DISSERTATION

FOREST SOIL C AND N RESPONSES TO SALVAGE LOGGING AND BELOWGROUND C INPUTS IN BARK BEETLE INFESTED STANDS

Submitted by

Bethany N. Avera

Graduate Degree Program in Ecology

In partial fulfillment of the requirements

For the Degree of Doctor of Philosophy

Colorado State University

Fort Collins, Colorado

Summer 2020

Doctoral Committee:

Advisor: M. Francesca Cotrufo

Charles Rhoades
Monique Rocca
Linda van Diepen

ABSTRACT

FOREST SOIL C AND N RESPONSES TO SALVAGE LOGGING AND BELOWGROUND C INPUTS IN BARK BEETLE INFESTED STANDS

Managing forest ecosystems in this era of global change requires a fundamental understanding of forest soil properties and processes. Forest disturbance events are projected to increase in severity and frequency, requiring a better understanding of how post-disturbance management will impact ecological processes such as soil nutrient dynamics and stocks of soil carbon (C). The research in this dissertation focused on areas of widespread mortality in lodgepole pine (*Pinus contorta* var. *latifolia*) in northern Colorado due to the most recent outbreak of the endemic mountain pine beetle (MPB; *Dendroctonus ponderosae* Hopkins). The goal of this research was to examine soil nitrogen (N) stocks, plant N uptake, and changes in forest soil C stocks in soil organic matter (SOM) due to tree mortality and subsequent salvage logging and from different belowground C inputs. To achieve this aim, I compared the three most prevalent management options: 1) uncut beetle-infested lodgepole pine stands and clear-cut salvage logged areas with either 2) post-harvest residue retention or 3) post-harvest residue removal.

To determine the impacts of MPB-infestation and salvage logging on ecosystem N stocks and plant N uptake, I implemented an experimental field study by adding ^{15}N-labeled ammonium sulfate to research plots centered over lodgepole pine seedlings. Measuring N stocks and ^{15}N recovery in soil and vegetation pools over two growing seasons highlighted the coupled nature of forest C and N cycling between plant and soil forest ecosystem compartments. The majority of the ^{15}N label was recovered in the soil and was not impacted by the management treatments. In contrast, the N uptake by lodgepole

pine seedlings was driven primarily by the amount of C fixation and the patterns of C fixation, in turn, related to other environmental factors modulated by the management treatment, such as available light.

An observational field study sought to quantify changes in forest soil C stocks in the bulk soil and SOM fractions and detect any changes in C chemistry as a result of management that may impact C persistence. In the dry, high elevation forests studied, soil C increased with salvage logging likely due to mixing of surface residues and O horizon C into the mineral soil during logging. The distribution of C stocks among the mineral soil fractions and the chemistry of those fractions indicated that root C accumulation in the particulate organic matter (POM, >53 µm) is an important mechanism of soil C accumulation in these forest soils.

A mechanistic laboratory incubation evaluated the efficiency of mineral-associated organic matter (MAOM, <53 µm) formation from root and hyphal necromass inputs with different C chemistries. This study showed that rye root necromass with more labile and less structural C than pine roots, was processed most in the 38-day incubation and contributed much more efficiently to the formation of MAOM than did the pine roots. Despite less processing, the arbuscular and ectomycorrhizal fungal necromass both contributed as efficiently as rye roots to MAOM formation. These results indicate that both C chemistry and C/N ratio exert controls on residue processing and MAOM formation.

Together, this dissertation work showed that salvage logging stimulated the growth of lodgepole pine seedlings, resulting in increased storage of both C and N in the plant biomass above- and belowground. As this pine root biomass turns over, the root necromass will contribute C to the POM fraction, the largest pool of soil C in this system. The net increase of forest soil C with salvage logging found in this study is notable as it suggests that the MPB-infested lodgepole pine forests of Colorado can be salvage logged with a low risk of significant soil C loss. Additionally, the highest recovery of the N

label was in the soil, thus the high soil N recovery with higher soil C supports SOM is a sink of N reducing N losses. Finally, pine seedling colonization by ectomycorrhizal fungi may further aid with nutrient retention and the efficient formation of MAOM during regeneration.

ACKNOWLEDGEMENTS

Completion of my doctoral dissertation would not have been possible without the support, guidance, and the support of numerous people along the way. First, I thank my advisor Dr. M Francesca Cotrufo who has been a great mentor; I am very fortunate to have been able to work with her and be supported by her personally. I greatly appreciate the assistance and advising from my committee member Dr. Charles C. Rhoades who, along with many other contributions, helped me with the 18+ hour field day when we applied the ^{15}N-label for Chapter 2. I would also like to thank my committee members Dr. Monique Rocca and Dr. Linda van Diepen and my collaborator Dr. Francisco Calderón who have all provided valuable insight and guidance. Dr. Jocelyn Lavallee has been a valuable mentor, in addition to past and present Cotrufo lab members and other GDPE students who have provided valuable insight along the way: Y. Pressler, E. Foster, K. Barker, K. Rocci, M. Machmuller, S. Mosier, R. Even, M. Ramlow, L. van der Pol, H. Oleszak, S. Leichty, E. Cubley, I. Oleksy, A. Foster, and S. Hoosein.

I received generous assistance in the laboratory, greenhouse and field that made these projects feasible. I would like to thank M. Haddix, D. Reuss, G. Beresford, T. Brenner, P. Freebury, D. Meraz, R. Tyler, Y. Pressler, R. Even, X. Tan, T. Fegel, J. Enigawaza, C. McCarty, C. Livensperger, A. Fairfield, C. Knebel, and S. Telander.

I would like to thank my family and friends for their encouragement throughout my PhD, particularly S. Ogburn and R. Taylor for housing me in Fort Collins regularly over the past 1.5 years and for those who made sure I did not feel isolated as I finished writing my dissertation in the midst of a stay-at-home order. Matthew Sparacino and Sprout have provided the strongest support through all of this, listening to endless ramblings about soil fungi, making sure I never went to campus without lunch, and accompanying me on many runs to bring balance throughout the process.

TABLE OF CONTENTS

ABSTRACT ii

ACKNOWLEDGEMENTS v

CHAPTER 1: INTRODUCTION 1

CHAPTER 2: VEGETATION RESPONSE TO RESOURCE AVAILABILITY MEDIATES NITROGEN DYNAMICS IN BARK BEETLE-INFESTED AND SALVAGE LOGGED LODGEPOLE PINE ECOSYSTEMS 9

CHAPTER 3: SOIL C STORAGE FOLLOWING SALVAGE LOGGING AND RESIDUE MANAGEMENT IN BARK BEETLE-INFESTED LODGEPOLE PINE FORESTS 38

CHAPTER 4: CONTRIBUTIONS OF ROOT AND HYPHAL NECROMASS TO THE FORMATION OF MINERAL-ASSOCIATED ORGANIC MATTER 72

CHAPTER 5: SUMMARY AND CONCLUSIONS 104

CHAPTER 1: INTRODUCTION

Forested ecosystems cover approximately 1/3 of the global terrestrial land surface and provide important ecosystem services such as mediating atmospheric composition through taking up carbon dioxide and serving as a large store of terrestrial carbon (C), regulating the water cycle, and provisioning timber products. Notably, >40% of terrestrial organic C globally is stored in forest soils (IPCC., 2007) as the main component of soil organic matter (SOM). SOM provides nutrients and nutrient storage, supports nutrient cycling, energy for soil microbial processes, and water retention (Smith et al., 2015), thus the forest ecosystem services that we rely upon are rooted in forest soils.

Global climate change will lead to more forest mortality and novel stand conditions (Millar and Stephenson, 2015; Seidl et al., 2017). In the Rocky Mountain Region an unprecedented, synchronous outbreak of mountain pine beetle (*Dendroctonous ponderosae* Hopkins) from mid-1990's to a peak circa 2008-2009 led to high rates of forest mortality from Colorado to northern British Columbia, across the range of lodgepole pine (*Pinus contorta* var. *latifolia*) (Raffa et al., 2008). In response, clear-cut salvage logging (harvesting of dead or dying trees) rates increased, particularly in Colorado, with the objective to reduce tree fall hazards, decrease wildfire risk and promote regeneration (Collins et al., 2010). The large amounts of sub-merchantable woody residues generated as a biproduct of salvage logging raised the possibility of a bioenergy market (Chung et al., 2017), but also highlighted the uncertainties remaining about the ecological impacts of salvage logging with different levels of residue retention.

Excess N mineralization and concentrations of inorganic-N have been measured in MPB-infested stands in Colorado and Wyoming (Brouillard et al., 2017; Griffin et al., 2011; Griffin and Turner, 2012); however, nitrate (NO_3^-) leaching losses have been minimal (Rhoades et al., 2017). Ecosystem N retention in MPB-infested stands is more highly correlated to the percentage of forest cover within a basin than

tree mortality rates (Clow et al., 2011). But comparisons of management and disturbance effects on ecosystem N retention predicted that clear-cut salvage logging of MPB-infested stands was likely to increase N leaching losses (Rhoades et al., 2013). Still, lodgepole pine ecosystems in the region are known to be highly retentive of N (Fahey et al., 1985), and N uptake by residual live vegetation and soil microorganisms were suggested as potential mechanisms to ameliorate N losses in salvage logged MPB-infested stands (Rhoades et al., 2013). Resolving the importance of different soil and vegetation pools for N uptake and recovery will improve our understanding of N sinks in response to disturbance and the implications for coupled C stocks.

Understanding of how specific management practices and land-use changes impact soil C stores and mechanisms of soil C accrual is still lacking. The impacts of forest harvesting on soil C stocks has been extensively studied, yet factors such as soil type, species composition and logging system, makes this a complex and highly nuanced question. Salvage logging, however, has received less attention and the majority of salvage logging research focuses on wildfire (Leverkus et al., 2018). Several recent studies have targeted this gap (e.g., Fornwalt et al., 2018; Hood et al., 2017; Rhoades et al., 2020a, 2020b), yet none have explicitly addressed soil C.

Detecting changes in forest soil C in response to salvage logging is notoriously challenging because of the high spatial variability of both soil C stocks and harvest impacts (Yanai et al., 2003). Investigating changes in soil C by physically fractionating the SOM into particulate organic matter (POM) and mineral-associated organic matter (MAOM) is likely to be a useful approach to increase our ability to detect changes in soil C stocks and their functional significance. The POM and MAOM are physically distinct pools, that are hypothesized to form from different pathways (Cotrufo et al., 2015). The POM is characterized as primarily plant and fungal structural compounds that have undergone little decomposition and will remain in the soil on the order of years to decades if not protected in microaggregates, whereas the MAOM is characterized by low molecular weight compounds, primarily of

microbial origin, chemically bonded to minerals and therefore has the potential to be retained in soil on the order of decades to centuries (Lavallee et al., 2020).

In addition to changes in aboveground C inputs, forest disturbances, management and changes in species composition associated with land use or climate change all have the possibility of altering belowground C inputs. Accumulation of soil C in POM vs. MAOM across forest systems has been found to covary with the dominant mycorrhizal fungal association, arbuscular mycorrhizal (AMF) or ectomycorrhizal (EMF) fungi (Cotrufo et al 2019). However, the role of residue quality vs. mycorrhizal activity in driving these trends is unclear. More evidence is continuing to emerge that points towards the importance of root inputs to forming SOM both in the POM (Fulton-Smith and Cotrufo, 2019) and MAOM (Sokol et al., 2019). Mycorrhizal fungi link the flow of C from the atmosphere into the soil as root symbionts, but the specific contribution of root-symbiotic mycorrhizal fungal necromass to POM and MAOM has been largely overlooked. Root and hyphal necromass with more labile chemistry should form MAOM more efficiently (Lavallee et al., 2018), but how root and hyphal chemistry differs between species and growth forms and the relationship to formation of MAOM still remains largely unknown. Managing forests also for SOM will require a better understanding of how different types of residues contribute to POM vs. MAOM and how disturbance and management will impact this.

This dissertation sought to advance understanding of forest soil properties and processes related to post-disturbance and salvage logging N uptake and recovery, and SOM formation response to management and with different residue inputs. To achieve this aim, my dissertation focused on the following questions:

1) How do plant N stocks in MPB-infested lodgepole pine areas differ between management treatments of uncut MPB-infested lodgepole pine stands and clear-cut salvage logged areas with

either post-harvest residue retention or removal, and what is the role of understory vs. pine seedlings for total N recovery?

2) Is N uptake by lodgepole pine responsive to differences in growth conditions (e.g., light, moisture) between cut and uncut areas associated with salvage logging?
3) Are soil N stocks or availability related to the management treatments or vegetation N stocks?
4) How does forest harvest and residue management impact forest soil C stocks, C distribution between the O horizon and the upper 10 cm of mineral soil and among light and heavy POM and MAOM fractions, and forest soil C chemistry in MPB-infested lodgepole areas?
5) Do necromass types (e.g., root and extraradical mycorrhizal hyphae) differ in efficiency of MAOM formation?
6) How does necromass processing relate to necromass chemistry?

I addressed these questions in three studies presented in the following chapters: an experimental field study (Chapter 2), and an observational field study (Chapter 3), and a mechanistic laboratory incubation (Chapter 4). I reflect on the overall conclusions in the final chapter (Chapter 5).

REFERENCES

Brouillard, B.M., Mikkelson, K.M., Bokman, C.M., Berryman, E.M., Sharp, J.O., 2017. Extent of localized tree mortality influences soil biogeochemical response in a beetle-infested coniferous forest. Soil Biology and Biochemistry 114, 309–318. https://doi.org/10.1016/j.soilbio.2017.06.016

Chung, W., Evangelista, P., Anderson, N., Vorster, A., Han, H., Poudel, K., Sturtevant, R., 2017. Estimating Aboveground Tree Biomass for Beetle-Killed Lodgepole Pine in the Rocky Mountains of Northern Colorado. Forest Science 63, 413–419. https://doi.org/10.5849/FS.2016-065

Clow, D.W., Rhoades, C., Briggs, J., Caldwell, M., Lewis, W.M., 2011. Responses of soil and water chemistry to mountain pine beetle induced tree mortality in Grand County, Colorado, USA. Applied Geochemistry 26, S174–S178. https://doi.org/10.1016/j.apgeochem.2011.03.096

Collins, B.J., Rhoades, C.C., Underhill, J., Hubbard, R.M., 2010. Post-harvest seedling recruitment following mountain pine beetle infestation of Colorado lodgepole pine stands: a comparison using historic survey records. Can. J. For. Res. 40, 2452–2456. https://doi.org/10.1139/X10-172

Cotrufo, M.F., Soong, J.L., Horton, A.J., Campbell, E.E., Haddix, M.L., Wall, D.H., Parton, W.J., 2015. Formation of soil organic matter via biochemical and physical pathways of litter mass loss. Nature Geosci 8, 776–779. https://doi.org/10.1038/ngeo2520

Fahey, T.J., Yavitt, J.B., Pearson, J.A., Knight, D.H., 1985. The nitrogen cycle in lodgepole pine forests, southeastern Wyoming. Biogeochemistry 1, 257–275. https://doi.org/10.1007/BF02187202

Fornwalt, P.J., Rhoades, C.C., Hubbard, R.M., Harris, R.L., Faist, A.M., Bowman, W.D., 2018. Short-term understory plant community responses to salvage logging in beetle-affected lodgepole pine forests. Forest Ecology and Management 409, 84–93. https://doi.org/10.1016/j.foreco.2017.10.056

Fulton-Smith, S., Cotrufo, M.F., 2019. Pathways of soil organic matter formation from above and belowground inputs in a Sorghum bicolor bioenergy crop. GCB Bioenergy 11, 971–987. https://doi.org/10.1111/gcbb.12598

Griffin, J.M., Turner, M.G., 2012. Changes to the N cycle following bark beetle outbreaks in two contrasting conifer forest types. Oecologia 170, 551–565. https://doi.org/10.1007/s00442-012-2323-y

Griffin, J.M., Turner, M.G., Simard, M., 2011. Nitrogen cycling following mountain pine beetle disturbance in lodgepole pine forests of Greater Yellowstone. Forest Ecology and Management 261, 1077–1089. https://doi.org/10.1016/j.foreco.2010.12.031

Hood, P.R., Nelson, K.N., Rhoades, C.C., Tinker, D.B., 2017. The effect of salvage logging on surface fuel loads and fuel moisture in beetle-infested lodgepole pine forests. Forest Ecology and Management 390, 80–88. https://doi.org/10.1016/j.foreco.2017.01.003

IPCC., 2007. Climate change 2007: The physical science basis. Cambridge University Press, Cambridge, UK and New York, USA.

Lavallee, J.M., Conant, R.T., Paul, E.A., Cotrufo, M.F., 2018. Incorporation of shoot versus root-derived 13C and 15N into mineral-associated organic matter fractions: results of a soil slurry incubation with dual-labelled plant material. Biogeochemistry 137, 379–393. https://doi.org/10.1007/s10533-018-0428-z

Lavallee, J.M., Soong, J.L., Cotrufo, M.F., 2020. Conceptualizing soil organic matter into particulate and mineral-associated forms to address global change in the 21st century. Glob Change Biol 26, 261–273. https://doi.org/10.1111/gcb.14859

Leverkus, A.B., Rey Benayas, J.M., Castro, J., Boucher, D., Brewer, S., Collins, B.M., Donato, D., Fraver, S., Kishchuk, B.E., Lee, E.-J., Lindenmayer, D.B., Lingua, E., Macdonald, E., Marzano, R., Rhoades, C.C., Royo, A., Thorn, S., Wagenbrenner, J.W., Waldron, K., Wohlgemuth, T., Gustafsson, L.,

2018. Salvage logging effects on regulating and supporting ecosystem services — a systematic map. Can. J. For. Res. 48, 983–1000. https://doi.org/10.1139/cjfr-2018-0114

Millar, C.I., Stephenson, N.L., 2015. Temperate forest health in an era of emerging megadisturbance. Science 349, 823–826. https://doi.org/10.1126/science.aaa9933

Raffa, K.F., Aukema, B.H., Bentz, B.J., Carroll, A.L., Hicke, J.A., Turner, M.G., Romme, W.H., 2008. Cross-scale Drivers of Natural Disturbances Prone to Anthropogenic Amplification: The Dynamics of Bark Beetle Eruptions. BioScience 58, 501–517. https://doi.org/10.1641/B580607

Rhoades, C.C., Hubbard, R.M., Elder, K., 2017. A Decade of Streamwater Nitrogen and Forest Dynamics after a Mountain Pine Beetle Outbreak at the Fraser Experimental Forest, Colorado. Ecosystems 20, 380–392. https://doi.org/10.1007/s10021-016-0027-6

Rhoades, C.C., Hubbard, R.M., Elder, K., Fornwalt, P.J., Schnackenberg, E., Hood, P.R., Tinker, D.B., 2020a. Tree regeneration and soil responses to management alternatives in beetle-infested lodgepole pine forests. Forest Ecology and Management 468, 118182. https://doi.org/10.1016/j.foreco.2020.118182

Rhoades, C.C., Hubbard, R.M., Hood, P.R., Starr, B.J., Tinker, D.B., Elder, K., 2020b. Snagfall the first decade after severe bark beetle infestation of high-elevation forests in Colorado, USA. Ecol Appl 30. https://doi.org/10.1002/eap.2059

Rhoades, C.C., McCutchan, J.H., Cooper, L.A., Clow, D., Detmer, T.M., Briggs, J.S., Stednick, J.D., Veblen, T.T., Ertz, R.M., Likens, G.E., Lewis, W.M., 2013. Biogeochemistry of beetle-killed forests: Explaining a weak nitrate response. Proceedings of the National Academy of Sciences 110, 1756–1760. https://doi.org/10.1073/pnas.1221029110

Seidl, R., Thom, D., Kautz, M., Martin-Benito, D., Peltoniemi, M., Vacchiano, G., Wild, J., Ascoli, D., Petr, M., Honkaniemi, J., Lexer, M.J., Trotsiuk, V., Mairota, P., Svoboda, M., Fabrika, M., Nagel, T.A.,

Reyer, C.P.O., 2017. Forest disturbances under climate change. Nature Clim Change 7, 395–402. https://doi.org/10.1038/nclimate3303

Smith, P., Cotrufo, M.F., Rumpel, C., Paustian, K., Kuikman, P.J., Elliott, J.A., McDowell, R., Griffiths, R.I., Asakawa, S., Bustamante, M., House, J.I., Sobocká, J., Harper, R., Pan, G., West, P.C., Gerber, J.S., Clark, J.M., Adhya, T., Scholes, R.J., Scholes, M.C., 2015. Biogeochemical cycles and biodiversity as key drivers of ecosystem services provided by soils. SOIL Discuss. 2, 537–586. https://doi.org/10.5194/soild-2-537-2015

Sokol, N.W., Kuebbing, Sara.E., Karlsen-Ayala, E., Bradford, M.A., 2019. Evidence for the primacy of living root inputs, not root or shoot litter, in forming soil organic carbon. New Phytol 221, 233–246. https://doi.org/10.1111/nph.15361

Yanai, R.D., Currie, W.S., Goodale, C.L., 2003. Soil carbon dynamics after forest harvest: an ecosystem paradigm reconsidered. Ecosystems 6, 197–212. https://doi.org/10.1007/s10021-002-0206-5

CHAPTER 2: VEGETATION RESPONSE TO RESOURCE AVAILABILITY MEDIATES NITROGEN DYNAMICS IN BARK BEETLE-INFESTED AND SALVAGE LOGGED LODGEPOLE PINE ECOSYSTEMS

2.1 Introduction

Lodgepole pine (*Pinus contorta* var. *latifolia*) forests from Colorado to southern British Columbia have experienced unprecedented outbreaks of endemic mountain pine beetle (MPB, *Dendroctonus ponderosae* Hopkins) from the late 1990's and peaking between 2007 and 2009 (Raffa et al. 2008). Increased beetle activity has been attributed to regional temperature increases favoring beetle survival coupled with the abundance of dense, lodgepole dominant stands weakened by drought (Raffa et al. 2008; Bentz et al. 2010). Beetles killed over 75% of overstory trees in many pine-dominated stands across the Southern Rockies (Collins et al. 2011), generating projections that climate-driven forest disturbances will become more frequent and severe in the coming decades (Seidl et al. 2017). Human safety and infrastructure concerns about treefall hazards, elevated wildfire risk and associated impacts on clean water supply prompted an active management response across the region (Collins et al. 2010). The MPB-infestation and subsequent salvage logging (harvesting to remove dead and dying trees) has created a range of stand conditions and many uncertainties remaining about associated ecological impacts, such as ecosystem nitrogen (N) retention and plant N availability and uptake.

The MPB-infestation resulted in higher rates of N mineralization and concentrations of soil inorganic-N under beetle infested trees, which were attributed to reduced evapotranspiration, lower tree N uptake and increased litter from needle fall of dead trees (Griffin et al. 2011; Griffin and Turner 2012; Brouillard et al. 2017). Yet very low rates of excess streamwater nitrate (NO_3^-) were measured following the beetle, and it was found that forest cover and other catchment factors mediated the influence of the percent MPB-mortality on NO_3^- leaching losses (Clow et al. 2011; Rhoades et al. 2017). In

a canopy-gap study investigating belowground response of a lodgepole pine stand in southeastern Wyoming, Parsons et al. (1994) found that mortality of 15-30 trees in a gap was required before elevated soil NO_3^- concentrations were detected. The absence of N loss at tree gaps <15 trees was attributed to uptake of N by remaining live trees, supporting previous studies in the area that concluded that lodgepole pine stands are highly retentive of N because plant demand exceeds rates of N inputs and internal N recycling (Fahey et al. 1985). However, a comparison of N loss from MPB-infestations to other forest disturbances indicated that clear cut harvesting could be expected to have a much bigger impact on nitrification and NO_3^- leaching losses (Rhoades et al. 2013). Subsequent studies in Colorado found that salvage logging did increase mineralization and nitrification with uncertain impacts to ecosystem N retention in soil and plant pools (Rhoades 2019; Rhoades et al. 2020).

Abatement of post-harvest rates of nitrification and elevated NO_3^- concentrations are closely connected to regeneration and growth of vegetation (Vitousek and Reiners 1975). Therefore, high N demand from residual live or regenerating vegetation may rapidly take-up the excess available soil N to help prevent leaching losses after salvage logging. Plant competition for soil N may have implications for total N uptake and ecosystem N recovery depending upon the productivity of each vegetation type and the associated amount of N stored in plant biomass. Salvage logging reduces understory cover (Fornwalt et al. 2018; Rhoades et al. 2018; Rhoades 2019) yet promotes lodgepole seedling regeneration and growth (Collins et al. 2012; Rhoades et al. 2020). Binkley et al. (2004) reframed the production ecology equation (Monteith 1977) to demonstrate that growth is a function of the resource supply, proportion of resources captured and the efficiency of resource use. Each of these three factors is likely to be affected by salvage logging and residue management, indicating that soil N availability is likely not enough to understand plant N uptake and demand.

The objective of this work was to assess the roles of understory vegetation and regenerating lodgepole pine seedlings in N storage and uptake in MPB-infested and salvage logged lodgepole pine

areas. To evaluate the impact of salvage logging on soil and plant N stocks we compared uncut MPB-infested stands and clear-cut salvage logged areas with two levels of post-harvest residue management. Further, we added a ^{15}N tracer and measured uptake and recovery of the ^{15}N tracer in vegetation and soil pools over two growing seasons. The ^{15}N addition approach is a robust method for integrating soil and vegetative processes to identify those contributing to ecosystem N retention on a seasonal and annual timescales (Templer et al. 2012; Goodale et al. 2015). Specifically, we sought to address the following questions: 1) how do plant N stocks differ between the management treatments?, 2) what is the role of understory and pine seedlings for total ^{15}N recovery?, 3) is the N uptake by lodgepole pine responsive to the different growth conditions in the uncut vs. cut areas?, and 4) are soil N stocks or availability related to the management treatments or vegetation N stocks?

2.2 Materials and Methods

2.2.1 Site and treatment descriptions

We conducted this study in northern Colorado at the US Forest Service Fraser Experimental Forest (FEF) on the Sulphur Ranger District of the Arapaho-Roosevelt National Forest. The study site was located between 2700-3000 m. At this elevation in FEF the temperature ranges from -40°C to 32°C with a mean annual temperature of 1°C and an annual precipitation of 71-76 cm, two-thirds of which fall as snow (Alexander and Watkins 1977; Collins et al. 2011). The overstory of the study area was predominantly lodgepole pine (>90%) and beetle attacks caused 70% overstory mortality or more (Klutsch et al. 2009; Collins et al. 2011). Soils were classified as Ustic Haplocryalfs and were well-drained, loams or sandy loams with gentle slopes (0-25%) (Collins et al. 2011).

For this experiment, we used established study sites with a complete block design to compare 1) uncut, beetle-infested lodgepole pine forest (hereafter “uncut”), to nearby salvage logged stands with 2) logging residue retention or 3) removal. Salvage logged treatments were harvested during the winter of

2007-2008 after trees had shed needles and were in the "gray stage" of the beetle outbreak (Fornwalt et al. 2018). Locations of three study blocks were selected using USFS pre-harvest stand exams (unpublished records) and stand inventories of uncut areas to minimize differences in forest species composition, slope and aspect between the adjacent harvested and untreated stands (Collins et al. 2011, 2012). Each block (n=3) consisted of a 900-m^2 (30-by-30 m) treatment area, with three treatments plots of 400 m^2 (20-by-20 m) demarcated within. For each block, the salvage logged treatments were randomly assigned to adjacent plots with a 10 m buffer between them and were ≤400 m from the paired uncut stand. In 2010, lodgepole pine seedlings grown from locally collected seed were planted in a 10-by-10 m corner of each treatment plot.

2.2.2 Experimental design and ^{15}N addition

In June 2016, four similar size, healthy lodgepole pine seedlings were selected per plot in pairs of approximately the same height. In two of the blocks suitable planted lodgepole seedlings could not be identified within the uncut plots and so naturally regenerated lodgepole seedlings were selected that were within the same height range of the planted seedlings chosen in the other plots. Plastic collars made of garden edging were installed around each seedling to demarcate the study unit. The collars were 76 cm in diameter resulting in a tree plot area of 0.454 m^2 centered over the seedling. The collars were trenched 10 cm in the soil.

Ten days after collar installation we applied a ^{15}N label to one seedling per pair (n=18) and an unlabeled N solution to the other tree (n=18). Both applications added 31.4 kg N ha^{-1} as ammonium sulfate ($(NH_4)_2SO_4$) with labeled trees receiving 98 atom % ^{15}N-$(NH_4)_2SO_4$. The N added was equivalent to ~2% of the total N in the mineral soil layer as the purpose of the N addition was not to stimulate growth. For each seedling, the $(NH_4)_2SO_4$ was diluted in 1.5 L of DI water and was sprayed homogeneously across the tree plot followed by the application of another 1 L of DI water sprayed evenly across the tree plot

to homogenize and rinse the $(NH_4)_2SO_4$ from litter and aboveground plant structures into the soil. Precipitation during the summer months (May-September) at FEF ranges from 3.2-4.7 cm per month with average rainfall events of 0.64 cm (Community Collaborative Rain, Hail and Snow Network, https://www.cocorahs.org), thus the 2.5 L DI water added to each plot was equivalent to an average summer rainfall event. Herbaceous vegetation in each tree plot was clipped prior to $(NH_4)_2SO_4$ application so that the uptake of ^{15}N of the understory could be more accurately measured at the end of the growing season. Large woody residue (greater than about 0.5 cm diameter) in each tree plot was removed prior to the $(NH_4)_2SO_4$ application and then returned after the application to minimize $(NH_4)_2SO_4$ interception by these residues.

2.2.3 Soil sampling and analysis

We sampled 3, 11 and 14 months after labeling to track ^{15}N recovery and analyze vertical movement into the soil over two growing seasons. During each sampling we collected two soil cores from each tree plot. At the first two harvests each soil core was separated into O horizon and mineral soil at 0-2, 2-5 and 5-15 cm depths and at the final harvest soil >15 cm was also collected to evaluate ^{15}N tracer movement below 15 cm. The cores were collected 15 cm from base of each seedling on opposite sides of the seedling using a 6.4 cm diameter split-corer (AMS, Inc., American Falls, Idaho, USA). The two soil cores for each seedling were composited by depth in the field and were transported on ice back to the lab where they were stored at 4°C until further analyses.

O horizon samples were oven dried at 60°C, weighed and a subsample was ground using a Wiley-Mill (Model No. 3, Arthur H. Thomas Co., Philadelphia, USA) and mortar and pestle to pass through 20 µm mesh. Mineral soil samples were sieved and homogenized using a 2 mm sieve and then air dried. A subsample from each depth was dried at 105°C (Soong 2016) and ground to a fine powder using a roller-mill. The O horizon and mineral soil subsamples were analyzed for %C, %N, and $\delta^{15}N$ on an

elemental analyzer (Costech ECS 4010, Costech Analytical Technologies, Valencia, CA, USA) coupled to an isotope ratio mass spectrometer (Delta V Advantage IRMS, Thermo-Fisher, Bremen, Germany).

Due to the rockiness of the soils at FEF, soil pit excavations were used to measure soil bulk density (Page-Dumroese et al. 1999). Following the method in Avera et al. (2020), three pits were excavated in both the logged unit and uncut stand of each block (n=3) just outside the plots to minimize disturbance. We sampled the 0-5 cm and 5-15 cm depths separately. The volume of each depth was quantified by filling it with millet and measuring the volume of millet in a graduated cylinder (Boot et al. 2015). Excavated soil was returned to the laboratory, sieved to 2 mm, dried at 105°C and the mass of the 2 mm soil fraction and the volume of each depth was used to estimate soil bulk density (Throop et al. 2012).

Mineral soils were extracted with 0.5 M K_2SO_4 within 5 days of sampling. Extracts were shaken for 1hr, filtered using 0.5 M K_2SO_4-rinsed Whatman No. 42 filters, and frozen (-20°C) until further analysis (Brookes et al. 1985). Extract NH_4-N and NO_3-N concentrations were analyzed on a continuous flow colorimeter (Alpkem Flow Solution IV, O.I. Analytical, College Station, TX) with minimum detection limits of 4 $\mu g\ L^{-1}$ for both NO_3-N and NH_4-N.

2.2.4 Vegetation sampling and analysis

Understory samples were collected at the end of the 2016 and 2017 growing seasons. In Sept. 2016 all grass forb and shrub foliage was clipped and total wet mass recorded, a representative subsample was collected for further analysis and the remaining material was redistributed on the plot surface. The subsample was weighed, dried at 60°C and reweighed to calculate foliar moisture content and determine foliar dry mass, and then the subsample was ground as described for the O horizon. In Sept. 2017 at the final harvest at the end of the second growing season, all aboveground understory biomass was harvested and collected (prior to collection of the soil cores), mixing all graminoids, forbs

and shrub vegetation together as one sample. After the final soil cores were collected all understory root biomass was collected for each tree plot by excavating the entire remaining soil volume to a depth of 15 cm followed by sieving with a 4 mm sieve and picking out the roots. In the lab the root biomass was rinsed thoroughly with DI water over a 2 mm sieve to remove all adhering soil particles.

The lodgepole pine seedlings were also harvested in September 2017. Trees were severed at the ground level and their root systems were excavated to at least 15 cm. Needles, lateral branches and the main stem were collected separately for the 2015-2017 annual increments. Pine and 2017 understory samples were processed as described earlier for the 2016 understory samples and the pine, 2016 and 2017 understory samples were analyzed for %N and $\delta^{15}N$ as described earlier for soils.

We estimated the N content of each vegetation component (g N $plot^{-1}$ or $seedling^{-1}$) and summed them to the stand level. The understory values were extrapolated from the 0.45 m^2 plot area and seedling estimates were scaled using the density of naturally regenerating lodgepole pine (<1 m height) enumerated in nearby harvest areas and uncut stands at FEF (Rhoades et al. 2020). Those densities were 880, 2147 and 3189 trees ha^{-1} in 2015 for the uncut, retention and removal, respectively

2.2.5 ^{15}N recovery calculations and N budget

We used the atom% notation to report ^{15}N abundance values. For samples with a ^{15}N < 5atom%, this was calculated as (Equation 1):

$$\textit{Equation 1:atom \%} = \frac{\textit{area under Mass 29}}{\textit{(area under Mass 28+29)} \times 2}$$

For samples with ^{15}N >5 atom % we also included mass 30 (Fry 2006), this was calculated as (Equation 2):

$$\textit{Equation 2:atom \%} = \frac{\textit{area under Mass 29+(area under Mass 30} \times 2)}{\textit{(area under Mass 28+Mass 29+Mass 30)} \times 2}$$

We expressed enrichment of ^{15}N in each pool as ^{15}N atom percent excess (APE) (Equation 3) and measured the ^{15}N recovery of each pool by multiplying the APE by the pool's total N stock and measured percent recovery (% $^{15}N_{rec}$) dividing by the mass of ^{15}N added ($M_{15Naddded}$) (Equation 4). We assessed overall tracer recovery (mg ^{15}N) at the final harvest and total percent tracer recovery by summing each of them across all pools.

Equation 3: atom % excess =atom % enriched sample-atom % background sample (i.e., unlabeled)

$$Equation\ 4:\ \%^{15}N_{rec} = (atom\ \%\ excess \times N\ stock\ of\ pool\ (mg)) \div M_{15Nadded} \times 100$$

2.2.6 Statistical Analyses

Linear mixed models using *lmer* and the R packages *lme4*, lmerTEST, and lsmeans (Bates et al. 2015; R Core Team 2019) were used to test for the fixed effect of treatment on the variables of interest. Block was classified as a random effect for all models. For μg NH_4-N g^{-1} dry soil we also tested for differences between sampling date and soil depth and included all 2-way and 3-way interactions. Due to the heterogeneity within the system created by both the MPB and logging operations, we used an "extreme" criteria for removing outliers, which was outliers were removed prior to analysis based upon the criteria that they were 3 times the interquartile range outside either positive or negative. Data that were not normally distributed were first log transformed. Models were evaluated using analysis of variance followed by Tukey-adjusted pairwise comparisons. Linear regressions between needle mass (g) and woody biomass (g) and total lodgepole seedling mass (g) and available N (g NH_4-N m^{-2}) were fit using *lm* function. All statistical analyses were done using R version 3.6.1 (R Core Team 2019).

2.3 Results

2.3.1 Forest soil N pools

In the study system, over 97% of the N in the measured pools was stored in the soil. There was more N contained in the O horizon of the retention (p=0.02; Tukey's HSD) and removal (p=*0.08*; Tukey's HSD) treatments compared to the uncut stands. The mineral soil (0-15 cm) N stock differed between all treatments following management intensity, with highest values in the removal (p<0.0001 and p=0.001, compared to the uncut and retention respectively), and lowest in the uncut, which was significantly different from the retention too (p=0.04).

Extractable inorganic N was comprised of NH_4-N as NO_3-N was consistently below the instrument detection limit (4 μg L^{-1}). Extractable NH_4-N did not differ between treatments at any sampling or any depth and was highest in the 0-2 cm depth (Fig. 2.2.).

2.3.2 Plant biomass, nitrogen content and stoichiometry in response to treatments

Combined understory and lodgepole pine biomass at the end of the 2017 growing season was 436.7 g (±56.8 SE) in the uncut control and 640.6 g (±69.6) and 558.8 g (±46.5) in residue retention and removal treatments. Generally, the uncut stands had the highest understory and lowest lodgepole pine seedling biomass and conversely the retention treatment had the lowest understory and highest lodgepole pine seedling biomass (Table 2.1.). Across all three treatments, most of the understory biomass was in the roots. Seedlings grown in the salvage logged areas were larger overall, had greater biomass for all individual components and root-to-shoot (R/S) ratios were ~40% higher than the uncut control (Table 2.1.).

Neither the N concentration or C:N ratio of above or belowground tissues of understory vegetation differed between treatments (Table 2.1.). Harvesting had a greater effect on N concentration of lodgepole pine tissues. Pines growing in the uncut stands had higher foliar and branch N concentration that those in the harvested areas (Table 2.1.). Needle mass was 10-12 times more lodgepole seedling needle mass in salvage logged treatments as compared to uncut. The values were

4.19 (±0.56), 38.04 (±5.07) and 47.51 (±6.44) g needles m^{-2}, in the uncut, retention and removal, respectively (*F(2,31)*=128.49*, p*<0.0001), with the uncut differing by an order of magnitude from both salvage logged treatments (*p*<0.0001; Tukey's HSD). Despite the higher %N in the uncut needles (Table 2.2.), the needle N stock (g N m^{-2}) was driven by needle mass and followed the same pattern of significance. Needle and woody biomass were strongly related (R^2=0.91) and the allometric relation did not vary across treatments (Fig. 2.3.A.). Total lodgepole growth (needles, aboveground woody and roots) across all levels of N availability was higher in the salvage logged treatments (*p*<0.0001; Tukey's HSD) (Fig. 2.3.B.) and was not related to level of N availability (linear regressions not shown).

Across treatments the combined N stock of the understory aboveground and root tissues was the largest vegetation pool (Fig. 4.1.A.). The cumulative understory and seedling vegetation accounted for 2.37%, 1.51% and 1.73% of the measured N in the uncut, retention and removal treatments, respectively. The lodgepole pine seedlings were the smallest vegetation pool of N but the only one that differed between the uncut and cut treatments (*F(2, 31)*=108.63*, p*<0.0001), with a total of 0.08 (±0.01), 0.71 (±0.10), 0.83 (±0.10) g N m^2 in the uncut, retention and removal treatment, respectively. Due to high variability in biomass values, there were no differences between treatments for the understory vegetation (*F(2, 29)*=0.60*, p*=0.55).

2.3.3 ^{15}N atom percent excess and tracer recovery

Treatment did not influence the total amount of ^{15}N recovered. In total, ^{15}N recovery ranged from 49% of the added ^{15}N in the retention to 69% in the removal treatment (Table 2.2.). Recovery of the added ^{15}N label in the vegetation largely followed the patterns of biomass and vegetation N pool sizes of the understory and lodgepole pine seedlings in the uncut and salvage logged treatments. The uncut control recovered the most ^{15}N of the vegetation in the understory whereas in the salvage logged plots the total ^{15}N recovery in the lodgepole pine was about 33-35% higher than that of the uncut

control (Table 2.2.). Yet when considering the total vegetation pool there were no differences in ^{15}N recovery, with vegetation across treatments, accounting for 18-26% of the total ^{15}N recovered. The forest soil consistently recovered the largest share of added ^{15}N, averaging 49% across treatments, with 60% of this retention in the O horizon and 0-2 cm depth (Table 2.2.).

The understory aboveground tissues had the highest APE of all ecosystem pools measured in both fall 2016 and 2017, with higher values in 2016 than 2017. In 2016, the understory aboveground biomass in both salvage treatments took up more ^{15}N label with APE averaging just over 20% compared to 15-20% in the uncut control (Fig. 2.4.B). In 2017, however, there were no differences between treatments with the aboveground biomass of all treatments having ~10% APE and roots ~5% APE (Fig. 2.4.B). Overall, the lodgepole pine had a much lower APE than the understory aboveground biomass. Across all lodgepole pine pools the APE was ~5%.

Soil values for APE were lower than the vegetation biomass values. Of the soil values, the O horizon had the highest APE, ranging around 2-3% (Fig. 2.4.A). APE decreased with each soil depth, although there was some ^{15}N label detected below 15 cm for each seedling plot measured in fall 2017. Overall, there were no differences in APE between the treatments for any of the soil depths nor differences between years within any of the depths.

2.4 Discussion

2.4.1 Nitrogen is stored and recovered as soil organic N

The forest soil was a tremendous reservoir of N as it accounted for over 97% of measured ecosystem N and the majority of ^{15}N recovery (Table 2.2.). At the time of sampling we found no differences between the treatments in the amount of inorganic N as NH_4-N (Fig. 2.2.), while NO_3-N was below the detection limits and therefore not likely to be a significant contributor to differences in mineral N availability. Three years following salvage logging, elevated extractable NH_4^+ and NO_3^- were

measured in the retention treatment and elevated total inorganic N was measured in the retention and the removal in these and nearby sites (Rhoades et al. 2020). These results were supported by nearby findings in the first three years following salvage logging of higher dissolved inorganic N (particularly NO_3-N), dissolved total N, and higher plant available NH_4-N and NO_3-N measured by ion exchange resin bags in cut compared to uncut, upland MPB-infested lodgepole stands (Rhoades 2019). While our lack of detectable NO_3-N was therefore initially surprising, we interpret this finding to indicate that NO_3^- was past the peak of production eight to nine years following salvage logging, which is supported by previous work showing elevated post-harvest NO_3-N in the 3-5 years following logging but that those rates declined 6 years following harvest (Jerabkova et al. 2011).

Despite evidence of elevated inorganic N soon following harvest in these treatment plots (Rhoades et al. 2020), there is no evidence that salvage logging following MPB-infestation resulted in excess N loss in this system as total soil N values were higher with salvage logging (Fig. 2.1.A). Our ^{15}N addition was not designed to be a fertilizer experiment and was low, but we did add ca. 12-fold the N deposition rate in this area of 2.6 kg N ha^{-1} (Rhoades et al. 2017) and therefore we interpret our ^{15}N recovery values to be quite high. Water moves in FEF via subsurface flow without surface runoff, and our elevated APE values in soil >15cm (Fig. 2.4.A.) supports that much of the unrecovered label has likely redistributed deeper in the soil profile, with lateral transport and some loss via subsurface flow. But ca. 60% of the recovered label was in the O horizon and 0-2 cm of the mineral soil indicating that microbial immobilization (Turner et al. 2007) incorporated the ^{15}N into soil organic matter (SOM), perhaps binding with soil minerals and occlusion within aggregates (Bingham and Cotrufo 2016). This finding supports the N bank hypothesis that adds on to the Vitousek and Reiners (1975) model of nutrient retention in ecosystem succession by emphasizing the importance of SOM for ecosystem N retention (Lovett et al. 2018). In a previous study at these and nearby sites we found that salvage logging MPB-infested stands

led to an increase of SOM, which would support the N bank hypothesis and increase of soil N with logging found in this study (Fig. 2.4.A) (Avera et al. 2020).

2.4.2 Pine N uptake is an effect of growth, rather than a driver

Lodgepole seedling N was the smallest ecosystem N pool and the most responsive to salvage logging and residue management. Overall our findings reflected the fact that lodgepole pine is a shade-intolerant early-successional species that does well in full-sun (Mason 1915). The seedling N uptake was a function of the increased density and growth relative to the uncut treatment (Rhoades et al. 2020) and not a response to soil N availability. Across all levels of NH_4-N availability, the seedlings in the salvage logged treatments had higher total lodgepole pine biomass (Fig. 2.3.B). Thus, the lower foliar N concentration and higher C:N of the lodgepole needles in the salvage logged treatments (Table 2.2) point towards higher photosynthetic N use efficiency in the clear cuts rather than a reflection of nutrient status (Turner et al. 2019). Higher biomass in roots and R/S ratio of the salvage logged treatments compared to the uncut (Table 2.1.) further support for increased higher N use efficiency of the seedlings in the clear cut. We were anticipating that the seedlings in the clear cut might have a difference in N and C allocation aboveground, such as a preferential investment in needles to capture more C. However, the linear regression between needle mass and woody biomass across all treatments instead make it clear that aboveground allometry is consistent between treatments (R^2=0.91; Fig. 2.3.A.). Across a constant resource supply, we conclude that the increased efficiency of resource use is the primary factor leading to increased productivity of the regenerating seedlings in the salvage logged compared to uncut, creating a positive feedback that is also increasing the proportion or resources captured (Binkley et al. 2004).

Our study only focused on lodgepole seedling N uptake. Therefore, our study design does not allow for a perfect comparison of plant N uptake as there were residual live overstory and sub-canopy

trees in the uncut treatments (Collins et al. 2012) that may have taken up a portion of the added ^{15}N. Slightly lower ^{15}N APE in the >15 cm soil may support some canopy uptake, however the lack of differences in total ^{15}N recovery between the treatments in the vegetation or in the soil suggests that the remaining live trees were not a significant factor in the N dynamics of our seedling plots.

2.4.3 Understory vegetation is effective at N retention, particularly when lodgepole pine growth is limited

Compensatory uptake, as evidenced by the ^{15}N recovery in the vegetation of 12-13% when vegetation accounts for <3% of total ecosystem N in our seedling plots, suggests that continued plant uptake is an important process for helping to prevent N losses. In the uncut stands, the understory responded more to increases in soil N availability than the lodgepole pine seedlings but declines in understory biomass due to logging disturbance shifted N uptake to the lodgepole pine seedlings (Tables 2.1. and 2.2.). In the uncut stands vegetation biomass and N uptake was dominated by the understory, recovering ~75% of the ^{15}N label retained in the vegetation for this treatment (Table 2.2.). Whereas in the salvage logged treatments 67-70% of the ^{15}N label retained in the vegetation was recovered in the lodgepole pine seedlings (Table 2.2.). The trade-off in the growth and N uptake between the understory and lodgepole pine seedlings was particularly evident in the retention treatment that had the lowest understory biomass paired with the greatest lodgepole pine growth (Table 2.1.). Previous work in lodgepole has found growth responses of the understory vegetation to higher resource availability following bark beetles (Stone and Wolfe 1996; Brown et al. 2010; Bowler et al. 2012; Pec et al. 2015). This pattern was also observed by Turner et al. (2019) following wildfire, who showed a tradeoff between lodgepole pine and understory access to N, interpreted as N availability for the understory increasing when lodgepole pine are taking up less N. Our study also indicates that the understory may be particularly effective at competing for inorganic N; aboveground biomass had 2-3 times higher APE values in fall 2016 and 2017 (10-15 APE) compared to all lodgepole seedling pools (~5 APE) (Fig. 2.4.B).

The lower APE of the lodgepole seedlings compared to the understory may support the importance of organic N as a N source for conifers with symbiotic ectomycorrhizal fungi, however, that was beyond the scope of this study.

2.4.4 Conclusions

Over 97% of the measured ecosystem N was stored in the soil and tracking a ^{15}N label over two growing seasons, we found the highest ^{15}N label recovery in the soil. This result is in agreement with ^{15}N tracers studies across temperate forest ecosystems (Templer et al. 2012) and consistent with the hypothesis that soil organic matter can act as a N bank, reducing ecosystem N losses (Lovett et al. 2018). Despite the lack of treatment differences in NH_4-N concentrations 8-9 years following salvage logging, seedlings in the salvage logged areas recovered more of the ^{15}N tracer and had higher N stocks because the seedlings were larger and more dense than in the uncut. These findings show that the success of lodgepole pine in early succession environments is likely due to their ability to more efficiently use available N to fix more C in high light environments.

Table 1 Understory biomass (g dry wt. tree plot^{-1}), lodgepole pine seedling biomass (g dry wt. seedling^{-1}), and total N (%N) for the understory and lodgepole pine after the second growing season in fall 2017. Data are means (± 1 S.E.) (n=3).

	Uncut	**Retention**	**Removal**	**p-value***
		Understory biomass (g dry wt. tree plot^{-1})		
Aboveground biomass	39.64 (7.52) a†	23.69 (4.41) b	26.30 (4.36) ab	0.08
Roots	235.23 (51.63) a	97.66 (13.13) b	129.86 (21.98) ab	0.03
		Lodgepole biomass (g dry wt. seedling^{-1})		
Bole and branches	90.66 (11.78) a	233.67 (31.53) b	177.83 (24.96) b	<0.0001
Needles	47.64 (6.35) a	177.18 (23.63) b	148.99 (20.19) b	<0.0001
Roots	23.50 (3.27) a	108.36 (18.85) b	75.84 (11.71) b	<0.0001
R/S ratio	0.27 (0.02) a	0.46 (0.03) b	0.43 (0.02) b	<0.0001
		Total N (%N)		
Understory aboveground biomass	1.00 (0.05)	0.96 (0.07)	1.03 (0.08)	0.70
Understory roots	0.72 (0.09)	0.78 (0.04)	0.80 (0.07)	0.66
Lodgepole bole§	0.30 (0.01)	0.28 (0.01)	0.31 (0.03)	0.69
Lodgepole branch§	0.58 (0.05) a	0.50 (0.02) ab	0.47 (0.03) b	0.02
Needles	1.19 (0.05) a	1.06 (0.03) b	1.07 (0.04) ab	0.03
Lodgepole root	0.40 (0.05)	0.47 (0.03)	0.48 (0.02)	0.11
		C:N Ratio		
Branch C:N ratio‡	84.13 (5.83) a	96.95 (4.18) ab	101.64 (6.75) b	0.05

Needle C:N ratio	46.10 (1.87) a	52.49 (1.61) b	51.53 (1.92) b	0.01

* p-values presented are from the linear mixed effects model testing for fixed effect treatment differences

† lowercase letters indicate that the pairwise differences between treatments had p-values≤0.05 by the Tukey method

§ Prior to averaging the bole and branch N across the respective growth year separations we tested for a significance of year and interaction of year*treatment on % N; year was significant but treatment*year was not and so the values in the table are mass weighted averages by summing the total g N and dividing by the total g of bole or branches.

‡ For these calculations the % C was estimated at 48% based upon (Prescott and Laiho 2002)

Table 2 Recovery of the added 1398 mg ^{15}N by treatment and ecosystem pool after two growing seasons in Sept. 2017, the final sampling. Recovery is reported in mg ^{15}N, with % ^{15}N recovery summed across all vegetation, soil and ecosystem pools. Data are means (± 1 S.E.) (n=3).

		Uncut	Retention	Removal	p-value*
		Vegetation (mg ^{15}N)			
Understory aboveground biomass		35.67 (11.58)	19.58 (4.69)	18.13 (3.99)	0.15
Understory roots		107.34 (32.47) a†	32.06 (6.05) b	38.48 (12.33) b	0.01
Lodgepole aboveground woody biomass		25.11 (5.93)	30.89 (2.81)	31.02 (3.54)	0.56
Lodgepole needles		40. 14 (13.56) a	72.17 (7.94) b	66.98 (9.65) ab	0.03
Lodgepole roots		5.36 (1.50) a	18.95 (3.11) b	18.77 (2.75) b	0.0003
		Soil (mg ^{15}N)			
O horizon		269.34 (50.98)	219.07 (71.91)	324.04 (107.46)	0.54
Mineral soil	0-2 cm	170.67 (51.09)	121.47 (43.58)	228.38 (72.40)	0.14
	2-5 cm	61.98 (15.56)	55.42 (11.69)	111.86 (53.48)	0.92
	5-15 cm	99.85 (27.62)	111.49 (22.97)	176.45 (42.54)	0.16
		Total (mg ^{15}N)			
Understory		143.00 (43.15) a	51.64 (6.76) b	56.61 (12.78) b	0.01
Lodgepole		78.80 (26.86)	122.01 (10.80)	116.77 (14.09)	0.23
Vegetation		191.95 (82.31)	173.65 (8.20)	173.37 (8.35)	0.71
Forest soil		601.83 (88.31)	507.45 (96.80)	786.73 (94.05)	0.21
Total		854.62 (145.34)	681.10 (101.31)	960.10 (92.74)	0.26
		Total (% added)			
Vegetation		13.73 (5.89)	12.42 (0.59)	12.40 (0.60)	0.71
Forest soil		43.05 (6.32)	36.30 (6.92)	56.28 (6.73)	0.21
Total		61.13 (10.40)	48.72 (7.25)	68.68 (6.63)	0.26

* p-values presented are from the linear mixed effects model testing for fixed effect treatment differences

† lowercase letters indicate that the pairwise differences between treatments had p-values ≤0.05 by the Tukey method

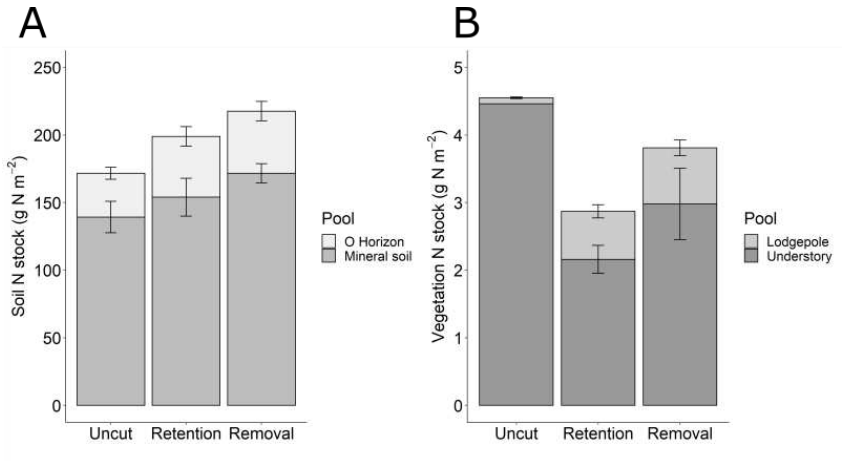

Fig. 2.1. Measured forest soil N stock (g N m^{-2}) in the O horizon and upper mineral soil (0-15 cm) (A) and vegetation N stock (g N m^{-2}) in the understory and lodgepole pine (B) for the uncut and salvage logged with residue retention and removal treatments at the final harvest in fall 2017. Data are mean and start error bars (n=3).

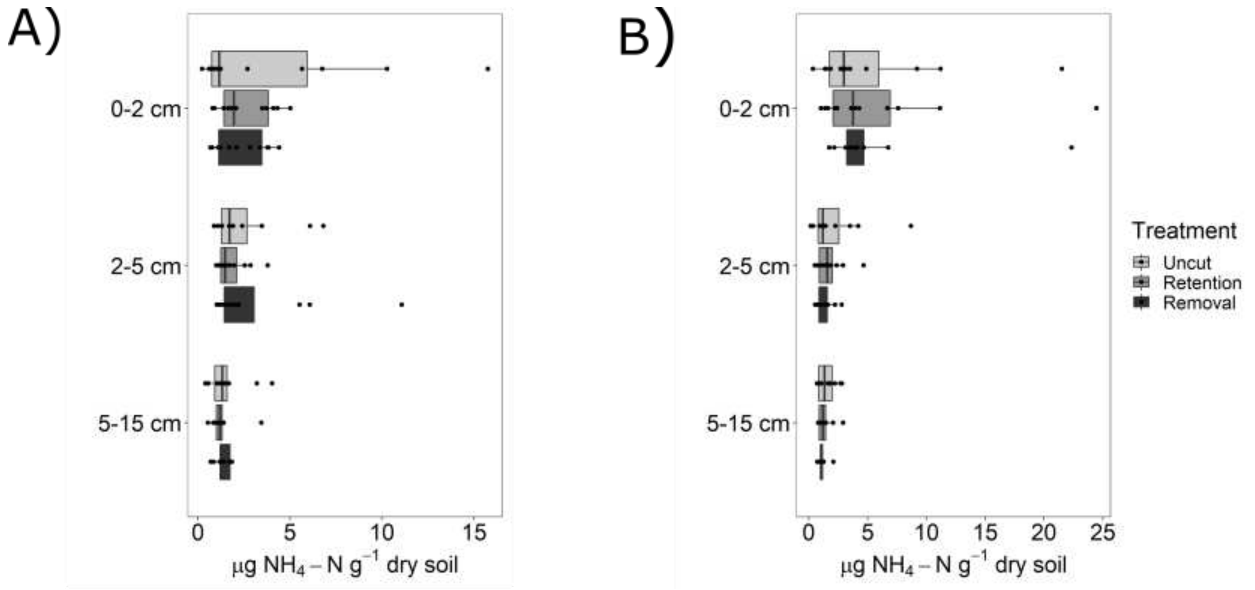

Fig. 2.2. Extractable inorganic N concentration in the form of NH_4-N by soil depth for spring (A) and fall (B) 2017. Black dots represent the individual raw data points (n=12). Overall treatments did not differ from each other (p=0.87), but there were seasonally dependent concentration differences with depth. In spring 2017 the 0-2 and 2-5 cm depths did not vary (p=1.0) but the 5-15 cm was less (p=0.08) that the shallower depths. In fall 2017 there was a notable decrease in the 2-5 and 5-15 cm depths than 0-2 cm (p<0.0001).

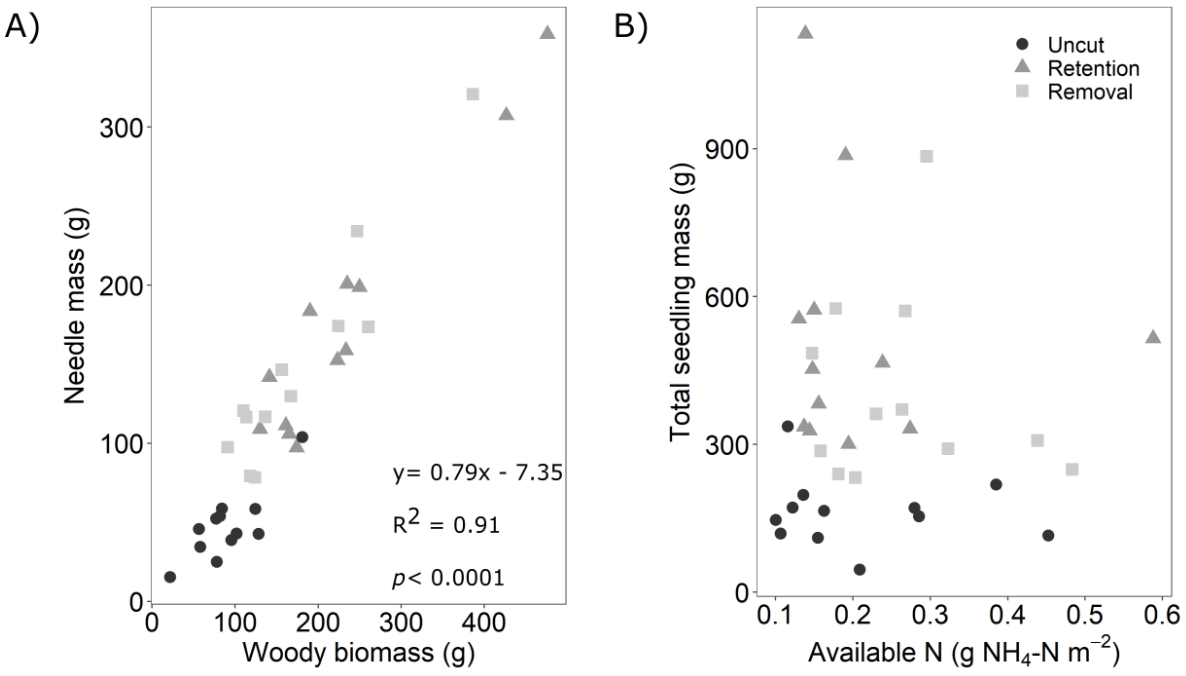

Fig. 2.3. Relation between the needle mass (g) to the aboveground woody biomass (g; bole and branches) for each seedling (A) and total seedling mass (g; needle, bole, branches and roots) to available N (g NH_4-N m^{-2}) (B). Each point represents a seedling in the study (n=36). For (A) the linear regression was fitted across all treatments and for (B) no linear relationships were found.

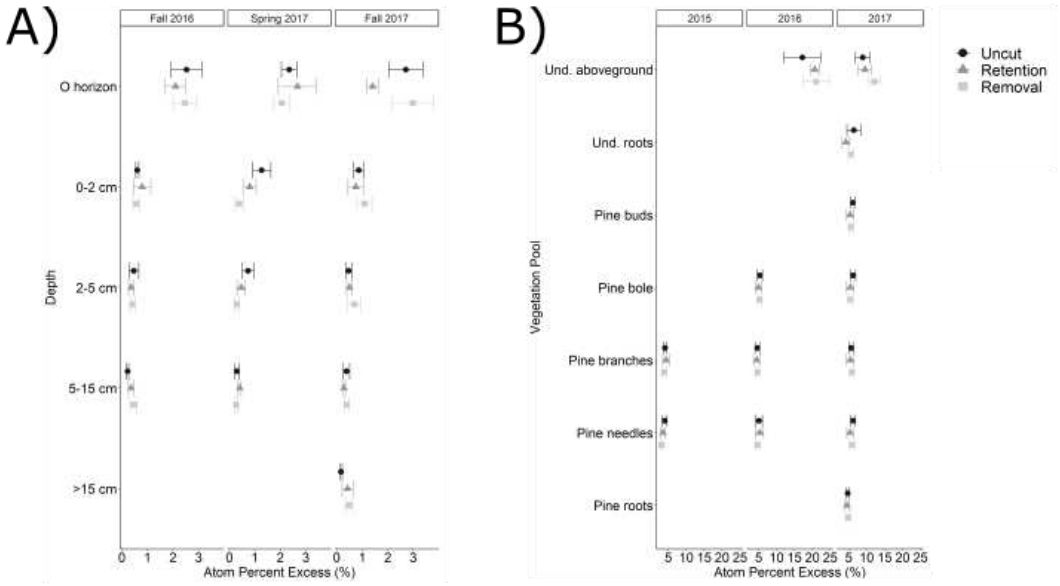

Fig. 2.4. ^{15}N atom percent (%) excess (APE) measured in the sampled soil depth (A) and vegetation pools (B). The soil APE vales are represented by sampling date and the vegetation APE are represented by year of growth, with the exception of the roots which were all sampled in 2017 without knowing the year of growth. Data are means with standard error bars (n=3).

REFERENCES

Alexander, R.R., and Watkins, R.K. 1977. The Fraser Experimental Forest, Colorado. USDA Forest Service.

Avera, B.N., Rhoades, C.C., Calderón, F., and Cotrufo, M.F. 2020. Soil C storage following salvage logging and residue management in bark beetle-infested lodgepole pine forests. Forest Ecology and Management, 472(15):118251.

Bates, D., Maechler, M., Bolker, B., and Walter, S. 2015. Fitting Linear Mixed-Effects Models Using lme4. Journal of Statistical Software.

Bentz, B.J., Régnière, J., Fettig, C.J., Hansen, E.M., Hayes, J.L., Hicke, J.A., Kelsey, R.G., Negrón, J.F., and Seybold, S.J. 2010. Climate Change and Bark Beetles of the Western United States and Canada: Direct and Indirect Effects. BioScience 60(8): 602–613. doi:10.1525/bio.2010.60.8.6.

Bingham, A.H., and Cotrufo, M.F. 2016. Organic nitrogen storage in mineral soil: Implications for policy and management. Science of The Total Environment 551–552: 116–126. doi:10.1016/j.scitotenv.2016.02.020.

Binkley, D., Smith, F.W., and Son, Y. 1995. Nutrient supply and declines in leaf area and production in lodgepole pine. Canadian Journal of Forest Research 25: 621–628.

Binkley, D., Stape, J.L., and Ryan, M.G. 2004. Thinking about efficiency of resource use in forests. Forest Ecology and Management 193(1–2): 5–16. doi:10.1016/j.foreco.2004.01.019.

Blevins, D.P., Prescott, C.E., Allen, H.L., and Newsome, T.A. 2005. The effects of nutrition and density on growth, foliage biomass, and growth efficiency of high-density fire-origin lodgepole pine in central British Columbia. 35: 9.

Boot, C.M., Haddix, M., Paustian, K., and Cotrufo, M.F. 2015. Distribution of black carbon in ponderosa pine forest floor and soils following the High Park wildfire. Biogeosciences 12(10): 3029–3039. doi:10.5194/bg-12-3029-2015.

Bowler, R., Fredeen, A.L., Brown, M., and Andrew Black, T. 2012. Residual vegetation importance to net CO2 uptake in pine-dominated stands following mountain pine beetle attack in British Columbia, Canada. Forest Ecology and Management 269: 82–91. doi:10.1016/j.foreco.2011.12.011.

Brookes, P.C., Landman, A., Pruden, G., and Jenkinson, D.S. 1985. Chloroform fumigation and the release of soil nitrogen: A rapid direct extraction method to measure microbial biomass nitrogen in soil. Soil Biology and Biochemistry 17(6): 837–842. doi:10.1016/0038-0717(85)90144-0.

Brouillard, B.M., Mikkelson, K.M., Bokman, C.M., Berryman, E.M., and Sharp, J.O. 2017. Extent of localized tree mortality influences soil biogeochemical response in a beetle-infested coniferous forest. Soil Biology and Biochemistry 114: 309–318. doi:10.1016/j.soilbio.2017.06.016.

Brown, M., Black, T.A., Nesic, Z., Foord, V.N., Spittlehouse, D.L., Fredeen, A.L., Grant, N.J., Burton, P.J., and Trofymow, J.A. 2010. Impact of mountain pine beetle on the net ecosystem production of lodgepole pine stands in British Columbia. Agricultural and Forest Meteorology 150(2): 254–264. doi:10.1016/j.agrformet.2009.11.008.

Clow, D.W., Rhoades, C., Briggs, J., Caldwell, M., and Lewis, W.M. 2011. Responses of soil and water chemistry to mountain pine beetle induced tree mortality in Grand County, Colorado, USA. Applied Geochemistry 26: S174–S178. doi:10.1016/j.apgeochem.2011.03.096.

Collins, B.J., Rhoades, C.C., Battaglia, M.A., and Hubbard, R.M. 2012. The effects of bark beetle outbreaks on forest development, fuel loads and potential fire behavior in salvage logged and untreated lodgepole pine forests. Forest Ecology and Management 284: 260–268. doi:10.1016/j.foreco.2012.07.027.

Collins, B.J., Rhoades, C.C., Hubbard, R.M., and Battaglia, M.A. 2011. Forest Ecology and Management Tree regeneration and future stand development after bark beetle infestation and harvesting in Colorado lodgepole pine stands. Forest Ecology and Management 261(11): 2168–2175. Elsevier B.V. doi:10.1016/j.foreco.2011.03.016.

Collins, B.J., Rhoades, C.C., Underhill, J., and Hubbard, R.M. 2010. Post-harvest seedling recruitment following mountain pine beetle infestation of Colorado lodgepole pine stands: a comparison using historic survey records. Can. J. For. Res. 40(12): 2452–2456. doi:10.1139/X10-172.

Fahey, T.J., Yavitt, J.B., Pearson, J.A., and Knight, D.H. 1985. The nitrogen cycle in lodgepole pine forests, southeastern Wyoming. Biogeochemistry 1(3): 257–275. doi:10.1007/BF02187202.

Fornwalt, P.J., Rhoades, C.C., Hubbard, R.M., Harris, R.L., Faist, A.M., and Bowman, W.D. 2018. Short-term understory plant community responses to salvage logging in beetle-affected lodgepole pine forests. Forest Ecology and Management 409: 84–93. doi:10.1016/j.foreco.2017.10.056.

Fry, B. 2006. Stable Isotope Ecology. Springer, New York.

Goodale, C.L., Fredriksen, G., Weiss, M.S., McCalley, C.K., Sparks, J.P., and Thomas, S.A. 2015. Soil processes drive seasonal variation in retention of 15 N tracers in a deciduous forest catchment. Ecology 96(10): 2653–2668. doi:10.1890/14-1852.1.

Griffin, J.M., and Turner, M.G. 2012. Changes to the N cycle following bark beetle outbreaks in two contrasting conifer forest types. Oecologia 170(2): 551–565. doi:10.1007/s00442-012-2323-y.

Griffin, J.M., Turner, M.G., and Simard, M. 2011. Nitrogen cycling following mountain pine beetle disturbance in lodgepole pine forests of Greater Yellowstone. Forest Ecology and Management 261(6): 1077–1089. doi:10.1016/j.foreco.2010.12.031.

Jerabkova, L., Prescott, C.E., Titus, B.D., Hope, G.D., and Walters, M.B. 2011. A meta-analysis of the effects of clearcut and variable-retention harvesting on soil nitrogen fluxes in boreal and temperate forests. Can. J. For. Res. 41(9): 1852–1870. doi:10.1139/x11-087.

Klutsch, J.G., Negrón, J.F., Costello, S.L., Rhoades, C.C., West, D.R., Popp, J., and Caissie, R. 2009. Stand characteristics and downed woody debris accumulations associated with a mountain pine beetle (Dendroctonus ponderosae Hopkins) outbreak in Colorado. Forest Ecology and Management 258(5): 641–649. doi:10.1016/j.foreco.2009.04.034.

Lovett, G.M., Goodale, C.L., Ollinger, S.V., Fuss, C.B., Ouimette, A.P., and Likens, G.E. 2018. Nutrient retention during ecosystem succession: a revised conceptual model. Front Ecol Environ 16(9): 532–538. doi:10.1002/fee.1949.

Mason, D.T. 1915. The life history of lodgepole pine in the Rocky Mountains. US Department of Agriculture. Available from https://books.google.com/books?hl=en&lr=&id=qL8eAAAAIAAJ&oi=fnd&pg=PA1&ots=TgxUvuH6ke&sig=V9_aLi-kP73PdqP6lqW2UAo4bkk#v=onepage&q&f=false.

Monteith, J.L. 1977. Climate and the Efficiency of Crop Production in Britain. Phil. Trans. R. Soc. Lond. B. 281: 277–294.

Page-Dumroese, D.S., Brown, R.E., Jurgensen, M.F., and Mroz, G.D. 1999. Comparison of methods for determining bulk densities of rocky forest soils. Soil Science Society of America Journal 63(2): 379. doi:10.2136/sssaj1999.03615995006300020016x.

Parsons, W.F.J., Knight, D.H., and Miller, S.L. 1994. Root Gap Dynamics in Lodgepole Pine Forest: Nitrogen Transformations in Gaps of Different Size. Ecological Applications 4(2): 354–362. doi:10.2307/1941939.

Pec, G.J., Karst, J., Sywenky, A.N., Cigan, P.W., Erbilgin, N., Simard, S.W., and Cahill, J.F. 2015. Rapid Increases in Forest Understory Diversity and Productivity following a Mountain Pine Beetle (Dendroctonus ponderosae) Outbreak in Pine Forests. PLoS ONE 10(4): e0124691. doi:10.1371/journal.pone.0124691.

Prescott, C.E., Corbin, J.P., and Parkinson, D. 1992. Immobilization and availability of N and P in the forest floors of fertilized Rocky Mountain coniferous forests. Plant Soil 143(1): 1–10. doi:10.1007/BF00009123.

Prescott, C.E., and Laiho, R. 2002. The Nutritional Significance of Coarse Woody Debris in Three Rocky Mountain Coniferous Forests. : 12.

R Core Team. 2019. R: A language and environment for statistical computing. R Foundation for Statistical Computing, Vienna, Austria. Available from https://www.R-project.org/.

Raffa, K.F., Aukema, B.H., Bentz, B.J., Carroll, A.L., Hicke, J.A., Turner, M.G., and Romme, W.H. 2008. Cross-scale Drivers of Natural Disturbances Prone to Anthropogenic Amplification: The Dynamics of Bark Beetle Eruptions. BioScience 58(6): 501–517. doi:10.1641/B580607.

Rhoades, C., Pelz, K., Fornwalt, P., Wolk, B., and Cheng, A. 2018. Overlapping bark beetle outbreaks, salvage logging and wildfire restructure a lodgepole pine ecosystem. Forests 9(3): 101. doi:10.3390/f9030101.

Rhoades, C.C. 2019. Soil nitrogen leaching in logged beetle-killed forests and implications for riparian fuel reduction. Journal of Environment Quality 48(2): 305. doi:10.2134/jeq2018.04.0169.

Rhoades, C.C., Hubbard, R.M., and Elder, K. 2017. A Decade of Streamwater Nitrogen and Forest Dynamics after a Mountain Pine Beetle Outbreak at the Fraser Experimental Forest, Colorado. Ecosystems 20(2): 380–392. doi:10.1007/s10021-016-0027-6.

Rhoades, C.C., Hubbard, R.M., Elder, K., Fornwalt, P.J., Schnackenberg, E., Hood, P.R., and Tinker, D.B. 2020. Tree regeneration and soil responses to management alternatives in beetle-infested lodgepole pine forests. Forest Ecology and Management accepted.

Rhoades, C.C., McCutchan, J.H., Cooper, L.A., Clow, D., Detmer, T.M., Briggs, J.S., Stednick, J.D., Veblen, T.T., Ertz, R.M., Likens, G.E., and Lewis, W.M. 2013. Biogeochemistry of beetle-killed forests: Explaining a weak nitrate response. Proceedings of the National Academy of Sciences 110(5): 1756–1760. doi:10.1073/pnas.1221029110.

Seidl, R., Thom, D., Kautz, M., Martin-Benito, D., Peltoniemi, M., Vacchiano, G., Wild, J., Ascoli, D., Petr, M., Honkaniemi, J., Lexer, M.J., Trotsiuk, V., Mairota, P., Svoboda, M., Fabrika, M., Nagel, T.A., and Reyer, C.P.O. 2017. Forest disturbances under climate change. Nature Clim Change 7(6): 395–402. doi:10.1038/nclimate3303.

Soong, J.L. 2016. Soil microarthropods support ecosystem productivity and soil C accrual: Evidence from a litter decomposition study in the tallgrass prairie. Soil Biology: 9.

Stone, W.E., and Wolfe, M.L. 1996. Response of understory vegetation to variable tree mortality following a mountain pine beetle epidemic in lodgepole pine stands in northern Utah. Vegetatio 122(1): 1–12. doi:10.1007/BF00052811.

Templer, P.H., Mack, M.C., Iii, F.S.C., Christenson, L.M., Compton, J.E., Crook, H.D., Currie, W.S., Curtis, C.J., Dail, D.B., D'Antonio, C.M., Emmett, B.A., Epstein, H.E., Goodale, C.L., Gundersen, P., Hobbie, S.E., Holland, K., Hooper, D.U., Hungate, B.A., Lamontagne, S., Nadelhoffer, K.J., Osenberg, C.W., Perakis, S.S., Schleppi, P., Schimel, J., Schmidt, I.K., Sommerkorn, M., Spoelstra, J., Tietema, A., Wessel, W.W., and Zak, D.R. 2012. Sinks for nitrogen inputs in terrestrial ecosystems: a meta-analysis of 15 N tracer field studies. Ecology 93(8): 1816–1829. doi:10.1890/11-1146.1.

Throop, H.L., Archer, S.R., Monger, H.C., and Waltman, S. 2012. When bulk density methods matter: Implications for estimating soil organic carbon pools in rocky soils. Journal of Arid Environments 77: 66–71. doi:10.1016/j.jaridenv.2011.08.020.

Turner, M.G., Smithwick, E.A.H., Metzger, K.L., Tinker, D.B., and Romme, W.H. 2007. Inorganic nitrogen availability after severe stand-replacing fire in the Greater Yellowstone ecosystem. Proceedings of the National Academy of Sciences 104(12): 4782–4789. doi:10.1073/pnas.0700180104.

Turner, M.G., Whitby, T.G., and Romme, W.H. 2019. Feast not famine: Nitrogen pools recover rapidly in 25-yr-old postfire lodgepole pine. Ecology 100(3): e02626. doi:10.1002/ecy.2626.

Vitousek, P.M., and Reiners, W.A. 1975. Ecosystem Succession and Nutrient Retention: A Hypothesis. BioScience 25(6): 376–381. doi:10.2307/1297148.

CHAPTER 3: SOIL C STORAGE FOLLOWING SALVAGE LOGGING AND RESIDUE MANAGEMENT IN BARK BEETLE-INFESTED LODGEPOLE PINE FORESTS[1]

3.1. Introduction

Widespread mortality of lodgepole pine (*Pinus contorta* var. *latifolia* Engelm. ex Wats.) in the Rocky Mountain region of western North America due to a climate-driven outbreak of the endemic mountain pine beetle (MPB; *Dendroctonus ponderosae* Hopkins) has significantly altered ecosystem carbon (C) dynamics (Edburg et al., 2011; Hansen, 2014). During the most recent outbreak, bark beetles killed 70% or more of the lodgepole pine overstory basal area in many Colorado forests (Collins et al., 2011; Klutsch et al., 2009). Clear cut salvage logging of MPB-infested lodgepole pine stands has taken place in Colorado (Collins et al., 2010) and across western North America to reduce fuel loads and wildfire risk, reduce treefall hazards, recover the economic value of the timber, and regenerate new forests. Post-beetle salvage has the potential to increase C captured within rapidly growing young forests and store it in timber and other wood products (Malmsheimer et al., 2011). Yet, a recent systematic map of primary studies evaluating post-disturbance salvage logging cited 51 publications on post-wildfire salvage, 26 publications on post-wind salvage and only 13 publications on post-insect salvage, less than a quarter of the cited studies (Leverkus et al., 2018). Studies following this most recent MPB outbreak are starting to fill this gap in understanding and have found that salvage logging reduces canopy fuels and wildfire risk, and regenerates new trees without negatively effecting plant diversity or soil nitrogen availability (Collins et al., 2012, 2011; Fornwalt et al., 2018; Griffin et al., 2013; Hood et al.,

[1] Avera, B.N., Rhoades, C.C., Calderón, F., and Cotrufo, M.F. 2020. Soil C storage following salvage logging and residue management in bark beetle-infested lodgepole pine forests. Forest Ecology and Management, 472(15):118251.

2017; Rhoades et al., 2018, 2020a); however, none of the aforementioned studies directly evaluated changes to forest soil C.

Soils store half of the C in forest ecosystems of the conterminous U.S. (Turner et al., 1995), totaling approximately 13-28 Pg of soil organic C (Lajtha et al., 2018). Following the MPB-outbreak in Colorado, upper mineral soil (0-5 cm) % C declined by 38-49% under beetle-killed lodgepole pine compared to live, green trees at Niwot Ridge Long-Term Ecological Research site, which the authors attributed to declines in C inputs to the rhizosphere (Xiong et al., 2011). This finding supported initial model-based predictions that decreases in net primary production (NPP) due to tree mortality would convert infested stands into net sources of atmospheric C due to reduced new C inputs, respiration during decomposition and salvage logging (Kurz et al., 2008). However, other studies have documented the recovery of NPP and net ecosystem production within 4-7 years following MPB (Brown et al., 2010, 2012) due to the increased photosynthetic activity and C uptake of residual vegetation (Bowler et al., 2012; Romme et al., 1986). Compensatory increases in C uptake by understory vegetation, new recruits or residual trees were not accounted for in the Kurz et al. (2008) model. Salvage logging increases new seedling establishment and growth of residual trees, though it reduces understory plant cover in beetle-killed Colorado forests (Collins et al., 2012; Fornwalt et al., 2018). Changes in soil C quality have also been detected in Colorado in MPB-infested stands. Brouillard et al. (2017) reported lower soil C to nitrogen (N) ratios and increased aromaticity under MPB-killed lodgepole compared to green trees. The quality and distribution of soil C among soil organic matter (SOM) fractions may also be vulnerable to post-bark beetle salvage logging or other management (Lajtha et al., 2018) with implications for function, mechanisms of C persistence and turnover times (Christensen, 2001; von Lützow et al., 2008).

Forest soil C is distributed vertically with an accumulation of surface organic inputs forming the O horizon above the mineral soil. While C concentrations are highest in the O horizon, the majority of C in temperate forest systems is stored in the upper 100 cm of the mineral profile as a component of soil

organic matter (SOM) (Nave et al., 2010; Shaw et al., 2008). SOM can be separated based on size and/or density into particulate (POM) and mineral-associated organic matter (MAOM) fractions with different chemical properties and potential turnover times (Christensen, 2001; Lavallee et al., 2020; Sollins et al., 2006). Forest soils typically store a high proportion of soil C (i.e., ≥60%) as light POM (<1.85 g cm^{-3}) (Cotrufo et al., 2019; Denef et al., 2013; Sollins et al., 2006), characterized by structural plant residues with a high C:N ratio that have undergone little decomposition (Golchin et al., 1994; Gregorich et al., 2006). Light POM is formed through fragmentation and physical transfer of above or belowground plant C inputs (Cotrufo et al., 2015; Haddix et al., 2016). Microbial processing of plant residues and light POM mineralizes much of the C, with some of the residual C forming sand-sized heavy POM (>1.85 g cm^{-3} and >53 µm) (Grandy and Neff, 2008). In contrast to the POM fractions, MAOM (>1.85 g cm^{-3} and <53 µm) is thought to form from soluble compounds entering the mineral soil through root exudation, leaching from plant residues or from products of microbial transformation (Cotrufo et al., 2015; Liang et al., 2017; Sokol et al., 2019). The efficiency of SOM formation and distribution of C among SOM fractions is controlled by the chemistry and physical structure of the plant C inputs (Cotrufo et al., 2015, 2013; Haddix et al., 2016). While the chemical recalcitrance of the POM fractions may slow their decomposition, inaccessibility to microorganisms through protection within aggregates or mineral association are the most important mechanisms for stabilizing soil C (Lehmann and Kleber, 2015; Mikutta et al., 2006; Sollins et al., 2006). Formation of MAOM requires silt and clay particles and may be limited in forest soils with coarse texture and recalcitrant litter (Cotrufo et al., 2013).

Clear cut salvage logging and residue management may alter forest soil C through changing the microclimate and the quantity and type of plant C inputs contributing to the O horizon and available for mineral POM and MAOM formation. Changes in microclimate and microbial controls on decomposition—temperature, moisture and nitrogen availability—have been well studied (e.g., Prescott, 2010, 1997; Smolander et al., 2008). Overall, long-term changes in soil C stocks in response to

logging and residue management depend on the balance of soil C loss due to logging and the formation of new SOM, particularly MAOM, from the decaying residues and live plant inputs. A global meta-analysis found that forest harvesting decreased C storage in the O horizons of coniferous and mixed coniferous and broadleaf forests by 20% on average, but that changes within mineral soils were relatively minor (Nave et al., 2010). Site conditions, post-harvest site preparation, logging residue (e.g. slash) prescriptions influence whether O horizon C increases, decreases, or is unchanged (Johnson and Curtis, 2001). Many factors influence the amount of surface detritus contributing to the O horizon in both the uncut and salvage logged stands. In uncut stands, needles are shed 3-5 years following MPB-infestation, slowly contributing fine residues to the O horizon (Hicke et al., 2012; Schoennagel et al., 2012; Simard et al., 2011). In salvage logged stands, shatter of dry, MPB-killed tree crowns during felling increases foliage and branch residue inputs within the harvest unit, regardless of slash prescription. Soil C stocks might be most responsive to changes in the inputs of smaller residues in the first few decades following MPB infestation and salvage logging. Less than 20% of snags have fallen in the first decade following the beetle outbreak in Colorado (Rhoades et al., 2020b) and large diameter woody material decompose on the order of a century (Brown et al., 1998; Busse, 1994; Fahey, 1983), thus C inputs from snags and large woody residues are likely to have small contributions to soil C stocks early in the decomposition process.

This study documents changes in forest soil C following salvage logging and residue management of MPB-infested lodgepole pine forests. We sought to characterize how forest harvest and residue management impacted (1) forest soil C stocks, (2) its distribution, between the O horizon and the upper 10 cm of mineral soil, and among light and heavy POM and MAOM fractions, and (3) forest soil C chemistry. To address these objectives, we studied three management treatments: (1) uncut beetle-infested lodgepole pine forest and, adjacent areas that were clear cut salvage logged with either woody residue (2) retention or (3) removal. We quantified C stocks in the O horizon, bulk mineral soil

and mineral SOM fractions and characterized C chemistry using Fourier transformed mid-infrared spectroscopy (FTIR) and stable isotope analysis. We expected the O horizon and light POM to be the most responsive to surface residue manipulations (Bowden et al., 2014; Crow et al., 2009a; Lajtha et al., 2014), increasing in proportion to the woody residue load. Further, we expected that the O horizon and the light POM would be more chemically recalcitrant due to the contribution from woody inputs.

3.2. Materials and Methods

3.2.1. Experimental management area description and design

This study was conducted at four MPB management areas in northern Colorado on the Arapaho-Roosevelt National Forest (Fraser Experimental Forest; 'Fraser' hereafter), the Medicine Bow-Routt National Forest (Gore Pass and Willow Creek), and the Colorado State Forest State Park (State Forest). At all sites, lodgepole pine is dominant on lower elevations and drier, southern aspects (Alexander and Watkins, 1977), comprising 70 to >90% of the overstory cover (Collins et al., 2012, 2011). Other species include Engelmann spruce (*Picea engelmanni*), subalpine fir (*Abies lasiocarpa*), and Quaking aspen (*Populus tremuloides*). Bark beetle activity began in the region between 1998 and 2002, peaked between 2006 and 2009 and caused 79-91% mortality of lodgepole pine basal area (Collins et al., 2012). The management areas have a mean elevation range of 2750 to 2850 m (Fornwalt et al., 2018) and a continental climate with mean annual precipitation ranging from 544-687 mm and mean annual temperature ranging from 1.8-2.7°C (PRISM Climate Group, 2017).

The respective management agency at each of the four management areas determined where the harvest units were located. Three replicate blocks were established at each of the four management areas during summer 2009. Pre-harvest stand exams (USFS Region 2 and Colorado State Forest Service, unpublished records) and stand inventories of uncut areas (Collins et al., 2012, 2011) were used to identify paired uncut and salvage logged areas within each management area to establish the block

locations to minimize differences between treatments due to location of the harvested areas. Further, the uncut and salvage logged areas were located $\leq$ 400 m from each other on similar aspects and slopes (Collins et al., 2012) to achieve this goal. The three treatments were (1) uncut control, (2) clear cut salvage-logged with logging residue retention ('retention' hereafter), and (3) clear cut salvage-logged with logging residue removal ('removal' hereafter) (Fornwalt et al., 2018). Salvage-logged treatments were randomly assigned to treatment plots located adjacent to each other with a 10 m buffer between plots (Fornwalt et al., 2018) to reduce the variability between the salvage logged plots as much as possible so that the main difference was the application of the logging residues. Clear cut salvage logging coincided with the peak of the outbreak in northern Colorado (Fraser: winter 2007-2008; Other Areas: winter 2008-2009). Logging operations were restricted to times with dry or frozen soils or >1 m of snow to minimize soil disturbance (Collins et al., 2011). Each treatment was applied to a 30 x 30 m (900 m^2) area containing a 20 x 20 m (400 m^2) sampling plot. Logged areas were first whole-tree harvested (i.e., removal) and then experimental logging residue treatments (e.g., retention) were established in in 2009 by returning slash to the plots (Fornwalt et al., 2018).

3.2.2. O horizon and mineral soil sampling and processing

The O horizon and upper mineral soil (0-10 cm) were sampled in fall 2015. For this sampling each research plot was divided into four 10 x 10 m quadrants then the O horizon and upper mineral soil were sampled from the center of three quadrants. O horizon samples were collected from a 15 x 15 cm sample frame. A knife was used to separate the O horizon and a plastic scoop was used to collect the sample. All three O horizon samples from each plot were composited in the field and were transported on ice and stored at 4°C until processing. The composited samples were air-dried and sieved into three size classes: large residues (>8 mm), fine residues (2-8 mm), and organic material (<2 mm). Large residues were comprised of identifiable plant tissues including twigs, cones and needles and most closely resembled the litter or Oi horizon. The fine residues consisted of decomposing wood, needle

fragments and portions of cones and resembled the Oe horizon. The organic material resembled the Oa horizon and contained uniform, highly decomposed matter. The O horizon size classes were oven dried to a constant mass at 60°C, dry weight was recorded, and a representative subsample was finely ground on a Wiley-Mill (Model No. 3, Arthur H. Thomas Co., Philadelphia, USA) prior to further analysis.

After O horizon sampling, two, 10 cm deep mineral soil samples were collected from each of the three quadrants from the same location where the O horizon was sampled using a 5 cm diameter core (Giddings Machine Company, Windsor, CO, USA) for a total of 216 soil cores which were composited in the field at the plot level. Mineral soils were then transported on ice and stored at 4°C until processing. Mineral soils were sieved to 2 mm and air-dried. One subsample of the mineral soil was used for SOM physical fractionation and another was ground to a fine powder using a roller-mill, dried at 105°C and used for total soil C and $\delta^{13}C$ (Mosier et al., 2019).

Soil bulk density was measured by pit excavation due to the rockiness of the soils (Page-Dumroese et al., 1999). Three pits were dug within the uncut and salvage logged areas of each block, outside of the sampling plots, then the total volume of the excavated soil pit was measured using millet (Boot et al., 2015). The soil excavated from each pit was brought back to the lab, air-dried and 2 mm sieved to separate the coarse fraction (>2 mm) from the soil fraction (<2 mm). The mass of the soil fraction was weighed after sieving and a ~5g subsample was dried at 105°C to apply an air-dry to oven-dry moisture correction. Bulk density for each pit was calculated using the hybrid approach of Throop et al. (2012) using the oven-dry mass of the soil fraction divided by the volume of the entire pit. Soil texture was analyzed using the hydrometer method (Gee and Bauder, 1986).

We utilized a physical fractionation scheme to separate the SOM into two uncomplexed POM fractions: light (<1.85 g cm^{-3}) and sand-sized heavy POM (>1.85 g cm^{-3} and >53 µm); and fine MAOM (>1.85 g cm^{-3} and <53 µm) (Christensen, 2001; Lavallee et al., 2020; Mosier et al., 2019). A 5 g oven-dry

subsample of each bulk soil sample was shaken for 18 h with 25 mL of 0.5% sodium hexametaphosphate (Na-HMP) and glass beads to disperse aggregates. After dispersion, centrifuge tubes were filled to 30 mL with 1.85 g cm^{-3} sodium polytungstate (SPT) (~25 mL SPT) and samples were centrifuged for 60 minutes at 2500 rpm to separate the light POM. Light POM was aspirated and filtered using a 20 µm Millipore glass filter, rinsed clean of SPT, and dried at 60°C. The remaining fractions were rinsed 3 times with DI water to remove SPT, then wet sieved through a 53 µm sieve to separate heavy POM from silt and clay sized MAOM. Fractions were rinsed into pre-weighed aluminum pans, dried at 60°C for two days, and weighed. Mass recovery was calculated by the difference between the starting soil weight and the combined weight of all fractions, with an accepted recovery of 100±5%. All dried fractions were ground to a fine powder using a mortar and pestle.

3.2.3. O horizon and mineral soil analyses

A subsample of each of the O horizon size classes, bulk mineral soil and mineral SOM fractions (light and heavy POM and MAOM) were analyzed for %C, %N, and $\delta^{13}C$ on an elemental analyzer (Costech ECS 4010, Costech Analytical Technologies, Valencia, CA, USA) coupled to an isotope ratio mass spectrometer (Delta V Advantage IRMS, Thermo-Fisher, Bremen, Germany). The analytical precision of the internal laboratory standards was <0.2‰ for $\delta^{13}C$. Additionally, the O horizon size classes and mineral SOM fractions were scanned for Fourier-transform infrared spectroscopy analysis (FTIR) on a Digilab FTS 700 Fourier transform spectrometer (Varian, Inc., Palo Alto, CA) with a deuterated, Peltier-cooled, triglycine sulfate detector and potassium bromide beam splitter and fitted with a Pike AutoDiFF diffuse reflectance accessory (Pike Technologies, Madison, WI). Potassium bromide was used as background. Spectra were collected at 4 cm^{-1} resolution, with 64 co-added scans per spectrum from 4000 to 400 cm^{-1}. Spectra were obtained as pseudo-absorbance (log[1/Reflectance]) in the method of Calderón et al. (2011). Two subsamples were scanned separately then averaged before statistical analyses and subtractions.

3.2.4. Data analyses

Linear mixed models using *lmer* and the R packages *lme4*, lmerTEST, and lsmeans (Bates et al., 2015; R Core Team, 2019) were used to test for the effect of treatment on the C stocks, C:N ratio, and $\delta^{13}C$ of the O horizon size classes and SOM fractions, and bulk density, % C, and C stocks of the bulk mineral soil. For all models, treatment was classified as a fixed effect. Management area and blocks nested within management area were classified as random effects. For bulk density there were just two treatments, uncut and salvage logged, while the other variables had all three treatments of uncut control and logged with residue retention and removal. For C:N ratio and $\delta^{13}C$, fraction (in this case the O horizon size classes and SOM fractions) was also included as a fixed effect. The interaction of treatment and fraction was not of interest for either variable, so it was dropped from both models due to non-significance. Data that were not normally distributed were first log transformed. Models were evaluated using analysis of variance using a significant alpha level at p=0.10 (Crow et al., 2009b) followed by Tukey-adjusted pairwise comparisons.

Principle component analysis (PCA) of the FTIR spectra was used to visualize differences between the forest management treatments, O horizon size classes, and SOM fractions in Unscrambler® X version 10.4 (CAMO, Oslo, Norway). Statistical assessment of differences among FTIR spectra as a function of fraction and treatment were tested with the permutational multivariate analysis of variance (PERMANOVA) ADONIS method in R using the vegan package using a Euclidean distance metric and 999 permutations (Oksanen et al., 2019) and pairwise comparisons were evaluated in PAST with Bonferroni adjustment (Hammer et al., 2001). All FTIR spectra were mean-centered prior to statistical analysis. Spectral averages and subtractions were carried out using Grams A/I version 9.3 (Thermo Fischer Scientific, Massachusetts, USA), using the default autoscale, optimal factor, and tolerance values suggested by the program.

We calculated minimum detectable differences (MDD) between our uncut and logged treatments for the C fractions contained in the O horizon and upper mineral soil using the following paired sample equation (Schöning et al., 2006):

$$MDD \geq \sqrt{\frac{s^2}{n}}(t_{\alpha(2),v} + t_{\beta(1),v})^2$$

where the variables were the pooled variance (s^2), sample size (n) and degrees of freedom (v). We assigned a significance level (α) of 0.10, consistent with the rest of our study, and a statistical power ($1-\beta$) of 0.80 to the *t*-statistic (t). We calculated the percentage change needed to conclude that logged and uncut C stocks differed as follows:

$$MDD\ \% = \frac{MDD}{\bar{x}} \times 100\%$$

where $\bar{x}$ is the mean value of the uncut treatment for a specific C stock.

3.3. Results

3.3.1. O horizon carbon stocks

The C stock of the large residues (>8 mm) differed with treatment (*F(2, 22)*=4.27, *p*=0.03). The C stock in the large residues of the retention treatment was more than double that of the uncut control (Tukey's pairwise comparison, *p*=0.02) but not different than the residue removal treatment (Tukey's pairwise comparison, *p*=0.14; Fig. 3.1). There was a non-significant trend of highest C in the retention treatment for the fine residues (2-8 mm) (*F(2, 22)*=1.19, *p*=0.32) and no differences in the organic material (<2 mm) (*F(2, 22)*=0.24, *p* =0.79; Fig. 3.1). The MDD % needed to conclude treatment differences for fine residues and organic material were ≥95% and ≥102%, yet we measured 55% and 38% differences respectively. The mean total Mg C ha^{-1} (± 1 standard error) in the three O horizon size classes was 12.1 (1.80) for the uncut, 20.6 (3.83) for the retention and 14.8 (4.44) for the removal with

no treatment effect (*F(2, 22)*=1.44, *p*=0.26). The MDD % for the total O horizon was ≥90% and the measured difference was ~71%.

3.3.2. Mineral soil C stocks and distribution among physically-defined SOM fractions

Both soil bulk density and bulk soil C concentration (%C) had a non-significant trend of increase with salvage logging and residue removal (Table 3.1), resulting in differences in bulk soil C stocks between treatments (*F(2, 22)*=3.10, *p*=0.07; Fig. 3.1). Pairwise comparisons showed that removal had the most upper mineral soil C (0-10 cm) with a mean increase of 8.5 (4.1) Mg ha^{-1} (± 1 standard error) more C than the uncut control, a 34% difference (Tukey's pairwise comparison, *p*=0.05; Fig 3.1). This analysis had a power (1-β) of 0.42 and the MDD calculations showed that a ≥59% difference was required to have 0.80 power or higher. Larger post-harvest upper mineral soil C stocks were driven by larger POM fractions relative to the uncut control (Fig. 3.2). However, only the heavy POM C stocks differed with treatment (*F(2, 22)*=4.63, *p*=0.02) and pairwise comparison showed that the removal treatment more C in heavy POM than the other two treatments (Tukey's pairwise comparison, *p*=0.02; Fig. 3.2). The measured difference in light POM between the uncut and removal treatments was 39%; to detect differences in that fraction our MDD analysis indicated that differences ≥75% would have been required. Independent of treatment, light POM was the largest soil C pool with approximately seven times more C than heavy POM, three times more C than MAOM and ~63% of total upper mineral soil C.

3.3.3. Soil C:N ratios, C chemistry, and ^{13}C

Overall, C:N ratios ranged from an average of 96.1 in large residues to an average of 14.2 in MAOM (Table 3.2). C:N ratios differed among fractions but not treatments (Table 3.3). The C:N ratio of each fraction was different from all others (Tukey's pairwise comparison, *p*<0.0001) except for the fine residues and light POM (Tukey's pairwise comparison, *p*=0.44). C:N ratio did not differ with treatment

for the bulk soil (*F(2, 22)*=0.08, *p*=0.93) and across all plots the mean C:N ratio (± 1 standard error) was 26.37 (0.55).

The $\delta^{13}C$ signature differed among fractions and treatments (Table 3.3). The large residues and mineral SOM fractions were significantly less depleted in ^{13}C than fine residues and organic material (Tukey's pairwise comparison, $p<0.0001$) and the organic material was also depleted relative to the fine residues (Tukey's pairwise comparison, $p=0.08$; Fig. 3.3). The MAOM fraction had the highest ^{13}C enrichment (Tukey's pairwise comparison, $p\leq0.01$). The retention treatment was depleted in ^{13}C in all fractions relative to the uncut (Tukey's pairwise comparison, $p<0.004$). Across fractions the removal treatment was not consistently enriched or depleted in ^{13}C relative to the retention or uncut treatment and thus the $\delta^{13}C$ of the removal did not differ from either treatment (removal-uncut Tukey's pairwise comparison, $p=0.24$; removal-retention Tukey's pairwise comparison, p=0.23).

PCA analysis of the FTIR spectra showed compositional differences among the O horizon and mineral SOM fractions. PERMANOVA showed that the spectra differed by fraction (*F(7, 244)*=261.52, *p*=0.001) as of all O horizon size classes and mineral SOM fractions were different from one another (Bonferroni corrected *p*=0.002), except for the large and fine residues (Bonferroni corrected *p*=0.48). There were no treatment effects (*F(2, 249)*=0.05, *p*=0.996), therefore, we averaged all FTIR spectra of the organic material and light POM and used spectral subtraction to help elucidate the unexpected C:N and $\delta^{13}C$ differences between these two fractions. The spectral subtraction showed that the organic material had different features than the light POM, in particular more amines and O-H functional groups (3400 cm^{-1}), aliphatics (2920-2850 cm^{-1}), esters (1750 cm^{-1}), amides (1750 cm^{-1}), and aromatic C=C (1515 cm^{-1}) (Fig. 3.4).

3.4. Discussion

Salvage logging MPB-killed lodgepole pine in Colorado has the potential to alter forest soil C by

removing C as tree biomass, transferring residue C to the soil surface where it may be more readily decomposed and altering root inputs and decomposition dynamics. Six to seven years following harvest, C stored in the O horizon and upper mineral soil was 11.4 (5.6) Mg C ha^{-1} higher on average in salvage-logged areas compared to uncut stands. Retention of large diameter woody residues (>7.62 cm) added 8.6 Mg C ha^{-1} to the O horizon compared to the uncut, equivalent to 41% more C (Table 3.1). But surprisingly, differences in upper mineral soil C did not parallel the treatment effects on C in woody residues or the O horizon and it was the residue removal treatment that had more upper mineral soil C compared to the uncut, a difference of 8.5 (4.1) Mg C ha^{-1} (Fig. 3.1; Table 3.1).

Studies of the effects of salvage logging on soil C following pest infestations are limited. The findings of this study are notable because they suggest that the MPB-infested lodgepole pine forests of Colorado can be salvage logged with a low risk of significant soil C loss. The differences in upper mineral soil C we measured were the result of modest differences in both soil bulk density and C concentration with salvage logging (Fig. 3.1; Table 3.1) and fell short of the 59% MDD needed to maintain power of 0.80. We suggest that the higher upper mineral soil C with post-beetle salvage logging can be attributed to direct inputs from surface organic matter in the cut areas through mixing of O horizon and harvest residues into the upper mineral soil by tracked equipment during logging operations (Rhoades et al., 2020a; Yanai et al., 2003). Mixing in of the surface organic matter during logging is supported by reduced O horizon cover and increased mineral soil exposure reported at these sites and nearby comparisons of cut and uncut beetle-killed lodgepole stands (Fornwalt et al., 2018; Rhoades et al., 2018; Rhoades, 2019). Mayer et al. (2020) concluded that soil C losses following clear cut harvesting are most closely tied to reduced litter C inputs and/or increased decomposition. Despite reduced cover of O horizon, the O horizon C stock was unchanged or increased in these dry, high elevation salvage logged areas and our data did not indicate that there was an increase in decomposition.

The chemical composition and $\delta^{13}C$ results show a decoupling of O horizon C from upper mineral

soil C and supports the idea that belowground C inputs are a dominant source of mineral soil C and in particular to POM (Bird et al., 2008; Fulton-Smith and Cotrufo, 2019; Puget and Drinkwater, 2001). The C:N of the light POM (39.7 ± 0.9) was higher than the organic material (28.8 ± 0.7) across all treatments, indicating that the light POM is less decomposed than the organic material (Table 3.2). Additionally, ^{13}C became ~1‰ more depleted moving from large residue litter to organic material (Fig. 3.3). In pine forests, needles and woody residues are high in lignin and lipids, which are 2-3‰ and ~4‰ depleted in ^{13}C, respectively, relative to bulk leaf tissue due to positional isotope effects (Bowling et al., 2008; Gleixner et al., 1993). Accumulation of lignin-derived C in fine residues and organic material would explain why the O horizon became depleted in ^{13}C with decomposition, and is consistent with higher abundance (e.g., absorbance) of aromatic C=C compounds on the mid-IR FTIR spectra of the organic material compared to the light POM (Fig. 3.4). Additionally, the spectral subtraction of the organic material and light POM FTIR spectra showed that the organic material had more microbial products with higher absorbance of aliphatic C-H and amide functional groups than the light POM (Fig. 3.4).

Chemical recalcitrance of the structural inputs contributing to light POM, results in POM decomposition and transformation on a yearly to decadal time frame . In these medium- to coarse-textured soils the two POM fractions together accounted for 76.7% of the C in the upper mineral soil (ranging from 65-95%) (Fig. 3.2), with the most C stored in the light POM fraction (63%). This finding is not surprising as coarse-textured forest soils with poor litter quality inputs will inherently have limited capacity to accumulate MAOM (Cotrufo et al., 2013). Yet, the importance of the POM fractions to maintaining the total soil C stock in this system, highlights the need to better understand what the dominant C inputs contributing to POM are and what management practices help build and preserve POM.

3.4.1 Conclusions and management implications

A better mechanistic understanding of how salvage logging and residue management alter SOM fractions will help guide management aimed at maintaining soil C stocks. We found that salvage logging with slash removal did not reduce soil C, instead upper mineral soil C was highest in this treatment. The C:N ratio, $\delta^{13}C$ and FTIR analyses of O horizon and upper mineral soil layers indicate that these two C stocks are likely derived from distinct organic matter sources. These results show the utility of separating SOM into POM and MAOM to identify differences in soil C stocks and chemical composition (Lavallee et al., 2020). Future studies that aim to link the manipulation of C inputs to changes in forest soil C stocks should attempt to quantify the contribution of various types of C inputs (e.g., aboveground litter, root residues, rhizodeposition) to each forest soil C pool. Within forest types that store a high percentage of the total soil C as POM, this pool should be the area of focus and further evaluation of the sensitivity of POM to disturbance and the ecosystem response will better inform system response to forest management.

Table 3.1 Bulk mineral soil characteristics (0-10 cm) of the four management areas of the study including soil texture, bulk density, and soil C concentration (%C), and the C stock of the woody residues (>7.62 cm) on the surface after treatment application. Data are means followed by the standard error (± 1 S.E.) in parentheses (n=3). Linear mixed model results for bulk density, soil C concentration and woody residue C stocks using the predictor effect treatment. Effects with $p < 0.05$ are emphasized in bold (n=12).

Management Area	Treatment	Soil Texture (% sand, % silt, % clay)	Bulk Density ($g\ cm^{-3}$)	Soil C Concentration (%C)	Woody Residue C Stocks ($Mg\ C\ ha^{-1}$)*
Fraser	Uncut	43, 40, 17	0.65 (0.06)	4.04 (0.88)	3.48 (1.82)
	Retention	52, 34, 14	0.73 (0.02)	3.63 (0.64)	21.88 (2.20)
	Removal	48, 38, 14		4.80 (0.42)	7.72 (0.52)
Gore Pass	Uncut	57, 33, 10	0.94 (0.07)	3.34 (0.54)	4.16 (2.48)
	Retention	60, 29, 11	0.77 (0.02)	4.60 (0.46)	16.28 (1.00)
	Removal	58, 32, 10		5.03 (1.25)	3.57 (1.32)
State Forest	Uncut	56, 36, 8	0.75 (0.03)	4.06 (0.96)	0.48 (0.27)
	Retention	47, 43, 10	0.93 (0.09)	4.28 (0.63)	27.54 (3.00)
	Removal	51, 39, 10		5.54 (2.05)	3.68 (0.78)
Willow Creek	Uncut	68, 24, 8	0.67 (0.03)	1.81 (0.26)	3.71 (1.79)
	Retention	72, 22, 6	0.79 (0.07)	1.53 (0.32)	23.76 (1.70)
	Removal	74, 21, 5		1.72 (0.22)	1.26 (0.39)

Model results				
	Num DF	1	2	2
	Den DF	11	22	22
	F value	0.56	1.466	97.514
	Pr > F	0.47	0.25	**<0.0001**

* The values were calculated by multiplying the loads (Mg ha^{-1}) of large diameter (>7.62 cm) downed wood and logging residues by 0.5 to convert to C stock (Mg C ha^{-1}). The loads of woody residues were estimated in 2010 along two, 20-m planar intercept transects in each plot and summed across decay classes and are derived from Collins et al. (2012).

Table 3.2 C:N ratio of the O horizon size classes and mineral SOM fractions for the uncut control and salvage logged plots with residue retention or removal. Data are means followed by the standard error (± 1 S.E.) in parentheses (n=12). The C:N ratio did not differ with treatment for any of the fractions.

	O Horizon C:N		
	Uncut	Retention	Removal
Large residues (>8 mm)	100.10 (11. 5)	89.01 (6.8)	99.15 (10.1)
Fine residues (2-8 mm)	41.86 (2.0)	44.33 (3.0)	46.10 (2.7)
Organic material (< 2mm)	28.31 (0.9)	29.05 (1.7)	28.97 (1.0)
	Mineral Soil (0-10cm) C:N		
Light POM (<1.85 g cm^{-3})	41.15 (2.0)	40.09 (1.9)	37.97 (0.8)
Heavy POM (> 53 µm)	18.86 (1.5)	19.72 (1.7)	22.35 (1.3)
MAOM (< 53 µm)	13.72 (0.6)	13.93 (0.5)	14.49 (0.7)

Table 3.3 Linear mixed model results for C:N ratio and $\delta^{13}C$ using the predictor effects treatment and fraction. In this analysis fraction included all the O horizon size classes and SOM fractions. Effects with $p < 0.05$ are emphasized in bold (n=12).

Effect	C:N				$\delta^{13}C$			
	Num DF	Den DF	F value	Pr>F	Num DF	Den DF	F value	Pr>F
Fraction	5	197	326.15	**<0.0001**	5	196.02	80.94	**<0.0001**
Treatment	2	197	0.97	0.38	2	196.02	5.25	**0.006**

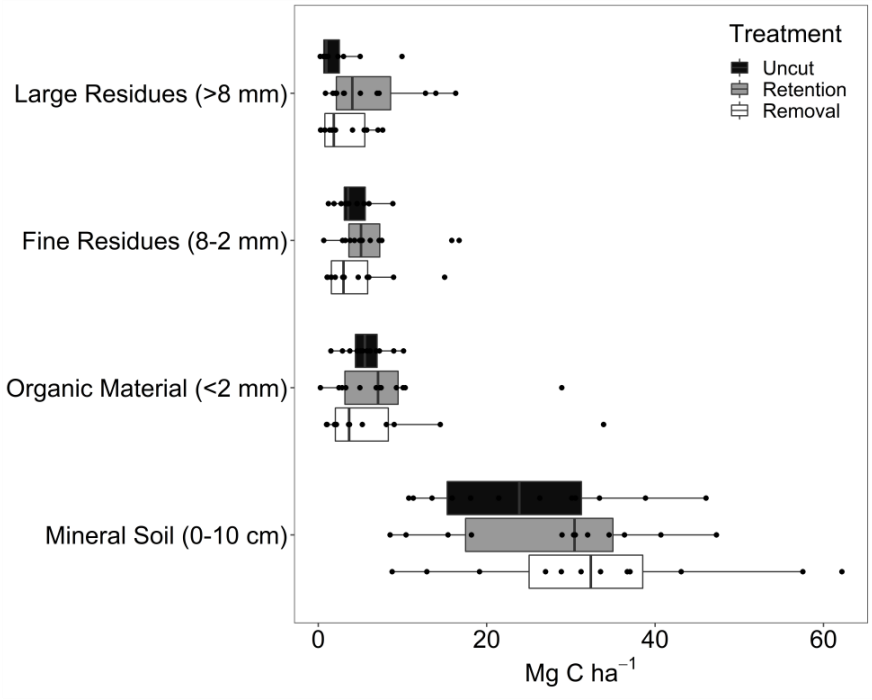

Figure 3.1 Carbon stocks (Mg C ha^{-1}) on the soil surface in the large and fine O horizon size classes, organic material, and in the bulk mineral soil for the uncut control and salvage logged plots with residue retention or removal. Black dots represent the individual raw data points (n=12).

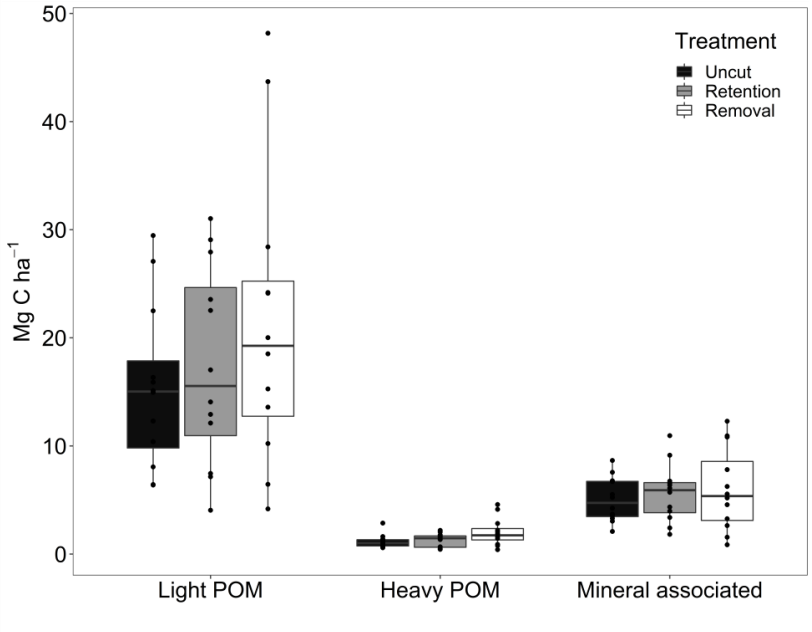

Figure 3.2 Carbon stocks (Mg C ha^{-1}) in the measured SOM fractions, light particulate organic matter (POM; <1.85 g cm^{-3}), heavy POM (>1.85 g cm^{-3}, >53 µm) and mineral-associated organic matter (>1.85 g cm^{-3}, <53 µm), for the uncut control and salvage logged plots with residue retention or removal. Black dots represent the individual raw data points (n=12).

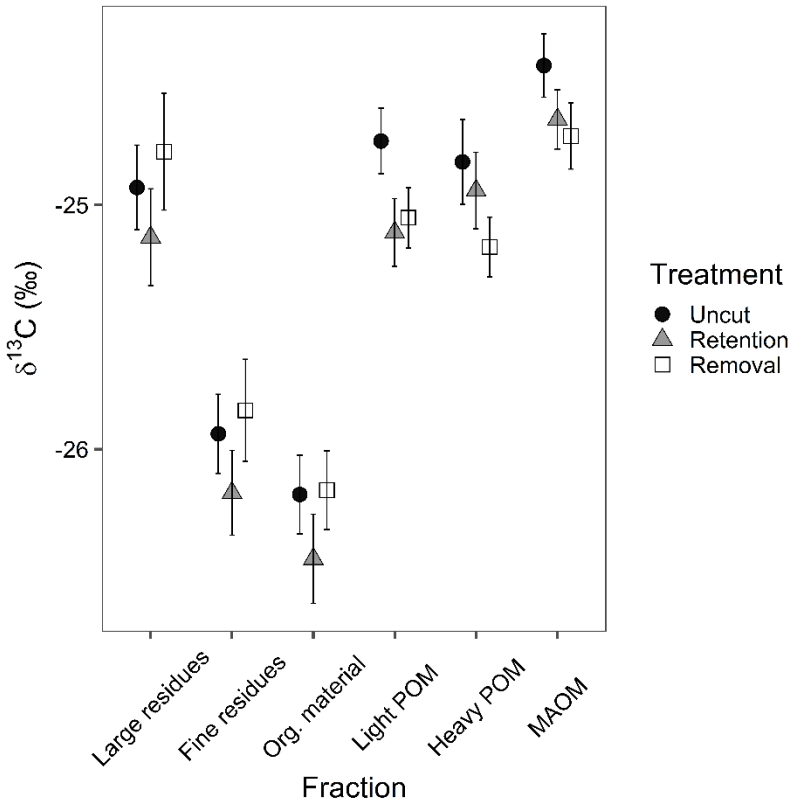

Figure 3.3 $\delta^{13}C$ of each O horizon size class and mineral SOM fraction by treatment for the uncut control and salvage logged plots with residue retention or removal. Data are means with standard errors (n=12).

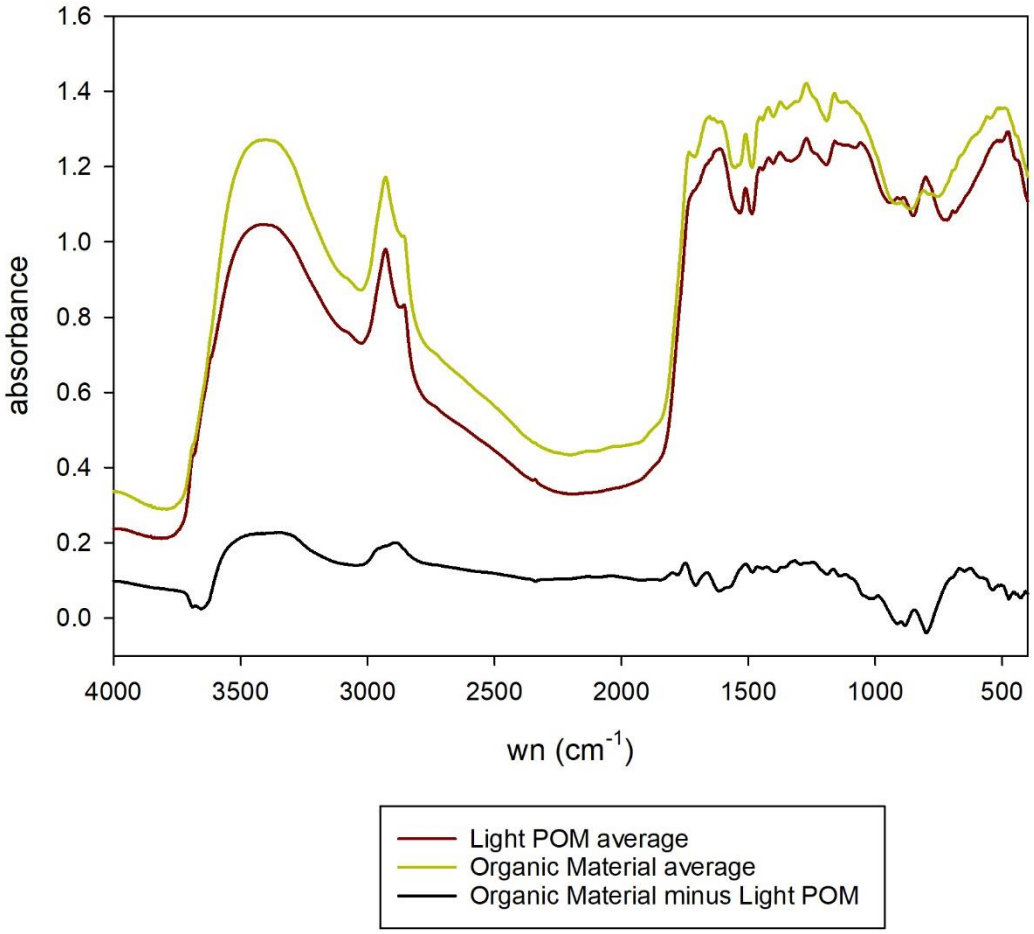

Figure 3.4 Mid-infrared FTIR spectra averaged across management area and treatment of the organic material of the O horizon and light particulate organic matter (POM) fraction of the mineral SOM and the spectral subtraction of the organic material minus the light POM. Absorbance is unitless and upward peaks in the subtraction denote bands that were more abundant in the organic material.

REFERENCES

Alexander, R.R., Watkins, R.K., 1977. The Fraser Experimental Forest, Colorado (No. General Technical Report RM-40). USDA Forest Service.

Bates, D., Maechler, M., Bolker, B., Walter, S., 2015. Fitting Linear Mixed-Effects Models Using lme4.

Bird, J.A., Kleber, M., Torn, M.S., 2008. ^{13}C and ^{15}N stabilization dynamics in soil organic matter fractions during needle and fine root decomposition. Organic Geochemistry 39, 465–477. https://doi.org/10.1016/j.orggeochem.2007.12.003

Boot, C.M., Haddix, M., Paustian, K., Cotrufo, M.F., 2015. Distribution of black carbon in ponderosa pine forest floor and soils following the High Park wildfire. Biogeosciences 12, 3029–3039. https://doi.org/10.5194/bg-12-3029-2015

Bowden, R.D., Deem, L., Plante, A.F., Peltre, C., Nadelhoffer, K., Lajtha, K., 2014. Litter input controls on soil carbon in a temperate deciduous forest. Soil Science Society of America Journal 78, S66. https://doi.org/10.2136/sssaj2013.09.0413nafsc

Bowler, R., Fredeen, A.L., Brown, M., Andrew Black, T., 2012. Residual vegetation importance to net CO_2 uptake in pine-dominated stands following mountain pine beetle attack in British Columbia, Canada. Forest Ecology and Management 269, 82–91. https://doi.org/10.1016/j.foreco.2011.12.011

Bowling, D.R., Pataki, D.E., Randerson, J.T., 2008. Carbon isotopes in terrestrial ecosystem pools and CO_2 fluxes. New Phytol 178, 24–40. https://doi.org/10.1111/j.1469-8137.2007.02342.x

Brouillard, B.M., Mikkelson, K.M., Bokman, C.M., Berryman, E.M., Sharp, J.O., 2017. Extent of localized tree mortality influences soil biogeochemical response in a beetle-infested coniferous forest. Soil Biology and Biochemistry 114, 309–318. https://doi.org/10.1016/j.soilbio.2017.06.016

Brown, M., Black, T.A., Nesic, Z., Foord, V.N., Spittlehouse, D.L., Fredeen, A.L., Grant, N.J., Burton, P.J., Trofymow, J.A., 2010. Impact of mountain pine beetle on the net ecosystem production of

lodgepole pine stands in British Columbia. Agricultural and Forest Meteorology 150, 254–264. https://doi.org/10.1016/j.agrformet.2009.11.008

Brown, M.G., Black, T.A., Nesic, Z., Fredeen, A.L., Foord, V.N., Spittlehouse, D.L., Bowler, R., Burton, P.J., Trofymow, J.A., Grant, N.J., Lessard, D., 2012. The carbon balance of two lodgepole pine stands recovering from mountain pine beetle attack in British Columbia. Agricultural and Forest Meteorology 153, 82–93. https://doi.org/10.1016/j.agrformet.2011.07.010

Brown, P.M., Shepperd, W.D., Mata, S.A., McClain, D.L., 1998. Longevity of windthrown logs in a subalpine forest of central Colorado. Canadian Journal of Forest Research 28, 932–936.

Busse, M.D., 1994. Downed Bole-Wood Decomposition in Lodgepole Pine Forests of Central Oregon. Soil Science Society of America J 58, 221–227.

Calderón, F.J., Iii, J.B.R., Collins, H.P., Paul, E.A., 2011. Chemical Differences in Soil Organic Matter Fractions Determined by Diffuse-Reflectance Mid-Infrared Spectroscopy 75. https://doi.org/10.2136/sssaj2009.0375

Christensen, B.T., 2001. Physical fractionation of soil and structural and functional complexity in organic matter turnover. European Journal of Soil Science 52, 345–353. https://doi.org/10.1046/j.1365-2389.2001.00417.x

Collins, B.J., Rhoades, C.C., Battaglia, M.A., Hubbard, R.M., 2012. The effects of bark beetle outbreaks on forest development, fuel loads and potential fire behavior in salvage logged and untreated lodgepole pine forests. Forest Ecology and Management 284, 260–268. https://doi.org/10.1016/j.foreco.2012.07.027

Collins, B.J., Rhoades, C.C., Hubbard, R.M., Battaglia, M.A., 2011. Tree regeneration and future stand development after bark beetle infestation and harvesting in Colorado lodgepole pine stands. Forest Ecology and Management 261, 2168–2175. https://doi.org/10.1016/j.foreco.2011.03.016

Collins, B.J., Rhoades, C.C., Underhill, J., Hubbard, R.M., 2010. Post-harvest seedling recruitment following mountain pine beetle infestation of Colorado lodgepole pine stands: a comparison using historic survey records. Can. J. For. Res. 40, 2452–2456. https://doi.org/10.1139/X10-172

Cotrufo, M.F., Ranalli, M.G., Haddix, M.L., Six, J., Lugato, E., 2019. Soil carbon storage informed by particulate and mineral-associated organic matter. Nat. Geosci. 12, 989–994. https://doi.org/10.1038/s41561-019-0484-6

Cotrufo, M.F., Soong, J.L., Horton, A.J., Campbell, E.E., Haddix, M.L., Wall, D.H., Parton, W.J., 2015. Formation of soil organic matter via biochemical and physical pathways of litter mass loss. Nature Geosci 8, 776–779. https://doi.org/10.1038/ngeo2520

Cotrufo, M.F., Wallenstein, M.D., Boot, C.M., Denef, K., Paul, E., 2013. The Microbial Efficiency-Matrix Stabilization (MEMS) framework integrates plant litter decomposition with soil organic matter stabilization: do labile plant inputs form stable soil organic matter? Glob Change Biol 19, 988–995. https://doi.org/10.1111/gcb.12113

Crow, S.E., Lajtha, K., Bowden, R.D., Yano, Y., Brant, J.B., Caldwell, B.A., Sulzman, E.W., 2009a. Increased coniferous needle inputs accelerate decomposition of soil carbon in an old-growth forest. Forest Ecology and Management 258, 2224–2232. https://doi.org/10.1016/j.foreco.2009.01.014

Crow, S.E., Lajtha, K., Filley, T.R., Swanston, C.W., Bowden, R.D., Caldwell, B.A., 2009b. Sources of plant-derived carbon and stability of organic matter in soil: implications for global change. Global Change Biology 15, 2003–2019. https://doi.org/10.1111/j.1365-2486.2009.01850.x

Denef, K., Galdo, I.D., Venturi, A., Cotrufo, M.F., 2013. Assessment of soil C and N stocks and fractions across 11 European soils under varying land uses. OJSS 03, 297–313. https://doi.org/10.4236/ojss.2013.37035

Edburg, S.L., Hicke, J.A., Lawrence, D.M., Thornton, P.E., 2011. Simulating coupled carbon and nitrogen dynamics following mountain pine beetle outbreaks in the western United States. Journal of Geophysical Research 116. https://doi.org/10.1029/2011JG001786

Fahey, T.J., 1983. Nutrient Dynamics of Aboveground Detritus in Lodgepole Pine (Pinus contorta ssp. latifolia) Ecosystems, Southeastern Wyoming. Ecological Monographs 53, 51–72. https://doi.org/10.2307/1942587

Fornwalt, P.J., Rhoades, C.C., Hubbard, R.M., Harris, R.L., Faist, A.M., Bowman, W.D., 2018. Short-term understory plant community responses to salvage logging in beetle-affected lodgepole pine forests. Forest Ecology and Management 409, 84–93. https://doi.org/10.1016/j.foreco.2017.10.056

Fulton-Smith, S., Cotrufo, M.F., 2019. Pathways of soil organic matter formation from above and belowground inputs in a *Sorghum bicolor* bioenergy crop. GCB Bioenergy 11, 971–987. https://doi.org/10.1111/gcbb.12598

Gee, G.W., Bauder, J.W., 1986. Particle-size Analysis, in: Page, A.L. (Ed.), Methods of Soil Analysis, Part 1, Physical and Mineralogical Methods. American Society of Agronomy, Madison, WI, pp. 383–411.

Gleixner, G., Danier, H.J., Werner, R.A., Schmidt, H.L., 1993. Correlations between the ^{13}C content of primary and secondary plant products in different cell compartments and that in decomposing basidiomycetes. Plant Physiol. 102, 1287–1290. https://doi.org/10.1104/pp.102.4.1287

Golchin, A., Oades, J., Skjemstad, J., Clarke, P., 1994. Study of free and occluded particulate organic matter in soils by solid state ^{13}C Cp/MAS NMR spectroscopy and scanning electron microscopy. Soil Res. 32, 285. https://doi.org/10.1071/SR9940285

Grandy, A.S., Neff, J.C., 2008. Molecular C dynamics downstream: The biochemical decomposition sequence and its impact on soil organic matter structure and function. Science of The Total Environment 404, 297–307. https://doi.org/10.1016/j.scitotenv.2007.11.013

Gregorich, E.G., Beare, M.H., McKim, U.F., Skjemstad, J.O., 2006. Chemical and biological characteristics of physically uncomplexed organic matter. Soil Science Society of America Journal 70, 975. https://doi.org/10.2136/sssaj2005.0116

Griffin, J.M., Simard, M., Turner, M.G., 2013. Salvage harvest effects on advance tree regeneration, soil nitrogen, and fuels following mountain pine beetle outbreak in lodgepole pine. Forest Ecology and Management 291, 228–239. https://doi.org/10.1016/j.foreco.2012.11.029

Haddix, M.L., Paul, E.A., Cotrufo, M.F., 2016. Dual, differential isotope labeling shows the preferential movement of labile plant constituents into mineral-bonded soil organic matter. Glob Change Biol 22, 2301–2312. https://doi.org/10.1111/gcb.13237

Hammer, Ø., Harper, D.A.T., Ryan, P.D., 2001. PAST: Paleontological Statistics Software Package for Education and Data Analysis. Palaeontologia Electronica.

Hansen, E.M., 2014. Forest development and carbon dynamics after mountain pine beetle outbreaks. Forest Science 60, 1–13. http://dx.doi.org/10.5849/forsci.13-039

Hicke, J.A., Johnson, M.C., Hayes, J.L., Preisler, H.K., 2012. Effects of bark beetle-caused tree mortality on wildfire. Forest Ecology and Management 271, 81–90. https://doi.org/10.1016/j.foreco.2012.02.005

Hood, P.R., Nelson, K.N., Rhoades, C.C., Tinker, D.B., 2017. The effect of salvage logging on surface fuel loads and fuel moisture in beetle-infested lodgepole pine forests. Forest Ecology and Management 390, 80–88. https://doi.org/10.1016/j.foreco.2017.01.003

Johnson, D.W., Curtis, P.S., 2001. Effects of forest management on soil C and N storage: Meta analysis. Forest Ecology and Management 140, 227–238. https://doi.org/10.1016/S0378-1127(00)00282-6

Klutsch, J.G., Negrón, J.F., Costello, S.L., Rhoades, C.C., West, D.R., Popp, J., Caissie, R., 2009. Stand characteristics and downed woody debris accumulations associated with a mountain pine beetle

(Dendroctonus ponderosae Hopkins) outbreak in Colorado. Forest Ecology and Management 258, 641–649. https://doi.org/10.1016/j.foreco.2009.04.034

Kurz, W.A., Dymond, C.C., Stinson, G., Rampley, G.J., Neilson, E.T., Carroll, A.L., Ebata, T., Safranyik, L., 2008. Mountain pine beetle and forest carbon feedback to climate change. Nature 452, 987–990. https://doi.org/10.1038/nature06777

Lajtha, K., Bailey, V., McFarlane, K., Paustian, K., Bachelet, D., Abramoff, R., Angers, D., Billings, S.A., Cerkowniak, D., Dialynas, Y.G., Finzi, A., French, N., Frey, S., Gurwick, N., Harden, J., Johnson, J.M.F., Johnson, K., Lehmann, J., (Leo) Liu, S., McConkey, B., Mishra, U., Ollinger, S., Paré, D., Paz, F., Richter, D. deB., Schaeffer, S.M., Schimel, J., Shaw, C., Tang, J., Todd-Brown, K., Trettin, C., Waldrop, M., Whitman, T., Wickland, K., Cavallaro, N., Shrestha, G., Birdsey, R., Mayes, M.A., Najjar, R., Reed, S., Romero-Lankao, P., Zhu, Z., 2018. Chapter 12: Soils. Second State of the Carbon Cycle Report. U.S. Global Change Research Program. https://doi.org/10.7930/SOCCR2.2018.Ch12

Lajtha, K., Townsend, K.L., Kramer, M.G., Swanston, C., Bowden, R.D., Nadelhoffer, K., 2014. Changes to particulate versus mineral-associated soil carbon after 50 years of litter manipulation in forest and prairie experimental ecosystems. Biogeochemistry 119, 341–360. https://doi.org/10.1007/s10533-014-9970-5

Lavallee, J.M., Soong, J.L., Cotrufo, M.F., 2020. Conceptualizing soil organic matter into particulate and mineral-associated forms to address global change in the 21st century. Glob Change Biol 26, 261–273. https://doi.org/10.1111/gcb.14859

Lehmann, J., Kleber, M., 2015. The contentious nature of soil organic matter. Nature 528, 60–68. https://doi.org/10.1038/nature16069

Leverkus, A.B., Rey Benayas, J.M., Castro, J., Boucher, D., Brewer, S., Collins, B.M., Donato, D., Fraver, S., Kishchuk, B.E., Lee, E.-J., Lindenmayer, D.B., Lingua, E., Macdonald, E., Marzano, R., Rhoades,

C.C., Royo, A., Thorn, S., Wagenbrenner, J.W., Waldron, K., Wohlgemuth, T., Gustafsson, L., 2018. Salvage logging effects on regulating and supporting ecosystem services — a systematic map. Can. J. For. Res. 48, 983–1000. https://doi.org/10.1139/cjfr-2018-0114

Liang, C., Schimel, J.P., Jastrow, J.D., 2017. The importance of anabolism in microbial control over soil carbon storage. Nat Microbiol 2, 17105. https://doi.org/10.1038/nmicrobiol.2017.105

Malmsheimer, R.W., Fried, J.S., Gee, E., Oneil, E., 2011. Managing forests because carbon matters: Integrating energy, products, and land management policy. Journal of Forestry 109, S7–S50.

Mayer, M., Prescott, C.E., Abaker, W.E.A., Augusto, L., Cécillon, L., Ferreira, G.W.D., James, J., Jandl, R., Katzensteiner, K., Laclau, J.-P., Laganière, J., Nouvellon, Y., Paré, D., Stanturf, J.A., Vanguelova, E.I., Vesterdal, L., 2020. Tamm Review: Influence of forest management activities on soil organic carbon stocks: A knowledge synthesis. Forest Ecology and Management 466, 118127. https://doi.org/10.1016/j.foreco.2020.118127

Mikutta, R., Kleber, M., Torn, M.S., Jahn, R., 2006. Stabilization of soil organic matter: Association with minerals or chemical recalcitrance? Biogeochemistry 77, 25–56. https://doi.org/10.1007/s10533-005-0712-6

Mosier, S., Paustian, K., Davies, C., Kane, M., Cotrufo, M.F., 2019. Soil organic matter pools under management intensification of loblolly pine plantations. Forest Ecology and Management 447, 60–66. https://doi.org/10.1016/j.foreco.2019.05.056

Nave, L.E., Vance, E.D., Swanston, C.W., Curtis, P.S., 2010. Harvest impacts on soil carbon storage in temperate forests. Forest Ecology and Management 259, 857–866.

Oksanen, J., Blanchet, F.G., Friendly, M., Kindt, R., Legendre, P., McGlinn, D., Minchin, P.R., O'Hara, R.B., Simpson, G.L., Solymos, P., Stevens, M.H.H., Szoecs, E., Wagner, H., 2019. vegan: Community Ecology Package.

Page-Dumroese, D.S., Brown, R.E., Jurgensen, M.F., Mroz, G.D., 1999. Comparison of Methods for Determining Bulk Densities of Rocky Forest Soils. Soil Science Society of America Journal 63, 379. https://doi.org/10.2136/sssaj1999.03615995006300020016x

Prescott, C.E., 2010. Litter decomposition: what controls it and how can we alter it to sequester more carbon in forest soils? Biogeochemistry 101, 133–149. https://doi.org/10.1007/s10533-010-9439-0

Prescott, C.E., 1997. Effects of clearcutting and alternative silvicultural systems on rates of decomposition and nitrogen mineralization in a coastal montane coniferous forest. Forest Ecology and Management 95, 253–260. https://doi.org/10.1016/S0378-1127(97)00027-3

PRISM Climate Group, 2017. PRISM Climate Data. Oregon State University. URL http://prism.oregonstate.edu/ (accessed 3.24.17).

Puget, P., Drinkwater, L.E., 2001. Short-term dynamics of root- and shoot-derived carbon from a leguminous green manure. Soil Sci. Soc. Am. J. 65, 771–779. https://doi.org/10.2136/sssaj2001.653771x

R Core Team, 2019. R: A language and environment for statistical computing. R Foundation for Statistical Computing, Vienna, Austria.

Rhoades, C., Pelz, K., Fornwalt, P., Wolk, B., Cheng, A., 2018. Overlapping bark beetle outbreaks, salvage logging and wildfire restructure a lodgepole pine ecosystem. Forests 9, 101. https://doi.org/10.3390/f9030101

Rhoades, C.C., 2019. Soil nitrogen leaching in logged beetle-killed forests and implications for riparian fuel reduction. Journal of Environment Quality 48, 305. https://doi.org/10.2134/jeq2018.04.0169

Rhoades, C.C., Hubbard, R.M., Elder, K., Fornwalt, P.J., Schnackenberg, E., Hood, P.R., Tinker, D.B., 2020a. Tree regeneration and soil responses to management alternatives in beetle-infested

lodgepole pine forests. Forest Ecology and Management 468, 118182. https://doi.org/10.1016/j.foreco.2020.118182

Rhoades, C.C., Hubbard, R.M., Hood, P.R., Starr, B.J., Tinker, D.B., Elder, K., 2020b. Snagfall the first decade after severe bark beetle infestation of high-elevation forests in Colorado, USA. Ecol Appl 30. https://doi.org/10.1002/eap.2059

Romme, W.H., Knight, D.H., Yavitt, J.B., 1986. Mountain pine beetle outbreaks in the Rocky Mountains: Regulators of primary productivity? The American Naturalist 127, 484–494. https://doi.org/10.1086/284497

Schoennagel, T., Veblen, T.T., Negron, J.F., Smith, J.M., 2012. Effects of mountain pine beetle on fuels and expected fire behavior in lodgepole pine forests, Colorado, USA. PLoS ONE 7, e30002. https://doi.org/10.1371/journal.pone.0030002

Schöning, I., Totsche, K.U., Kögel-Knabner, I., 2006. Small scale spatial variability of organic carbon stocks in litter and solum of a forested Luvisol. Geoderma 136, 631–642. https://doi.org/10.1016/j.geoderma.2006.04.023

Shaw, C.H., Banfield, E., Kurz, W.A., 2008. Stratifying soils into pedogenically similar categories for modeling forest soil carbon. Can. J. Soil. Sci. 88, 501–516. https://doi.org/10.4141/CJSS07099

Simard, M., Romme, W.H., Griffin, J.M., Turner, M.G., 2011. Do mountain pine beetle outbreaks change the probability of active crown fire in lodgepole pine forests? Ecological Monographs 81, 3–24. https://doi.org/10.1890/10-1176.1

Smolander, A., Levula, T., Kitunen, V., 2008. Response of litter decomposition and soil C and N transformations in a Norway spruce thinning stand to removal of logging residue. Forest Ecology and Management 256, 1080–1086. https://doi.org/10.1016/j.foreco.2008.06.008

Sokol, N.W., Sanderman, J., Bradford, M.A., 2019. Pathways of mineral-associated soil organic matter formation: Integrating the role of plant carbon source, chemistry, and point of entry. Glob Change Biol 25, 12–24. https://doi.org/10.1111/gcb.14482

Sollins, P., Swanston, C., Kleber, M., Filley, T., Kramer, M., Crow, S., Caldwell, B.A., Lajtha, K., Bowden, R., 2006. Organic C and N stabilization in a forest soil: Evidence from sequential density fractionation. Soil Biology and Biochemistry 38, 3313–3324. https://doi.org/10.1016/j.soilbio.2006.04.014

Throop, H.L., Archer, S.R., Monger, H.C., Waltman, S., 2012. When bulk density methods matter: Implications for estimating soil organic carbon pools in rocky soils. Journal of Arid Environments 77, 66–71. https://doi.org/10.1016/j.jaridenv.2011.08.020

Turner, D.P., Koerper, G.J., Harmon, M.E., Lee, J.J., 1995. A carbon budget for forests of the conterminous United States. Ecological Applications 5, 421–436. https://doi.org/10.2307/1942033

von Lützow, M., Kögel-Knabner, I., Ekschmitt, K., Flessa, H., Guggenberger, G., Matzner, E., Marschner, B., 2007. SOM fractionation methods: Relevance to functional pools and to stabilization mechanisms. Soil Biology and Biochemistry 39, 2183–2207. https://doi.org/10.1016/j.soilbio.2007.03.007

von Lützow, M., Kögel-Knabner, I., Ludwig, B., Matzner, E., Flessa, H., Ekschmitt, K., Guggenberger, G., Marschner, B., Kalbitz, K., 2008. Stabilization mechanisms of organic matter in four temperate soils: Development and application of a conceptual model. J. Plant Nutr. Soil Sci. 171, 111–124. https://doi.org/10.1002/jpln.200700047

Xiong, Y., D'Atri, J.J., Fu, S., Xia, H., Seastedt, T.R., 2011. Rapid soil organic matter loss from forest dieback in a subalpine coniferous ecosystem. Soil Biology and Biochemistry 43, 2450–2456. https://doi.org/10.1016/j.soilbio.2011.08.013

Yanai, R.D., Currie, W.S., Goodale, C.L., 2003. Soil carbon dynamics after forest harvest: an ecosystem paradigm reconsidered. Ecosystems 6, 197–212. https://doi.org/10.1007/s10021-002-0206-5

CHAPTER 4: CONTRIBUTIONS OF ROOT AND HYPHAL NECROMASS TO THE FORMATION OF MINERAL-ASSOCIATED ORGANIC MATTER

4.1 Introduction

Soils are critical reservoirs of carbon (C) and thus understanding the factors that control C sequestration in soil organic matter (SOM) is necessary to inform land management actions and policies that aim to sequester C in soil (Lajtha et al., 2018). Recent conceptual advances in our understanding of SOM composition, protection mechanisms and stabilization have been made as a result of physically separating the SOM into distinct fractions (Christensen, 2001). Numerous physical fractionation schemes have been developed based upon size and density, but the simple physical separation at 53 μm is deemed to be the most effective (Poeplau et al., 2018), because it results in a particulate organic matter (POM, >53 μm) and a mineral associated organic matter (MAOM, <53 μm) fraction that are the most distinct in chemistry, formation pathways and mechanisms of stabilization (Lavallee et al., 2020). SOM is formed from plant C inputs, with more structural or recalcitrant plant C inputs contributing primarily to the POM fraction by fragmentation and physical transfer, while more labile plant C compounds contribute to the MAOM (Cotrufo et al., 2015).

Accumulating evidence is pointing towards the importance of belowground C inputs over aboveground plant C inputs for forming SOM (e.g., Crow et al., 2009; Rasse et al., 2005; Sokol and Bradford, 2019). Across forest ecosystems, partitioning of plant C to the total belowground C flux (TBCF = Net Primary Production$_{root}$ + Respiration$_{root}$ + exudates + mycorrhizae) ranges from ~21-75% of gross primary productivity (Gill and Finzi, 2016; Litton et al., 2007), supporting the importance of roots for SOM formation. Allocation of C to root symbiotic mycorrhizal fungi is included in the TBCF and can be a significant conduit of root C into the soil. Extraradical hyphae (the vegetative biomass) of mycorrhizal

fungi are much more efficient at colonizing the soil than the fine roots of most plants due to smaller diameters that allow the hyphae to grow through smaller soil pore spaces, acting as a conduit for plant C into areas of the soil matrix beyond the root zone. Pulse labeling experiments with ^{13}C-CO_2 have confirmed this function of arbuscular mycorrhizal fungi (AMF), as a significant fraction of the recently fixed plant C was assimilated by AMF and distributed to the soil microbial community (Drigo et al., 2010; Kaiser et al., 2015).

While the role of soil microorganisms in the formation of SOM has focused largely on the mineralization and transformation of plant inputs into SOM, recent work has made it clear that microbial products, metabolites, and necromass (residues of biomass) are important contributors of MAOM (Kallenbach et al., 2016; Kleber et al., 2015; Liang et al., 2017). Therefore, mycorrhizal hyphal necromass may be an important source of mineral associated C (Frey, 2019). Using conversion factors based on the abundance of amino sugars in soil and microbial stoichiometry, Liang et al. (2019) estimated that 23-87% of total soil organic C in the topsoil (<0.25 m) may be of fungal necromass origin. Root necromass contribution to the formation of MAOM is thought to be mediated by microbial *in vivo* or *ex vivo* processing (Liang et al., 2017) and experiments that investigate the formation of MAOM from root and hyphal necromass will help quantify the contribution of these potentially significant MAOM C sources.

Hot water extractable (HWE) C, hemicellulose and other non-structural C compounds digested through chemical fractionation are the labile portion of plant litter that is easily decomposed and utilized by soil microorganisms (Soong et al., 2015). Cellulose and lignin are the primary plant structural compounds that are isolated during subsequent steps of chemical fractionation with sulfuric acid (Goering and Van Soest, 1970). Although both are structural, cellulose is much more decomposable than lignin and plant residues with a lower lignocellulose index, the ratio of lignin to total structural C, and higher nutrient contents are decomposed more rapidly (Aber et al., 1990; Soong et al., 2015). Likewise,

the necromass of fungal hyphae contains structural compounds that vary in recalcitrance and therefore in the efficiency with which soil microorganisms are likely to process them. Chitin is the N-rich, primary cell wall constituent of fungal hyphae and is now recognized to be readily decomposed and largely analogous to cellulose while fungal melanin, another complex cell wall biopolymer, is more recalcitrant like lignin (Fernandez and Koide, 2014, 2012). Other cell wall constituents (e.g., polysaccharides, proteins) and soluble cytoplasmic compounds may contribute to the lability of mycorrhizal necromass (Fernandez et al., 2016). There is no evidence, as historically thought, that the accumulation of lignin and other recalcitrant structural biopolymers, such as melanin, are selectively preserved to forming stable SOM (Lehmann and Kleber, 2015). Rather, chemical recalcitrance simply slows decomposition adding to short-term C storage and instead it is simple or low molecular weight compounds that are stabilized in the soil and persist decades to centuries through mineral-associations as part of the MAOM fraction (Cotrufo et al., 2013; Grandy and Neff, 2008; Schmidt et al., 2011). Similar links between chemistry and SOM formation have not been as well studied for roots or mycorrhizae (Poirier et al., 2018).

Broad patterns in the distribution of SOM between POM and MAOM have emerged in the literature between AMF- and EMF-associating systems with AMF systems storing more soil C in MAOM and EMF systems storing more C in POM (Cotrufo et al., 2019; Craig et al., 2018). However, questions remain surrounding the importance of fungal vs. plant traits in driving these patterns, such as the role of plant litter quality inputs vs. the enzymatic capacity and functional roles of the mycorrhizal symbionts. Focusing on how the chemistry of belowground inputs differs among plant growth forms and mycorrhizal functional types and how the chemistry relates to residue decomposition and MAOM formation will help us build an understanding of SOM formation from different belowground inputs.

Across systems major gaps remain in our understanding of the importance of different belowground C inputs in contributing to soil organic C storage, specifically in MAOM. Few studies have

looked explicitly at fungal hyphal necromass contribution to MAOM. We incubated dual isotopically labeled (^{13}C and ^{15}N) pine and rye grass root necromass and AMF and EMF hyphal necromass grown in a continuous isotope labeling chamber (Soong et al., 2014). We measured the CO_2 efflux over the course of a 38-day incubation and fractionated the incubated soils into dissolved organic matter (DOM), POM and MAOM at the end of the incubation using physical separation. Our goal was to address the following questions: (1) Do the plant and mycorrhizal necromass types differ in efficiency of MAOM formation? and (2) How does the necromass decomposition relate to the necromass chemistry? We predicted that the decomposition rate of residue C and MAOM formation efficiency would be positively related to the amount of low molecular weight or non-structural C, and that each hyphal necromass type would form MAOM more efficiently than their respective root symbiont due to the known decomposability of chitin and the higher N content in fungal necromass.

4.2 Methods

4.2.1 Growth of isotopically labeled root and fungal hyphal necromass

Scotch pine (*Pinus sylvestris* Czech. Rep. Krtiny) and perennial ryegrass (*Lolium perenne*) seedlings were grown in a dual isotope labeling chamber in the Plant Growth Facility (PGF) at Colorado State University, details on chamber design and operation are described by Soong et al. (2014). Scotch pine is widely distributed and is a very common species in temperate managed coniferous forests (Sullivan, 1993), while ryegrass is a valuable forage plant used throughout Europe and in the United States (Peterson, 2002); Scotch pine and ryegrass were chosen for this study for their contrasting chemistries and mycorrhizal associations.

The pine and rye for the experiment were grown from seed. Pine seeds (Sheffield's Seed Co., Inc., Locke, NY) were soaked in cold water for 24 hours and then cold stratified for two weeks at 4˚C prior to planting and the ryegrass seeds (American Meadows, Shelburne, VT) were surface sterilized

with 2% sodium hypochlorite for 30 min and then rinsed six times with sterile DI water. The pine and rye grass were germinated in separate flats of autoclaved sand, ceramic and vermiculite on a misting bench in the PGF.

Four pine seedlings and four clumps of ryegrass were planted in 19-liter pots (n=20 each for pine and rye) with a growth substrate mixture of 3 parts vermiculite, 2 parts sand and 3 parts baked ceramic. A fungal in-growth bag using 37 μm mesh (Elko Filtering Co., Tamarac, FL) filled with autoclave-sterilized sand was placed in the center of each pot to collect the extraradical hyphal biomass during the growth period (Wallander et al., 2001). Prior to planting into the pots, the ryegrass pots were inoculated with the AMF taxa *Rhizophagus intraradices* acquired from INVAM (West Virginia University, Morgantown, WV) by mixing in ~5 g of the AMF inocula mixture into the soil where each ryegrass clump was planted, for a total of ~20 g per pot. After planting, the pine seedlings were inoculated with the EMF taxa *Pisolithus tinctorious* and *Rhizopogan* spp. (Mycorrhizal Applications, Grants Pass, OR). To make the EMF inocula, 0.5 g of *Rhizopogan* and 1 g of *P. tinctorious* were mixed with 250 mL of deionized (DI) water. During inoculation the EMF inocula was placed on a stir plate and a 5 mL pipet fitted with a wide bore pipet tip was used to inoculate each seedling with 3 mL of the inocula mixture for a total of 12 mL per pot. All pots were watered weekly with a ^{15}N-labeled Hoagland's solution with a constant label of 7 atom % ^{15}N. The Hoagland's solution was modified to contain half the concentration of inorganic N, because 19 g of ground, dual labeled blue gramma aboveground necromass was added to each pot to help promote mycorrhizal growth, particularly of the EMF which are known to help supply organic N to plant symbionts (Nicolás et al., 2019). The amount of fertilizer delivered weekly was increased as plant biomass increased. Throughout the growth period CO_2 levels were maintained at a concentration of 360-400 ppm using ^{13}C enriched CO_2 at a target enrichment level of 4 atom %.

After 9 months, all 40 pots were removed from the labeling chamber and the aboveground biomass was immediately harvested by clipping the pine and rye aboveground biomass at the surface of

the growth media to stop photosynthesis and C and N accumulation. Fungal in-growth bags were then removed from each pot and frozen at -20°C until processed. The root system of each pot was harvested and rinsed free of the growth substrate. After rinsing, the root systems were dried at 60°C until constant weight. Fungal in-growth bags were thawed to collect the extraradical fungal hyphae. The contents of each bag were emptied into a beaker, stirred and decanted with DI water through a 53 µm mesh sieve (van Diepen et al., 2010). The hyphae were then pooled by type (AMF and EMF), frozen, freeze-dried and weighed.

4.2.2 Chemical characterization of roots and hyphal necromass

A subsample of each dried root type was finely ground on a Wiley Mill (Model No. 3, Arthur H. Thomas Co., Philadelphia, PA) equipped with a 40 µm mesh screen and a subsample of each dried hyphal necromass type was finely clipped using scissors. The hyphal necromass was not ground on the Wiley Mill because we had a low starting biomass and were concerned about sample loss. The rye roots, pine roots and AMF were analyzed for %C, %N, $\delta^{13}C$ and $\delta^{15}N$ on an elemental analyzer (Costech ECS 4010, Costech Analytical Technologies, Valencia, CA, USA) coupled to an isotope ratio mass spectrometer (Delta V Advantage IRMS, Thermo Fisher, Bremen, DE). The EMF was only analyzed for $\delta^{13}C$ and $\delta^{15}N$ and not for %C and %N because there was not enough sample for accurate element concentration values.

Three replicates each of the pine and rye roots were characterized using a hot water extraction based upon Lavallee et al. (2018) to separate the metabolic portion of the root residue from the structural component. The hot water extract (HWE) was separated by adding 0.4 g of oven dried root residue to 35 mL hot, DI water in covered glass digestion tubes and placed in a 100°C digestion block. After 3 hours, each replicate extract was filtered through a 20 µm nylon mesh filter, analyzed for organic C and N using a TOC analyzer (Shimadzu TOC-L, Shimadzu, Scientific Instruments, Inc., Kyoto, JP), and freeze-dried. The remaining hot water residue (HWR) was rinsed with DI water and oved dried at 60°C.

Both the HWE and HWR masses were quantified and the freeze-dried HWE and oven dried HWR were analyzed for %C, %N, $\delta^{13}C$, and $\delta^{15}N$ just like the bulk residue (TOC values were used for the %C and %N of the HWE).

To analyze the structural component of the root residues we did a wet chemical fractionation on three replicates of each root type using the acid detergent fiber (ADF) digestion method (Goering and Van Soest PJ, 1970). Subsamples of the ground roots were dried at 105°C and then 0.3 g samples were weighed into the glass digestion tubes and 35 mL of acid-detergent fiber digest solution made of cetyl trimethylammonium bromide (CTAB) and sulfuric acid was added to each tube to remove the non-structural carbohydrates and lipids. The acid hydrolyzable fiber (AHF), which is used as a proxy for cellulose (McKee et al., 2016), was then removed with a 73% sulfuric acid digest. This left acid-unhydrolyzable residue (AUR) and ash. The final step was to muffle furnace the digested residue for 2 hours at 525°C to correct for ash content. The AUR fraction is used as a proxy for lignin as previous studies have shown that in plant samples AUR is primarily composed of lignin, although it may also contain significant amounts of other more recalcitrant compounds such as plant waxes, cutin, suberin, and condensed tannins (Preston and Trofymow, 2015). At each step of the ADF digestion the residues were dried overnight at 105°C prior to weighing to solve for the AHF and AUR components. The lignocellulose index was calculated according to Soong et al. (2015): AUR/(AUR + AHF).

To characterize and compare the structural C chemistry across all four necromass types, we scanned a subsample of each dried and ground necromass using diffuse reflectance infrared Fourier-transform infrared spectroscopy (FTIR) (Nicolet iS50 Spectrometer, Thermo Fisher, Bremen, DE). We used KBr as a background and each spectrum was collected with 64 scans from 4000 to 400 cm^{-1} at 4 cm^{-1} resolution. Data were obtained as pseudo-absorbance (log[1/reflectance).

4.2.3 Incubation experiment

We incubated each of the four necromass residue types in native forest soil in a complete block design with four replicates. For this experiment, we chose a native forest soil from an uncut, mixed conifer stand in northern Colorado that has both EMF and AMF plant symbionts. The soil had 3.7% C, 0.16% N, -24.94‰ $\delta^{13}C$, 1.75‰ $\delta^{15}N$ and was a loam (34% sand, 42% silt, 24% clay). This soil was chosen because of the low C concentration and high % of fine particles (silt and clay) which provided plenty of opportunity for SOM formation, particularly in the MAOM fraction since its mineral fraction was far from saturation (Castellano et al., 2015). For each replicate of the four residue types, ~0.004 g of root or hyphal necromass was incubated in 5 g of native forest soil. The small masses of necromass and native forest soil were used because only 0.04 g of EMF hyphal necromass was produced. There were also three soil only control samples prepared and incubated the same as the necromass replicates, but without adding any residue.

Replicates were incubated in 50 mL centrifuge tubes at 60% water filled pore space (WFPS) throughout the incubation to optimize soil microbial activity (Linn and Doran, 1984). The soils had previously been air-dried for storage, so a subsample of the air-dried soil was oven-dried at 105°C to calculate the ~5 g of dry weight soil equivalent for each replicate, then the soil in each replicate was wetted to 60% WFPS and pre-incubated for two weeks so that the initial pulse of C from re-wetting would not be captured in our experiment. To start the incubation the necromass was mixed into the soil and thus became part of the POM fraction, aiding our goal of measuring MAOM formation from each of the necromass types. The soil only samples were also mixed to control for any disturbance effects. The centrifuge tube of each replicates was capped with a plug seal cap fitted with rubber septa and flushed with CO_2-free air for 10 minutes. All replicates were incubated at constant temperature, 25°C for 38 days, which is when the rate of residue-derived C respiration had reached an asymptote, and the experiment was thus harvested.

4.2.4 CO_2 measurements

The CO_2 flux was measured daily for the first 11 days and then every 1-3 days for the remainder of the 38-day incubation. To sample each replicate, the headspace of each was mixed with a 5-mL syringe then two 1-mL subsamples were taken sequentially and injected into a LI-6525 infrared gas analyzer (LI-COR, Lincoln, NE). The two subsamples were averaged to represent the value for each replicate for the sampling day. To calculate the CO_2 concentration in each replicate from the subsamples, a 5-point calibration curve for each day was used from a standard gas of known CO_2 concentration. Ten times during the incubation (on days 2, 4, 6, 9, 14, 17, 21, 28, 32, and 38), the $\delta^{13}C$ of the CO_2 was measured immediately after CO_2 concentration on a Gas Chromatograph-Isotope Ratio Mass Spectrometer (Optima IRMS, Isoprime Inc., Manchester, UK). Samples for the $\delta^{13}C$ analysis were taken directly from the incubation tubes without any intermediate storage. The $\delta^{13}C$-CO_2 was estimated for the days that $\delta^{13}C$-CO_2 was not measured by linear interpolation between the previous and subsequent measurements (Lavallee et al., 2018; Stewart et al., 2013). After each measurement all incubation replicates were flushed with CO_2-free air for 10 minutes.

4.2.5 SOM fractionation and formation analysis

At the conclusion of the incubation, the soils were then fractionated into DOM, POM and MAOM using centrifugation and wet sieving at 53 µm after aggregate dispersion (Cotrufo et al., 2019). Replicates were uncapped, dried at 60°C overnight and then the whole soil + residue was fractionated in the original centrifuge tube used for the incubation as we were concerned about losing soil. After each dried sample was weighed, it was filled with DI water to the 40 mL line. Centrifuges tubes were then placed on a horizontal shaker on low for 15 minutes then the caps and sides of the tubes were rinsed down with DI water and the samples were centrifuged at 3400 rpm for 15 minutes. The DOM was then collected by filtering the supernatant through a 20 µm nylon filter. The DOM was transferred to a pre-weighed, acid washed centrifuge tube. To disperse the soil, 12 glass beads were added to each original sample tube and 0.5% sodium hexametaphosphate was added to the 30 mL line. The samples were

placed back on the horizontal shaker on low. After 18 hours of shaking each sample was poured over a 2 mm sieve stacked on top of a 53 µm sieve in a large pan for the separation of POM and MAOM. The glass beads were collected from the 2 mm sieve and both the glass beads and sieve were rinsed clear with DI water. The top 2 mm sieve was then set aside and the POM that collected on the 53 µm was rinsed clear with DI water and was transferred to a pre-weighed aluminum pan and placed in the 60°C oven. The MAOM fraction remained in the large pan and was transferred to a second pre-weighed aluminum pan and was also placed in the 60°C oven. Once all the fractions were dried, 100±5% recovery was confirmed. A subsample of each fraction was then ground on a roller table and analyzed for %C, %N, $\delta^{13}C$, and $\delta^{15}N$ as described above for the necromass.

4.2.6 Data analyses

To calculate the fraction of residue-derived C respired with each CO_2 sampling and to determine the amount of residue-derived C (or N) in each SOM fraction (f_R), the isotopic mixing model was used:

(1) $$f_{residue} = \frac{(\delta^{13}C_{sample} - \delta^{13}C_{soil\ only\ control})}{(\delta^{13}C_{initial\ residue\ value} - \delta^{13}C_{soil\ only\ control})}$$

where $\delta^{13}C_{sample}$ (or $\delta^{15}N_{sample}$) is the value for each fraction for each sample including the CO_2-C, $\delta^{13}C_{soil\ only\ control}$ (or $\delta^{15}N_{soil\ only\ control}$) is the average value for the soil only controls, and $\delta^{13}C_{initial\ residue\ value}$ (or $\delta^{15}N_{initial\ residue\ value}$) is the initial starting value of the appropriate residue type measured prior to the incubation (as described in section *4.2.2;* Table 4.1).

Respiration of the residue-derived C in CO_2 (CO_{2R}) could then be calculated by multiplying $f_{residue}$ by the total CO_2 efflux for each sampling date:

(2) $$CO_{2R} = f_{residue} \times (CO_2)$$

Soil-derived CO_2 efflux (from the native forest soil) was then calculated by subtracting CO_{2R} from the total CO_2 efflux (Lavallee et al., 2018). The residue-derived C and N in each fraction by multiplying the $f_{residue}$ by the C and N in each fraction:

(3) $mg\ residue - derived\ C\ (or\ N)\ in\ fraction = mass\ soil \times$

$fractional\ mass\ of\ respective\ fraction\ \times \%C\ (or\ \%N)\ in\ fraction\ \times$

$f_{residue\ fraction}$

Total residue-derived C processed was calculated as the sum of the residue-derived C in CO_2, DOM, and MAOM and then MAOM formation efficiency (FE) was calculated by dividing the amount of residue-derived C in MAOM by the total residue-derived C processed (Lavallee et al., 2018):

(4) $FE = \frac{litter-derived\ C\ in\ MAOM}{litter-derived\ C\ processed}$

We tested for differences in chemical characteristics of the rye and pine roots types using two-sample t-tests. We tested for the effect of necromass type on the cumulative native soil-derived CO_2-C respired g^{-1} soil and the cumulative residue-derived CO_2-C respired g^{-1} soil using ANOVA with Tukey's post hoc test. We also used ANOVA with Tukey's post hoc test to evaluate differences in residue-derived C in each of the fractions (mg residue-derived C in fraction g^{-1} soil), residue-derived C processed, percent residue C processed, and MAOM formation efficiency. Prior to all ANOVA analyses, variables were tested for the ANOVA assumptions and variables that did not meet these assumptions of ANOVA were log-transformed prior to analysis. All statistical tests were carried out using R version 3.6.1 (R Core Team, 2019) using a significance value of $\alpha = 0.05$.

4.3 Results

4.3.1 Initial root and hyphal necromass chemistry

All necromass initial $\delta^{13}C$ and $\delta^{15}N$ are reported in Table 4.1. The AMF hyphal necromass used in the incubation was 44.9% C, and 1.08% N, resulting in a C/N ratio of 41.6. The rye roots and pine roots differed in stoichiometry and C chemistry. The rye roots had a higher C/N (59.8) than pine roots (37.6), but generally contained more labile C with a higher % of total C in HWE than the pine roots (Table 4.2). The first step of the ADF digest removes the non-structural C compounds from the residue and therefore

the difference between the starting mass of the necromass and the after the first step of the ADF digest gives an indication of the differences in hemicellulose and non-structural carbohydrates and lipids (McKee et al., 2016), between the two root necromass types. This calculation showed that the rye roots had almost twice as much non-structural and hemicellulose mass % as the pine roots, while the pine roots had much higher mass % in the AHF and AUR (Table 4.2). The lignocellulose index of the pine roots was therefore 33% higher than that of the rye roots, but the AUR/N ratio did not differ between the rye and pine roots (Table 4.2).

Results of the FTIR analysis qualitatively showed some differences in the chemical composition of the four necromass types. All necromass had bands at ~3400, 2950-2870, 1740-1700, ~1435, and 897 cm^{-1} (Fig. 4.1 A-D). The bands at ~3400 cm^{-1} are expected and attributed to O-H/N-H stretching (Galletti et al., 1993) and the features between 2950-2870 to aliphatic C-H stretching (Dokken and Davis, 2007). The pine roots had the most distinct peak at the ester carbonyl band from polysaccharides or fatty acids at 1737 cm^{-1} while the other three necromass types had shoulder peaks at 1735 cm^{-1} for the EMF and 1711 cm^{-1} for both the rye roots and AMF (Fig. 4.1 A-D) (Dokken and Davis, 2007). The bands from 1700 to 1250 cm^{-1} are called the fingerprint region and as the bands here have a lot of information about functional groups (Calderón et al., 2011). The rye roots, pine roots and AMF were very similar, with peaks between 1660-1605 cm^{-1}, near 1510 or 1512 cm^{-1}, and between 1170-1100 cm^{-1} (Fig. 4.1 A-C). The series of peaks between 1660-1605 cm^{-1} contains a range of protein (1660 cm^{-1}) to aromatic C=C (1610 cm^{-1}) (Dokken and Davis, 2007). The peaks near 1510 or 1512 cm^{-1} are aromatic and generally attributed to aromatic C=C of lignin (White et al., 2011) and the peaks between 1170-1100 cm^{-1} are part of the carbohydrate region of -C-C-C or -O-C bond stretching associated with polysaccharides, cellulose, hemicellulose and pectin (Dokken and Davis, 2007). The EMF was the most unique from the other necromass types, with single strong peaks near 1659, 1547, 1089, and 782 cm^{-1} (Fig. 4.1 D). Peaks near 1660 and 1550 cm^{-1} suggest esters in amide I and amide II (Dokken and Davis, 2007; Galletti et al., 1993).

The AMF differed from the other necromass types with peaks 1270-1240 cm^{-1}, which is a C-O-H or C-C-O stretch of ester and considered a diagnostic peak for hemicellulose or cellulose (Fig. 4.1 B) (Dokken and Davis, 2007).

4.3.2 Processing of residue-derived C

The cumulative total respiration (soil- and residue-derived respiration, mg CO_2-C g^{-1} soil) evaluated at the end of the 38-day incubation did not differ based upon necromass type (F=1.25, p=0.33). Partitioning the CO_2 efflux into soil-derived and residue-derived CO_2-C showed that most of the CO_2-C was soil-derived, which did not differ based upon necromass type (F=2.02, p=0.15; Fig. 4.2). While a small component of the CO_2-C flux, the residue-derived CO_2-C (mg CO_2-C g^{-1} soil) did differ based upon necromass type (F=11.82, p=0.0007), with the highest residue-derived CO_2-C in the rye root treatment (*Tukey's HSD*, $p \leq 0.03$; Fig. 4.2).

The rye root treatment showed the greatest decomposition through the highest residue-derived C lost as CO_2-C and highest residue-derived C processed, while the other three necromass types did not differ for either of these metrics (Table 4.3). On average, residue-derived C processed was 32% higher for the rye roots than the other necromass types (Table 4.3). Using the instrument values for the rye, pine and AMF and an average of 44% C for the EMF from a meta-analysis of fungal stoichiometry (Zhang and Elser, 2017) the percent of residue-derived C processed in our study was calculated to be 31.5% for the rye, 22.3% for the AMF, 22.9% for the pine and 21.3% for the EMF (Table 4.3). However, despite differences in the total amount of C processed, the percent of C processed that was lost as CO_2-C differed consistently between the roots and hyphae with 60-61% of the residue-derived C processed lost as CO_2-C for both the rye and pine root necromass in comparison to 54% for the AMF and EMF necromass.

The majority of residue-derived C (mg C g^{-1} soil) remained in the POM fraction except for the EMF treatment which had the lowest POM recovery than all the other treatments (F=17.12, p=0.0001; Fig. 4.3.A). In agreement with the results presented in Table 4.3, the residue-derived C in MAOM (mg C g^{-1} soil) was lower in the pine treatment than the other three treatments (F=8.626, p=0.003) and the residue-derived C in DOM (mg C g^{-1} soil) was higher in the pine treatment than both the rye and AMF treatments (F=4.655, p=0.02; Fig. 4.3.A). The residue-derived C in CO_2 (mg CO_2-C g^{-1} soil) was highest in the rye treatment, as reported above. The residue-derived N (mg N g^{-1} soil) distributed more evenly through the measured fractions than the residue-derived C, except for the pine roots that had much higher residue-derived N retained in the POM (*Tukey's HSD*, $p \leq 0.02$; Fig. 4.3.B). Residue-derived N in the MAOM trended higher in the EMF, but this was not significant as this treatment had the highest variability and the trend was influenced by a split in the four replicates, with two higher than the others (F=2.56, p=0.10; Fig. 4.3.B). Higher residue-derived N in DOM in the pine and EMF treatments was significant (*Tukey's HSD*, $p \leq 0.04$; Fig. 4.3.B).

The mg of residue-derived C that formed MAOM for the pine and EMF were lower than the rye roots (Table 4.3). Because the pine root had also a higher % C processed than the other treatment, consequently it had the lowest MAOM formation efficiency across all treatments (Fig. 4.4).

4.4 Discussion

4.4.1 Processing and MAOM formation efficiency of root and hyphal necromass

At the end of the 38-day incubation we found that the residue quality traits that allowed for quicker processing rate did not also lead to higher processing efficiency. This was concluded from the fact that the rye root necromass was the most decomposed but had the same MAOM formation efficiency as the AMF and EMF necromass (Table 4.3). MAOM formation efficiency is useful as a metric to assess MAOM formation from residues in different states of decomposition because it standardizes

the amount of residue-derived C in MAOM to the amount of residue-derived C processed. After 38-days of incubation we found that all four necromass types in this study formed MAOM, however as hypothesized the MAOM formation efficiency differed among the four necromass types (Fig. 4.4).

The MAOM formation efficiency from the pine (0.18 ± 0.005) was lower than the rye grass (0.3 ± 0.02), AMF (0.32 ± 0.006) and EMF (0.28 ± 0.03), which did not differ from each other. Lavallee et al. (2018) evaluated the MAOM formation efficiency from big bluestem roots using litter-soil-slurries with silt and clay separately and found that after 7 days, ca. 14% litter-derived C was processed with a MAOM formation efficiency of 0.38 and 0.41 with silt and clay, respectively. In that study MAOM formation efficiency decreased to 0.18 in the silt and clay when measured again after 60 days, when ca. 48% litter-derived C had been processed. The stage of decomposition of our residues and the MAOM formation efficiency values of the rye, AMF and EMF were in between the two harvest dates of Lavallee et al. (2018). The rye roots in our study were more similar in mass % AHF and mass % AUR to the big bluestem (Lavallee et al., 2018) than the pine roots in our study. We anticipate that the MAOM formation efficiency would have decreased if our incubation had been longer as we could anticipate more structural litter to be processed and contribute less residue-derived C to MAOM (Cotrufo et al., 2015).

4.4.2 Effect of residue C chemistry on residue processing

Our measured values of residue chemistry indicate that C chemistry is an important predictor of residue processing. The rye roots had a higher C/N ratio than the pine roots (Table 4.2), however, the FTIR spectra indicated that this was because the rye roots had more labile, sugar/polysaccharide C than the pine roots (Fig. 4.1 A & C). The higher % of total C in HWE, higher mass % in hemicellulose and non-structural compounds, and lower lignocellulose index in the rye roots compared to the pine roots supports this conclusion from the FTIR spectra as the HWE are soluble C compounds that are known to be more labile (Lavallee et al., 2018; Soong et al., 2015). A compilation of studies shows that root decomposition is positively correlated with the concentration of hemicellulose and water-soluble

compounds and negatively correlated with root C/N and root cellulose and lignin concentrations (Poirier et al., 2018). These results were similar to Sun et al. (2018) who compared root decomposition in AMF and EMF systems and found that C chemistry not related to lignin or N content (and thus also C/N) predicted first-order root decomposition. We interpret our results to indicate that the labile C content of the rye roots allowed for more microbial processing, but also higher microbial use efficiency leading to the formation of MAOM (Cotrufo et al., 2013).

Our findings support patterns found of higher MAOM in AMF systems and higher POM in EMF systems (Cotrufo et al., 2019; Craig et al., 2018) by showing that rye roots and AMF both have a higher MAOM formation efficiency than pine roots. Our results for the pine-EMF system suggest that root C in pine systems will make a significant contribution to POM and due to the high structural C content will decompose more slowly than more labile roots, thus contributing to soil organic C in the short-term (e.g., years to decades). While the analysis of Liang et al. (2019) suggests that only ca. 30% of topsoil organic C (<0.25 m) in temperate forest ecosystems is from microbial necromass, we speculate that most of the MAOM in temperate forest ecosystems is from fungal necromass. The low efficiency of pine root processing in our study compared to the rye roots, supports the ex vivo pathway of microbial processing for low quality residues and more in vivo processing of high quality litters, leading to higher MAOM formation from microbial necromass in systems with higher quality litter inputs (Liang et al., 2019, 2017).

A targeted gap of this study that we did not fully address was the difference between roots and hyphal necromass in the grass-AMF system. The C/N ratio of the AMF necromass was higher than anticipated for fungal biomass, which averages 5-17 (Cleveland and Liptzin, 2007), and it was due to a lower %N than is expected with hyphal necromass. Our AMF %N value of 1.08 and C/N of 41.6, fell within the range of fungal biomass N content (percent of dry mass) of 0.97-11.4% N (median 3.70) and C/N of 3.5-54.33 (median 13.65) reported for ectomycorrhizal fungi by Zhang and Elser (2017), however

to our knowledge a similar analysis has not been done for AMF as less data is available for that functional guild. Calderón et al. (2009) showed that pure fungal cultures have broad peaks at ~3400, 2928, 1666, 1554, 1157-1085 and a broad peak at ca. 580 cm^{-1}. The spectrum of the EMF from this study almost perfectly lined up with these results, with the notable difference being that the EMF in this study just had a shoulder peak at 1157 cm^{-1} (Fig. 4.1.D). Our AMF had peaks at 3400, 2918, 1666 and ca. 1160, a small shoulder peak at 1085 cm^{-1}, but not at 1554 cm^{-1} (Fig. 4.1.B). Interpreting this spectrum was challenging because many of these peaks are also plant related and the AMF necromass additionally had peaks that are explicitly associated with plant compounds that the EMF did not have, such as the lignin associated peak at 1510 cm^{-1} (White et al., 2011).

McKee et al. (2016) concluded that using more than one chemical approach to characterize chemistry during litter decomposition is necessary because of the different information and limitations offered by different methods. Our results support this conclusion as our methods were much more effective at characterizing the root chemistry than the fungal chemistry, resulting in remaining questions regarding the MAOM formation efficiency patterns detected in the hyphal necromass treatments. Because of its high C/N ratio, low %N and the FTIR spectrum, we interpret the AMF necromass in our study to possibly be a mixture of fungal necromass and colonized fine roots, which may have grown through the seams of our hyphal in-growth bags in the rye treatment,. This interpretation still indicates that there can be both between- and within-species differences in C chemistry leading to differences in belowground C processing. White et al. (2011) showed species-specific differences in spectra from coarse and fine roots and highlighted the need to better resolve spectral characteristics of belowground-specific compounds such as suberin, which has been found to contribute to root C sequestration through recalcitrance, occlusion in aggregates and mineral associations (Poirier et al., 2018). We suggest that mycorrhizal colonization may be another factor contributing to the C chemistry differences detected between species and root diameters and conclude that multiple approaches used together as

suggested by McKee et al. (2016), that focus on belowground specific C compounds, including suberin and fungal chemistry are needed to resolve differences in patterns of belowground residue processing and MAOM formation efficiency.

4.4.3. Conclusions and future research directions

The need to accurately predict changes in soil C stocks and fluxes in response to management and global change calls for a more thorough understanding of the plant-fungal-soil C flow pathway and the formation of SOM from belowground residue inputs. Initial evidence from this study indicates that belowground inputs differ in C chemistry with implications for function and long-term C sequestration. Our analyses were constrained by the amount of necromass produced and our results are limited in their generalizability because we have chosen just one species of each taxa of interest. Yet, notable differences in the chemistry and the fate of the rye and pine roots, colonized rye roots/AMF, and EMF hyphal necromass indicates that these different types of belowground necromass may contribute differently to SOM and explain the patterns of POM and MAOM accumulation across different systems. We show that dual isotopic labeling of hyphal necromass paired with FTIR and soil fractionation is a promising avenue to mechanistically understand the connections between chemistry and accumulation of necromass-derived C in more stable MAOM across different ecological systems. While FTIR has promise as a method to be used to scan many different plant and fungal taxa to contribute towards this knowledge, better characterization of root and fungal chemistry through other methods need to be paired with FTIR for better interpretation of the spectra.

Table 4.1. Initial isotopic signatures ($\delta^{13}C$, atom % ^{13}C, $\delta^{15}N$ and atom % ^{15}N) of the four necromass types in the experiment: perennial ryegrass roots (*Lolium perenne*), AMF extraradical hyphae (*Rhizophagus intraradices*), Scotch pine roots (*Pinus Sylvestris* Czech Rep. Kritny), and EMF extraradical hyphae (*Pisolithus tinctorious* and *Rhizopogan* spp.).

	Rye Roots	AMF	Pine roots	EMF
$\delta^{13}C$	2871.4	2959.7	3044.5	2672.6
At. % ^{13}C	4.15	4.24	4.33	3.94
$\delta^{15}N$	13190.6	13280.0	13529.4	11407.0
At. % ^{15}N	4.96	4.96	5.07	4.37

Table 4.2. Chemical characterization of the rye (*Lolium perenne*) root and pine (*Pinus sylvestris*) root necromass, with p-values from two-sample t-tests comparing data in each row.

	Rye Roots	Pine roots	Pr(>F)
% C	44.7	45.2	
% N	0.8	1.4	
C/N ratio (mass)	59.8	37.6	
HWE Mass %	13.0 ± 1.0	12.2 ± 0.3	0.44
HWE % of total C	10.6 ± 0.7	8.7 ± 0.1	0.06
HWE % C	37.2 ± 5.5	32.3 ± 0.4	0.43
HWE % N	0.71 ± 0.09	0.70 ± 0.04	0.95
Non-structural mass %	58.9 ± 0.4	34.8 ± 0.3	<0.0001
AHF Mass %	26.5 ± 0.05	39.8 ± 0.3	<0.0001
AUR Mass %	9.7 ± 0.5	25.8 ± 0.1	<0.0001
AUR/N	12.2 ± 0.7	13.1 ± 0.03	0.26
Lignocellulose index	0.27 ± 0.01	0.40 ± 0.001	0.0003

Data are means ± 1 standard error (n = 1 for % C, % N, C/N; n = 3 for % HWE-C, % HWE-N, C/N of HWE, % AHF, % AUR, AUR/N, lignocellulose index)

Table 4.3. Residue-derived C (mg) respired as CO_2, in mineral-associated organic matter (MAOM, <53 μm), dissolved organic C (DOC), processed (sum of CO_2-C, MAOM-C and DOM-C) and remaining in particulate organic matter (POM, >53 μm) at the end of the 38-day incubation.

Fraction	Rye roots	AMF	Pine roots	EMF	Pr(>F) *
CO_2	0.37 ± 0.02 a	0.22 ± 0.02 b	0.27 ± 0.01 b	0.21 ± 0.03 b	0.0007
MAOM	0.18 ± 0.002 a	0.13 ± 0.002 ab	0.08 ± 0.001 b	0.11 ± 0.005 b	0.009
DOC	0.06 ± 0.003 a	0.06 ± 0.006 a	0.1 ± 0.004 b	0.08 ± 0.02 ab	0.02
Processed	0.60 ± 0.02 a	0.41 ± 0.03 b	0.44 ± 0.02 b	0.39 ± 0.07 b	0.02
% residue C processed†	31.5 ± 1.3 a	22.3 ± 1.8 ab	22.9 ± 0.9 ab	21.3 ± 3.9 b	0.03

Data are means (± 1 standard error) (n=4)

*Different letters indicate differences between treatments for each variable at p≤0.05

†For the EMF used mean value of 44% C from Zhang and Elser (2017) to estimate initial mg C in each EMF replicate

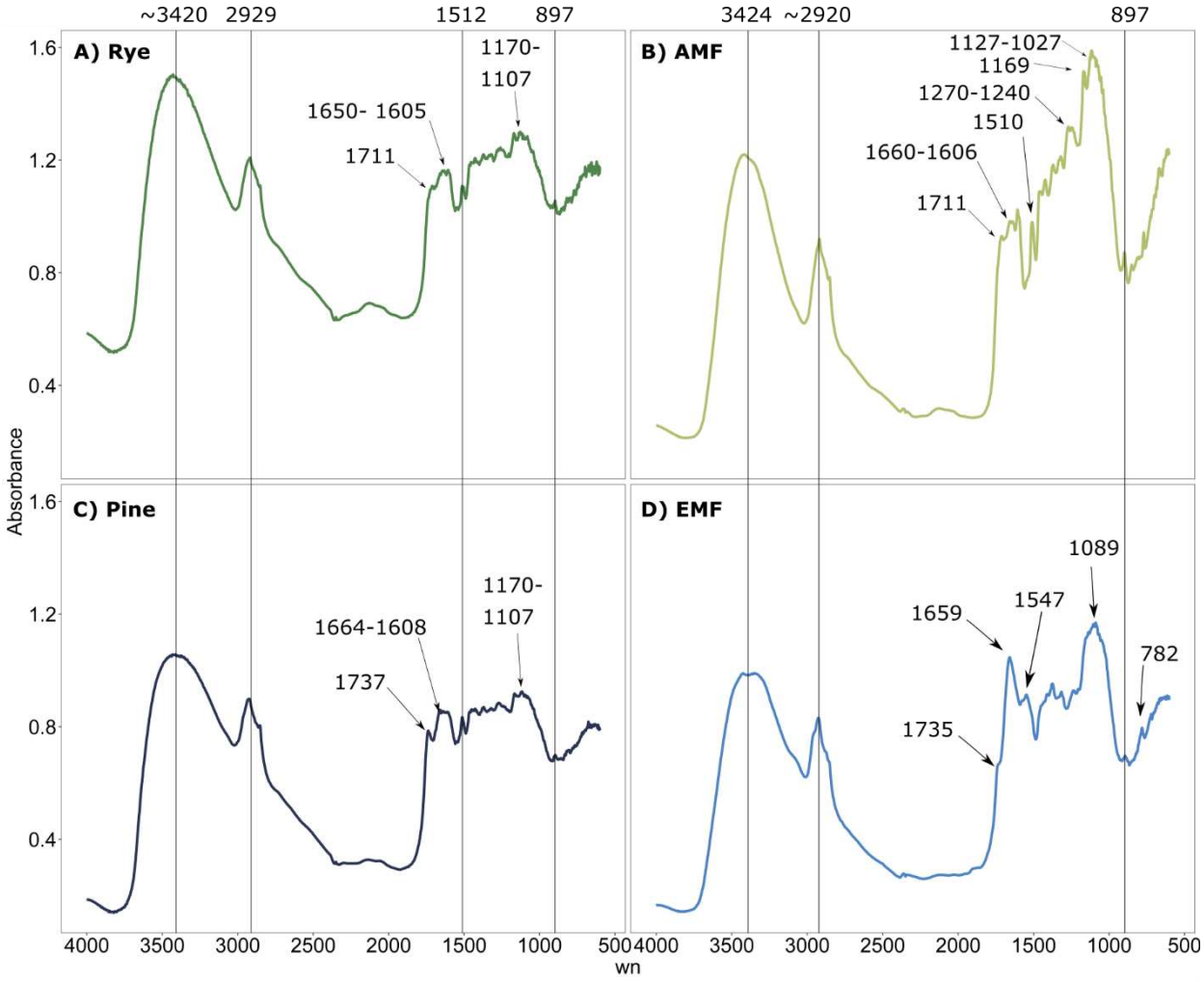

Fig. 4.1. FTIR spectra of all four residue types prior to incubation. Absorbance is unitless and wn is cm^{-1}. Peaks are defined in the results.

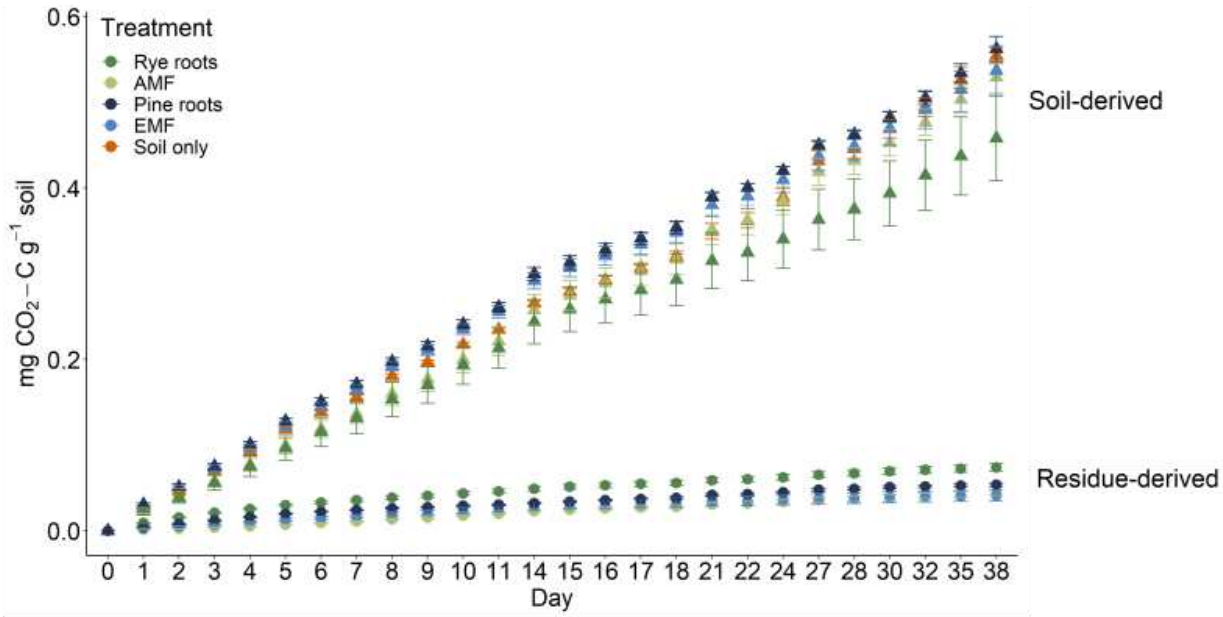

Fig. 4.2. Cumulative respiration of soil-derived and residue-derived C (mg CO_2-C g^{-1} soil) for each treatment over the 38-day incubation. Data are averages with bars as standard error (n=4).

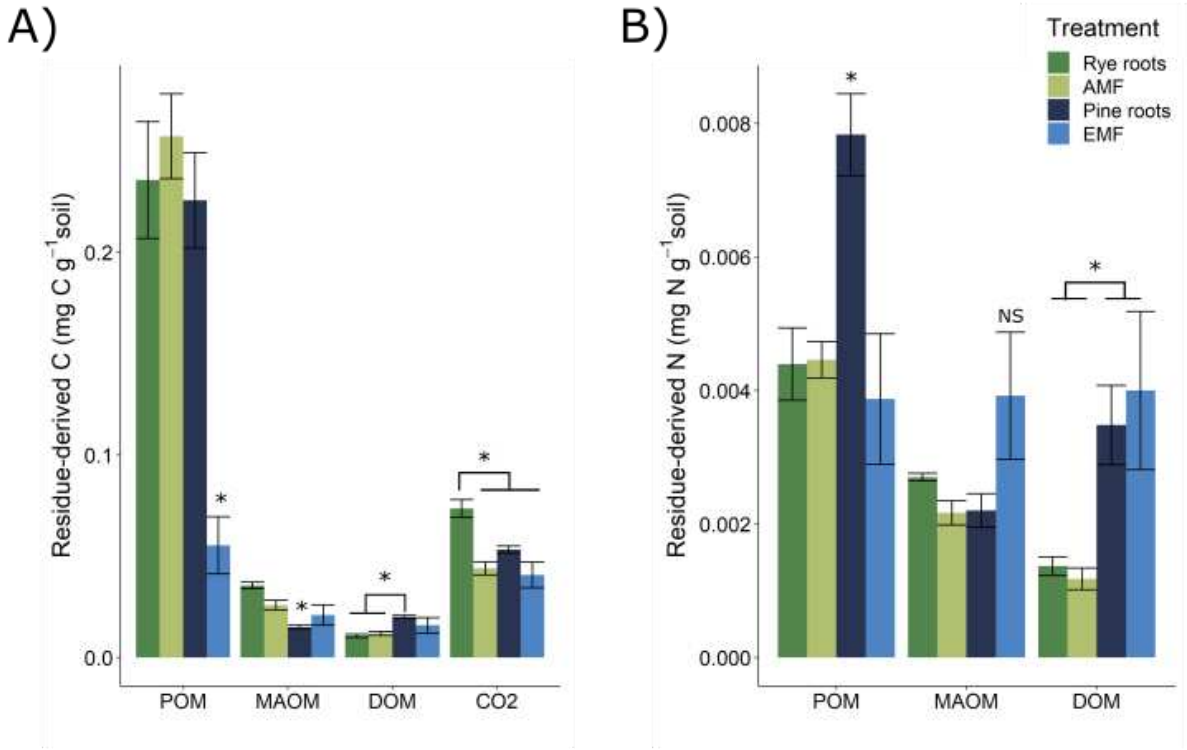

Fig. 4.3. A) residue-derived C (mg residue-derived C g^{-1} soil) and B) residue-derived N (mg residue-derived N g^{-1} soil) among the particulate organic matter (POM, >53 µm), mineral associated (MAOM, <53 µm) and dissolved organic matter (DOM) fractions and CO_2 at the end of the 38-day incubation. Data are means with 1 standard error bars (n=4). Astericks indicate a treatment or treatments that differs from the others.

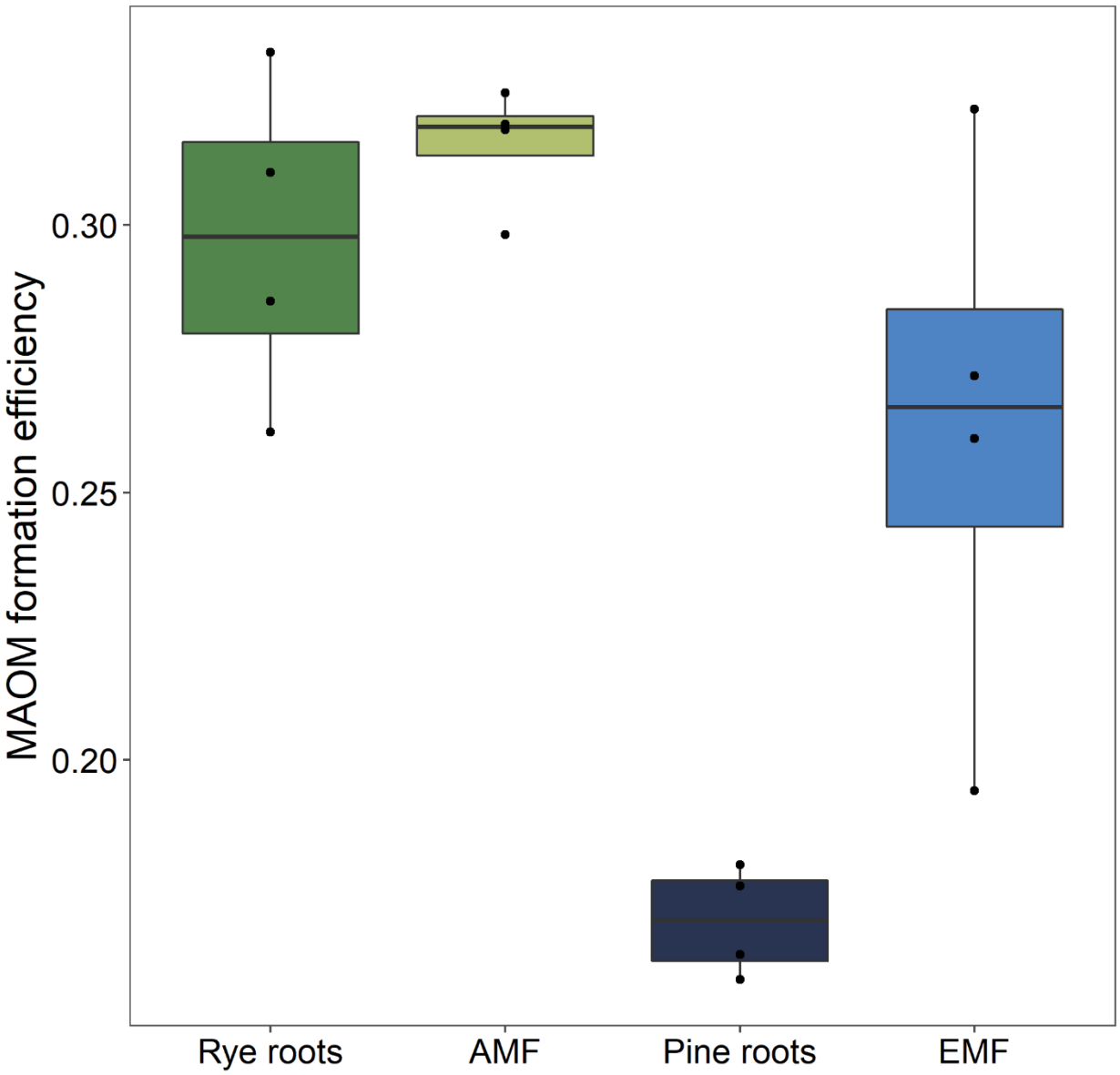

Fig. 4.4. The mineral associated organic matter (MAOM) formation efficiency calculated as the residue-derived C in MAOM divided by the total residue-derived C processed (CO_2 + DOM + MAOM) from each necromass type at the end of the 38-day soil incubation. The black dots are the values for each of the 4 replicates. The pine roots had a lower MAOM formation efficiency than the other three residue types (*Tukey's HSD*, $p \leq 0.006$) while the other three did not differ from each other.

REFERENCES

Aber, J.D., Melillo, J.M., McClaugherty, C.A., 1990. Predicting long-term patterns of mass loss, nitrogen dynamics, and soil organic matter formation from initial fine litter chemistry in temperate forest ecosystems. Can. J. Bot. 68, 2201–2208. https://doi.org/10.1139/b90-287

Calderón, F.J., Acosta-Martinez, V., Douds, D.D., Reeves, J.B., Vigil, M.F., 2009. Mid-Infrared and Near-Infrared Spectral Properties of Mycorrhizal and Non-Mycorrhizal Root Cultures. Appl Spectrosc 63, 494–500. https://doi.org/10.1366/000370209788346931

Calderón, F.J., Reeves, J.B., Collins, H.P., Paul, E.A., 2011. Chemical differences in soil organic matter fractions determined by diffuse-reflectance mid-infrared spectroscopy. Soil Science Society of America Journal 75, 568. https://doi.org/10.2136/sssaj2009.0375

Castellano, M.J., Mueller, K.E., Olk, D.C., Sawyer, J.E., Six, J., 2015. Integrating plant litter quality, soil organic matter stabilization, and the carbon saturation concept. Glob Change Biol 21, 3200–3209. https://doi.org/10.1111/gcb.12982

Christensen, B.T., 2001. Physical fractionation of soil and structural and functional complexity in organic matter turnover. Eur J Soil Science 52, 345–353. https://doi.org/10.1046/j.1365-2389.2001.00417.x

Cleveland, C.C., Liptzin, D., 2007. C:N:P stoichiometry in soil: is there a “Redfield ratio” for the microbial biomass? Biogeochemistry 85, 235–252. https://doi.org/10.1007/s10533-007-9132-0

Cotrufo, M.F., Ranalli, M.G., Haddix, M.L., Six, J., Lugato, E., 2019. Soil carbon storage informed by particulate and mineral-associated organic matter. Nat. Geosci. 12, 989–994. https://doi.org/10.1038/s41561-019-0484-6

Cotrufo, M.F., Soong, J.L., Horton, A.J., Campbell, E.E., Haddix, M.L., Wall, D.H., Parton, W.J., 2015. Formation of soil organic matter via biochemical and physical pathways of litter mass loss. Nature Geosci 8, 776–779. https://doi.org/10.1038/ngeo2520

Cotrufo, M.F., Wallenstein, M.D., Boot, C.M., Denef, K., Paul, E., 2013. The Microbial Efficiency-Matrix Stabilization (MEMS) framework integrates plant litter decomposition with soil organic matter stabilization: do labile plant inputs form stable soil organic matter? Glob Change Biol 19, 988–995. https://doi.org/10.1111/gcb.12113

Craig, M.E., Turner, B.L., Liang, C., Clay, K., Johnson, D.J., Phillips, R.P., 2018. Tree mycorrhizal type predicts within-site variability in the storage and distribution of soil organic matter. Global Change Biology 24, 3317–3330. https://doi.org/10.1111/gcb.14132

Crow, S.E., Lajtha, K., Bowden, R.D., Yano, Y., Brant, J.B., Caldwell, B.A., Sulzman, E.W., 2009. Increased coniferous needle inputs accelerate decomposition of soil carbon in an old-growth forest. Forest Ecology and Management 258, 2224–2232. https://doi.org/10.1016/j.foreco.2009.01.014

Dokken, K.M., Davis, L.C., 2007. Infrared Imaging of Sunflower and Maize Root Anatomy. J. Agric. Food Chem. 55, 10517–10530. https://doi.org/10.1021/jf072052e

Drigo, B., Pijl, A.S., Duyts, H., Kielak, A.M., Gamper, H.A., Houtekamer, M.J., Boschker, H.T.S., Bodelier, P.L.E., Whiteley, A.S., Veen, J.A. v., Kowalchuk, G.A., 2010. Shifting carbon flow from roots into associated microbial communities in response to elevated atmospheric CO2. Proceedings of the National Academy of Sciences 107, 10938–10942. https://doi.org/10.1073/pnas.0912421107

Fernandez, C.W., Koide, R.T., 2014. Initial melanin and nitrogen concentrations control the decomposition of ectomycorrhizal fungal litter. Soil Biology and Biochemistry 77, 150–157. https://doi.org/10.1016/j.soilbio.2014.06.026

Fernandez, C.W., Koide, R.T., 2012. The role of chitin in the decomposition of ectomycorrhizal fungal litter. Ecology 93, 24–28. https://doi.org/10.1890/11-1346.1

Fernandez, C.W., Langley, J.A., Chapman, S., McCormack, M.L., Koide, R.T., 2016. The decomposition of ectomycorrhizal fungal necromass. Soil Biology and Biochemistry 93, 38–49. https://doi.org/10.1016/j.soilbio.2015.10.017

Frey, S.D., 2019. Mycorrhizal Fungi as Mediators of Soil Organic Matter Dynamics. Annu. Rev. Ecol. Evol. Syst. 50, 237–259. https://doi.org/10.1146/annurev-ecolsys-110617-062331

Galletti, G.C., Reeves, J.B., Bloomfield, J., Vogt, K.A., Vogt, D.J., 1993. Analysis of leaf and fine root litter from a subtropical montane rain forest by pyrolysis—gas chromatography/mass spectrometry. Journal of Analytical and Applied Pyrolysis 27, 1–14. https://doi.org/10.1016/0165-2370(93)80018-U

Gill, A.L., Finzi, A.C., 2016. Belowground carbon flux links biogeochemical cycles and resource-use efficiency at the global scale. Ecol Lett 19, 1419–1428. https://doi.org/10.1111/ele.12690

Goering, H., Van Soest, P., 1970. Forage fiber analyses (apparatus, reagents, procedures, and some applications), in: USDA Agriculture Handbook No. 379. Washington, D.C.

Grandy, A.S., Neff, J.C., 2008. Molecular C dynamics downstream: The biochemical decomposition sequence and its impact on soil organic matter structure and function. Science of The Total Environment 404, 297–307. https://doi.org/10.1016/j.scitotenv.2007.11.013

Kaiser, C., Kilburn, M.R., Clode, P.L., Fuchslueger, L., Koranda, M., Cliff, J.B., Solaiman, Z.M., Murphy, D.V., 2015. Exploring the transfer of recent plant photosynthates to soil microbes: mycorrhizal pathway vs direct root exudation. New Phytol 205, 1537–1551. https://doi.org/10.1111/nph.13138

Kallenbach, C.M., Frey, S.D., Grandy, A.S., 2016. Direct evidence for microbial-derived soil organic matter formation and its ecophysiological controls. Nat Commun 7, 13630. https://doi.org/10.1038/ncomms13630

Kleber, M., Eusterhues, K., Keiluweit, M., Mikutta, C., Mikutta, R., Nico, P.S., 2015. Mineral–Organic Associations: Formation, Properties, and Relevance in Soil Environments, in: Advances in Agronomy. Elsevier, pp. 1–140. https://doi.org/10.1016/bs.agron.2014.10.005

Lajtha, K., Bailey, V., McFarlane, K., Paustian, K., Bachelet, D., Abramoff, R., Angers, D., Billings, S.A., Cerkowniak, D., Dialynas, Y.G., Finzi, A., French, N., Frey, S., Gurwick, N., Harden, J., Johnson, J.M.F., Johnson, K., Lehmann, J., (Leo) Liu, S., McConkey, B., Mishra, U., Ollinger, S., Paré, D., Paz, F., Richter, D. deB., Schaeffer, S.M., Schimel, J., Shaw, C., Tang, J., Todd-Brown, K., Trettin, C., Waldrop, M., Whitman, T., Wickland, K., Cavallaro, N., Shrestha, G., Birdsey, R., Mayes, M.A., Najjar, R., Reed, S., Romero-Lankao, P., Zhu, Z., 2018. Chapter 12: Soils. Second State of the Carbon Cycle Report. U.S. Global Change Research Program. https://doi.org/10.7930/SOCCR2.2018.Ch12

Lavallee, J.M., Conant, R.T., Paul, E.A., Cotrufo, M.F., 2018. Incorporation of shoot versus root-derived 13C and 15N into mineral-associated organic matter fractions: results of a soil slurry incubation with dual-labelled plant material. Biogeochemistry 137, 379–393. https://doi.org/10.1007/s10533-018-0428-z

Lavallee, J.M., Soong, J.L., Cotrufo, M.F., 2020. Conceptualizing soil organic matter into particulate and mineral-associated forms to address global change in the 21st century. Glob Change Biol 26, 261–273. https://doi.org/10.1111/gcb.14859

Lehmann, J., Kleber, M., 2015. The contentious nature of soil organic matter. Nature 528, 60–68. https://doi.org/10.1038/nature16069

Liang, C., Amelung, W., Lehmann, J., Kästner, M., 2019. Quantitative assessment of microbial necromass contribution to soil organic matter. Glob Change Biol 25, 3578–3590. https://doi.org/10.1111/gcb.14781

Liang, C., Schimel, J.P., Jastrow, J.D., 2017. The importance of anabolism in microbial control over soil carbon storage. Nat Microbiol 2, 17105. https://doi.org/10.1038/nmicrobiol.2017.105

Linn, D.M., Doran, J.W., 1984. Effect of Water-Filled Pore Space on Carbon Dioxide and Nitrous Oxide Production in Tilled and Nontilled Soils. Soil Science Society of America Journal 48, 1267–1272. https://doi.org/10.2136/sssaj1984.03615995004800060013x

Litton, C.M., Raich, J.W., Ryan, M.G., 2007. Carbon allocation in forest ecosystems. Global Change Biol 13, 2089–2109. https://doi.org/10.1111/j.1365-2486.2007.01420.x

McKee, G.A., Soong, J.L., Caldéron, F., Borch, T., Cotrufo, M.F., 2016. An integrated spectroscopic and wet chemical approach to investigate grass litter decomposition chemistry. Biogeochemistry 128, 107–123. https://doi.org/10.1007/s10533-016-0197-5

Nicolás, C., Martin-Bertelsen, T., Floudas, D., Bentzer, J., Smits, M., Johansson, T., Troein, C., Persson, P., Tunlid, A., 2019. The soil organic matter decomposition mechanisms in ectomycorrhizal fungi are tuned for liberating soil organic nitrogen. ISME J 13, 977–988. https://doi.org/10.1038/s41396-018-0331-6

Peterson, J.S., 2002. PERENNIAL RYEGRASS 2.

Poeplau, C., Don, A., Six, J., Kaiser, M., Benbi, D., Chenu, C., Cotrufo, M.F., Derrien, D., Gioacchini, P., Grand, S., Gregorich, E., Griepentrog, M., Gunina, A., Haddix, M., Kuzyakov, Y., Kühnel, A., Macdonald, L.M., Soong, J., Trigalet, S., Vermeire, M.L., Rovira, P., van Wesemael, B., Wiesmeier, M., Yeasmin, S., Yevdokimov, I., Nieder, R., 2018. Isolating organic carbon fractions with varying turnover rates in temperate agricultural soils – A comprehensive method comparison. Soil Biology and Biochemistry 125, 10–26. https://doi.org/10.1016/j.soilbio.2018.06.025

Poirier, V., Roumet, C., Munson, A.D., 2018. The root of the matter: Linking root traits and soil organic matter stabilization processes. Soil Biology and Biochemistry 120, 246–259. https://doi.org/10.1016/j.soilbio.2018.02.016

Preston, C.M., Trofymow, J.A., 2015. The chemistry of some foliar litters and their sequential proximate analysis fractions. Biogeochemistry 126, 197–209. https://doi.org/10.1007/s10533-015-0152-x

R Core Team, 2019. R: A language and environment for statistical computing. R Foundation for Statistical Computing, Vienna, Austria.

Rasse, D.P., Rumpel, C., Dignac, M.-F., 2005. Is soil carbon mostly root carbon? Mechanisms for a specific stabilisation. Plant Soil 269, 341–356. https://doi.org/10.1007/s11104-004-0907-y

Schmidt, M.W.I., Torn, M.S., Abiven, S., Dittmar, T., Guggenberger, G., Janssens, I.A., Kleber, M., Kögel-Knabner, I., Lehmann, J., Manning, D.A.C., Nannipieri, P., Rasse, D.P., Weiner, S., Trumbore, S.E., 2011. Persistence of soil organic matter as an ecosystem property. Nature 478, 49–56. https://doi.org/10.1038/nature10386

Sokol, N.W., Bradford, M.A., 2019. Microbial formation of stable soil carbon is more efficient from belowground than aboveground input. Nature Geosci 12, 46–53. https://doi.org/10.1038/s41561-018-0258-6

Soong, J.L., Parton, W.J., Calderon, F., Campbell, E.E., Cotrufo, M.F., 2015. A new conceptual model on the fate and controls of fresh and pyrolized plant litter decomposition. Biogeochemistry 124, 27–44. https://doi.org/10.1007/s10533-015-0079-2

Soong, J.L., Reuss, D., Pinney, C., Boyack, T., Haddix, M.L., Stewart, C.E., Cotrufo, M.F., 2014. Design and Operation of a Continuous ¹³C and ¹⁵N Labeling Chamber for Uniform or Differential, Metabolic and Structural, Plant Isotope Labeling. Journal of Visualized Experiments 1–8. https://doi.org/10.3791/51117

Stewart, C.E., Zheng, J., Botte, J., Cotrufo, M.F., 2013. Co-generated fast pyrolysis biochar mitigates green-house gas emissions and increases carbon sequestration in temperate soils. GCB Bioenergy 5, 153–164. https://doi.org/10.1111/gcbb.12001

Sullivan, J., 1993. Pinus sylvestris. Fire Effects Information System, [Online].

Sun, T., Hobbie, S.E., Berg, B., Zhang, H., Wang, Q., Wang, Z., Hättenschwiler, S., 2018. Contrasting dynamics and trait controls in first-order root compared with leaf litter decomposition. Proc Natl Acad Sci USA 115, 10392–10397. https://doi.org/10.1073/pnas.1716595115

van Diepen, L.T.A., Lilleskov, E.A., Pregitzer, K.S., Miller, R.M., 2010. Simulated Nitrogen Deposition Causes a Decline of Intra- and Extraradical Abundance of Arbuscular Mycorrhizal Fungi and Changes in Microbial Community Structure in Northern Hardwood Forests. Ecosystems 13, 683–695. https://doi.org/10.1007/s10021-010-9347-0

Wallander, H., Nilsson, L.O., Hagerberg, D., Bååth, E., 2001. Estimation of the biomass and seasonal growth of external mycelium of ectomycorrhizal fungi in the field. New Phytologist 151, 753–760. https://doi.org/10.1046/j.0028-646x.2001.00199.x

White, K.E., Reeves, J.B., Coale, F.J., 2011. Mid-infrared diffuse reflectance spectroscopy for the rapid analysis of plant root composition. Geoderma 167–168, 197–203. https://doi.org/10.1016/j.geoderma.2011.08.009

Zhang, J., Elser, J.J., 2017. Carbon:Nitrogen:Phosphorus Stoichiometry in Fungi: A Meta-Analysis. Front. Microbiol. 8, 1281. https://doi.org/10.3389/fmicb.2017.01281

CHAPTER 5: SUMMARY AND CONCLUSIONS

Forest ecosystems face an uncertain future in the face of global change, such as anticipated increases in disturbance frequency and severity (Seidl et al., 2017) and the functioning of forest soils will be critical to this response. How disturbances and subsequent management impact plant N uptake and soil C stocks, two very important functions of forest ecosystems, will depend on mechanisms of nutrient retention and availability and changes to soil organic matter (SOM) and soil C inputs. My dissertation focused on understanding these forest soil responses through focusing on mountain pine beetle infested lodgepole pine that had been salvage logged in northern Colorado.

To address the impacts of MPB-infestation and salvage logging on ecosystem N stocks and plant N uptake I labeled research plots centered over a lodgepole pine seedling with ^{15}N-$(NH_4)_2SO_4$ and measured label recovery over two growing seasons in soil and vegetation pools. The forest soil was the largest pool of ^{15}N recovery supporting the N sink hypothesis, which proposed that SOM is an important ecosystem N bank mediating leaching losses (Lovett et al., 2018). Soil microbial immobilization of N is the primary process mediating the formation of this sink, however great uncertainty remains surrounding the controls of this N sink, such as the long-term stability of the retained N.

Overall, the N uptake by the understory vegetation and lodgepole pine seedlings were the most responsive to the treatments. Our findings supported the understory vegetation playing an important role in compensatory N uptake, particularly in the uncut areas where there was less uptake by the lodgepole seedlings. Despite no differences in plant available N measured as salt extractable NH_4-N (NO_3-N was below the 4 ug/L detection limit), the lodgepole seedling N stock was an order of magnitude higher in the salvage logged treatments compared to the uncut. This difference was attributed to the

higher density of lodgepole seedlings in the clear-cuts and higher photosynthetic N use efficiency in the clear-cut because of the abundant light for photosynthesis. Thus, N uptake by the lodgepole seedlings was driven by C fixation in the seedlings, rather than N in the soil. Finally, this increased growth and C fixation by the seedlings in the clear-cut resulted in increased C allocation to the roots.

To address the impacts of MPB-infestation and salvage logging on forest soil C stocks I fractionated O horizon and upper mineral soil (0-10 cm) from uncut and salvage logged areas with residue retention and removal. I found that salvage logging and residue management treatments did not have negative impacts on soil C in the management areas studied and that soil C actually increased with management. The modest increases in C stock with logging were attributed to mixing in of O horizon and surface residues during forest harvest. While reduced cover of O horizon measured in these management areas supported this interpretation, we found that harvesting also increased the stock of surface C inputs. This was important because reductions in soil C following harvesting are generally associated with reduced C inputs and increased decomposition (Mayer et al., 2020) and we did not find evidence for either of those mechanisms in this context of salvage logging in dry, high elevation stands.

Using Fourier-transformed mid-infrared (FTIR) spectroscopy, natural abundance ^{13}C signatures, and the C/N ratios of the O horizon and mineral soil fractions indicated that vertical physical transfer of O horizon C is not a significant pathway of C input to forming SOM in the mineral soil. The large accumulation of the light particulate organic matter (<1.85 g cm^{-3}) in this study is consistent with fragmentation of low-quality root inputs that has been found in other systems (e.g., Bird et al., 2008; Fulton-Smith and Cotrufo, 2019; Rasse et al., 2005), supporting that the pine roots are not used efficiently by soil microorganisms and therefore contribute little C to MAOM through the ex vivo microbial modification pathway (Liang et al., 2017).

Changes in belowground C inputs due to disturbance or management may alter the formation of SOM. To understand potential implications for long-term soil C sequestration, I investigated MAOM formation efficiency from root and mycorrhizal hyphal necromass with different C chemistry. To do this, I produced dual ^{13}C- and ^{15}N-labeled ryegrass (*Lolium perenne*) and Scotch pine (*Pinus Sylvestris* Czech Rep. Krtiny) root and mycorrhizal extraradical hyphal necromass of arbuscular mycorrhizal (AMF) and ectomycorrhizal (EMF) grown in symbiosis with the rye and pine, respectively. The four, dual labeled necromass types were then incubated in soils from one of the uncut stands of the field experiments to determine differences in processing of the residue as a result of residue chemistry, with an emphasis on the mineral associated organic matter (MAOM, <53 μm) formation efficiency. The pine roots had a much higher mass % of structural C compounds than the rye roots and consequently we found that C processing rate and MAOM formation efficiency from the rye roots was consistently higher. This finding confirmed that more labile C chemistry increased microbial processing of the litter. However, the mycorrhizal hyphal necromass seemed to have a lower abundance of labile C and likely had more structural C compounds but had higher absorbances for protein and formed MAOM just as efficiently as the rye. Therefore this can be interpreted to support previous findings that the C/N ratio is important for forming MAOM (Lavallee et al., 2018). Synthesizing this information, we suggest that both C chemistry and C/N are important to determine residue decomposition efficiency and the formation of MAOM. The incubation results support a continent-scale analysis of European forest soils that showed that AMF and EMF systems differ in the distribution of SOM among the fractions with AMF-dominant systems characterized by more C in the MAOM and EMF-dominant systems characterized by POM (Cotrufo et al., 2019). Further, the incubation confirmed that residue C quality is important for the pathway of SOM formation (Cotrufo et al., 2015; Liang et al., 2017) and indicates that grass-AMF systems have more MAOM because both the root and necromass inputs form MAOM, whereas in the pine-EMF systems more the MAOM is primarily formed by the mycorrhizal necromass.

This dissertation used field experimental and observational studies and a mechanistic laboratory study, isotope labeling and natural abundance isotope patterns, physical fractionation of O horizon and mineral soil C stocks and chemical characterization of the SOM stocks and residue inputs, to study forest C and N stocks and processes of retention and accumulation. Through these methods I demonstrated the importance of understanding fundamental forest soil properties and processes to understand system function. My dissertation highlighted new questions and existing knowledge gaps that will provide a deeper understanding of the processes studied such as: What are the factors regulating the retention of N in SOM and how will this be affected by future changes in climate and disturbance? What is the efficiency of O horizon decomposition across forest systems? Are the results of the mechanistic laboratory incubation confirmed in the field across forest types? How do different mycorrhizal symbionts impact plant chemical root traits relevant to decomposition and SOM formation and how does this vary across plant functional types and taxa? These new research frontiers are exciting and promising in aiding goals to improve the management of forest ecosystems, necessary to preserve ecosystem function in the uncertain future.

REFERENCES

Bird, J.A., Kleber, M., Torn, M.S., 2008. ^{13}C and ^{15}N stabilization dynamics in soil organic matter fractions during needle and fine root decomposition. Organic Geochemistry 39, 465–477. https://doi.org/10.1016/j.orggeochem.2007.12.003

Cotrufo, M.F., Ranalli, M.G., Haddix, M.L., Six, J., Lugato, E., 2019. Soil carbon storage informed by particulate and mineral-associated organic matter. Nat. Geosci. 12, 989–994. https://doi.org/10.1038/s41561-019-0484-6

Cotrufo, M.F., Soong, J.L., Horton, A.J., Campbell, E.E., Haddix, M.L., Wall, D.H., Parton, W.J., 2015. Formation of soil organic matter via biochemical and physical pathways of litter mass loss. Nature Geosci 8, 776–779. https://doi.org/10.1038/ngeo2520

Fulton-Smith, S., Cotrufo, M.F., 2019. Pathways of soil organic matter formation from above and belowground inputs in a *Sorghum bicolor* bioenergy crop. GCB Bioenergy 11, 971–987. https://doi.org/10.1111/gcbb.12598

Lavallee, J.M., Conant, R.T., Paul, E.A., Cotrufo, M.F., 2018. Incorporation of shoot versus root-derived 13C and 15N into mineral-associated organic matter fractions: results of a soil slurry incubation with dual-labelled plant material. Biogeochemistry 137, 379–393. https://doi.org/10.1007/s10533-018-0428-z

Liang, C., Schimel, J.P., Jastrow, J.D., 2017. The importance of anabolism in microbial control over soil carbon storage. Nat Microbiol 2, 17105. https://doi.org/10.1038/nmicrobiol.2017.105

Lovett, G.M., Goodale, C.L., Ollinger, S.V., Fuss, C.B., Ouimette, A.P., Likens, G.E., 2018. Nutrient retention during ecosystem succession: a revised conceptual model. Front Ecol Environ 16, 532–538. https://doi.org/10.1002/fee.1949

Mayer, M., Prescott, C.E., Abaker, W.E.A., Augusto, L., Cécillon, L., Ferreira, G.W.D., James, J., Jandl, R., Katzensteiner, K., Laclau, J.-P., Laganière, J., Nouvellon, Y., Paré, D., Stanturf, J.A., Vanguelova,

E.I., Vesterdal, L., 2020. Tamm Review: Influence of forest management activities on soil organic carbon stocks: A knowledge synthesis. Forest Ecology and Management 466, 118127. https://doi.org/10.1016/j.foreco.2020.118127

Rasse, D.P., Rumpel, C., Dignac, M.-F., 2005. Is soil carbon mostly root carbon? Mechanisms for a specific stabilisation. Plant Soil 269, 341–356. https://doi.org/10.1007/s11104-004-0907-y

Seidl, R., Thom, D., Kautz, M., Martin-Benito, D., Peltoniemi, M., Vacchiano, G., Wild, J., Ascoli, D., Petr, M., Honkaniemi, J., Lexer, M.J., Trotsiuk, V., Mairota, P., Svoboda, M., Fabrika, M., Nagel, T.A., Reyer, C.P.O., 2017. Forest disturbances under climate change. Nature Clim Change 7, 395–402. https://doi.org/10.1038/nclimate3303